



**UNIVERSITY OF PATRAS  
DEPARTMENT OF ELECTRICAL ENGINEERING AND  
COMPUTER TECHNOLOGY**

**SECTOR Smart Grids with RES-High Voltages. LABORATORY  
of Power, Renewable and  
Distributed Production**

---

**"Analysis and improvement of  
operation/performance of a photovoltaic unit  
connected to the grid"**

**DIPLOMA THESIS  
of the student of the Department of Electrical Engineering and  
Computer Technology of the Faculty of Engineering of the University  
of Patras**

**(Stratakis Stavros son of Georgios)**

**Registration Number:1066687**

**SUPERVISOR: ANTONIOS ALEXANDRIDIS**

**PATRAS - MARCH 2024**

University of Patras, Department of Electrical Engineering and Computer Technology.

Stratakis Stavros

© 2024 – All rights reserved, the entire work is an original work, produced by Stratakis Stavros, and does not violate the rights of third parties in any way. If the work contains material that has not been produced by it, it is clearly visible and is explicitly mentioned in the text of the work as the work of a third party, noting in a similarly clear way the elements of the use of unaltered graphic representations, images, graphs, etc., has received the unrestricted permission of the copyright holder for the inclusion and subsequent publication of such material

## **CERTIFICATION**

It is certified that the Diploma Thesis entitled

### **Analysis and improvement of operation/performance of a grid-connected photovoltaic unit**

of the student of the Department of Electrical Engineering and Computer Technology

**STAVROS STRATAKIS SON OF GEORGIOS**

Registration Number: 1066687

It was presented publicly at the Department of Electrical Engineering and Computer Technology on

4/3/2024

and was examined by the following examination committee:

Antonios Alexandridis, Professor, HMTY (supervisor)

Georgios Konstantopoulos, Associate Professor, IMTY (committee member)

Panagis Vovos, Assistant Professor, HMTY (committee member)

The Supervisor

The Director of the Sector

Antonios Alexandridis  
Professor

Epaminondas Mitronikas  
Associate Professor



# **PROLOGOS**

First of all, I would like to thank the supervising professor of my diploma thesis, Mr. Antonios Alexandridis, who entrusted me with the elaboration of this interesting topic and provided me with assistance throughout its preparation. He is an example of a professor and president and is an example to all of us.

I would also like to thank doctoral candidate Zaid Alexakis for the time and energy he dedicated, helping me with a plethora of issues that I was asked to address during my thesis. His patience and the help he provided to me every time he was asked was invaluable and is an integral helper in this effort of mine. I wish him a brilliant academic career.

Last but not least, I would like to thank my family from the bottom of my heart, for the mental, financial and any other support they have provided me over the years. Without their support, understanding, faith and help, I would not have been able to choose this path and complete my studies. They, along with my friends, played a catalytic role in being able to have a pleasant and full of experiences and knowledge studies at the Department of Electrical Engineering and Computer Technology. I wish them all the best.

# **Summary**

## **Analysis and improvement of operation/performance of a grid-connected photovoltaic unit**

**STRATAKIS STAVROS:**

**ANTONIOS ALEXANDRIDIS:**

The purpose of this thesis is the modeling, control and mainly the improvement of the performance of photovoltaic systems connected to the grid. More specifically, the system studied consists of a photovoltaic array, a DC/DC Boost Converter, an Inventor and the simulation with the grid. Boost is controlled through Maximum Power Output Algorithms (MPPT Algorithms), from which we receive the reference current at which our system should operate and which we set control. We also control the Inventor appropriately, so that the appropriate amount of power is transferred from the system to the grid and under a specific voltage and frequency. This is achieved by using Park transform and Phased Locked Loop control. Of course, the use of filters and capacitors for the optimal operation of our system and the reduction of harmonics also played an important role. After taking into account the above, we built the corresponding models in MATLAB's Simulink, programmed the control algorithms appropriately and extracted the characteristics of the photovoltaic systems.

Of course, this process was completed in a series of steps, where each time we checked the proper functioning of our system. After we managed to extract these characteristics, and knew the points at which our system is in the optimal state, i.e. the maximum power output, we operated a series of MPPT Algorithms under various shading scenarios and observed the system responses. Thus, we were able to draw basic conclusions about their operation under conditions of no and partial shading, as well as the severity of taking into account the losses presented by the Boost Converter in the Algorithms. Finally, we confirmed the above results experimentally, using the Typhoon Hardware In The Loop device in combination with the C2000 microcontroller, observing the current to which our photovoltaic system was driven with the respective photovoltaics shading algorithm and model.

More specifically, in the first chapter we make a general introduction about SEUs and the importance of RES and solar energy, while also we analyze power converters and what is the purpose of this diploma thesis. In the second, we explain photovoltaic arrays, observe some of their characteristics, the equivalent circuit of photovoltaics, what MPPT means and explain how their characteristics are extracted and what information we can draw from there. We pay particular attention to the losses of Boost in the phenomenon of partial shading, how we deal with it and what we observe with the MPPT algorithms in these cases. In the third we do the modeling of the system, both DC and AC

side, while in the fourth we plan to control our system. In the fifth we introduce the HIL and the microcontroller while also designing the system in the Schematic Editor simulator and create the appropriate HIL SCADA file. Finally, in the sixth and seventh chapters we present the results of the simulations and experiments respectively along with a series of conclusions for improving the efficiency of a photovoltaic unit connected to the grid.

## **EXTENSIVE ENGLISH SUMMARY**

### **Analysis and improvement of operation/performance of a photovoltaic unit connected to the grid.**

**STRATAKIS STAVROS:**

**ALEXANDRIDIS ANTONIOS:**

The aim of this thesis is to model, control and mainly improve the performance of photovoltaic systems connected to the grid. More specifically, the system under study consists of a photovoltaic array , a DC/DC Boost Converter, an Inverter and the simulation of the grid. The Boost is controlled by means of Maximum Power Production Finding Algorithms (MPPT Algorithms) , from which we obtain the reference current at which our system should operate and which we set the control. We also control the Inverter appropriately , so that an appropriate amount of power is transferred from the system to the grid and under a specific voltage and frequency. This is achieved by using Park transformation and Phased Locked Loop control. Of course the use of filters and capacitors for optimal operation of our system and reduction of harmonics also played an important role. Having taken the above into account, we constructed the corresponding models in Simulink of MATLAB, programmed the control algorithms and extracted the characteristics of the photovoltaic systems. This process was completed in a series of several steps , where each time we checked the correct operation of our system. Once we were able to extract these characteristics , and we knew the points at which our system is in the optimal state, i.e. maximum power output, we ran a series of MPPT Algorithms under different shading scenarios and observed the system responses. Thus we were able to draw key conclusions about their operation under no and partial shading conditions, as well as the importance of factoring in the losses presented by the Boost Converter in the Algorithms. Finally, we confirmed the above results experimentally , using Typhoon's Hardware In The Loop device combined with the C2000 microcontroller , by observing the current at which our PV system was driven by each PV shading algorithm and model.

More specifically, in the first chapter we make a general introduction to the EEE and the importance of RES and solar energy while we also analyze the power converters and what is the purpose of this thesis. In the second we explain the PV arrays , we observe some of their characteristics, the equivalent circuit of the PV , what MPPT means and explain how their characteristics are extracted and what information we can derive from there. We pay special attention to the boost losses in the partial shading effect , how we deal with it and what we observe with the MPPT algorithms in these cases. In the third we do the system modeling , both the DC and AC side , and in the fourth we design our system control. In the fifth we introduce the HIL and the microcontroller while we also design the system in the Schematic Editor simulator and create the appropriate HIL SCADA file. And Finally in the sixth and seventh chapter we present the results of simulations and experiments respectively along with a set of conclusions to improve the performance of grid connected PV module.

## Table of Contents

Summary .....	4
Abstract .....	5
<b>CHAPTER 1: Electricity Systems .....</b>	<b>12</b>
1.1 Import.....	12
1.2 Microgrids-Dispersed Productions - RES.....	14
1.3 Power Converters.....	16
1.3.1 Import.....	16
1.3.2 Comparison with Past.....	20
1.3.3 Semiconductor Power Elements:.....	20
1.3.4 Pulse.....	22
1.4 Objectives of the Diploma Thesis.....	25
1.5 Steps and Implementation.....	26
<b>CHAPTER 2: Photovoltaic Systems.....</b>	<b>29</b>
2.1 Theory .....	29
2.1.1 Equivalent Circuit.....	32
2.1.2 Photovoltaic Performance.....	35
2.2 Maximum Power Point Algorithms (MPPT Algorithms).....	37
2.2.1 Perturb and Observe Algorithm.....	39
2.2.2 Particle Swarm Optimization Algorithm.....	41
2.3.1 Photovoltaic Array Losses.....	46
2.3.2 Modified P&O and PSO .....	50
<b>CHAPTER 3: Modeling.....</b>	<b>54</b>
3.1 Import.....	54
3.2 AC Side.....	57

3.2.1 Import.....	57
3.2.2 LC Filter and Coil Coupling:.....	61
3.3 DC Side.....	64
3.3.1 DC/DC Voltage Booster Transformer Model (Boost Conventer) .....	64
3.3.2 DC Bus Model (DC Link): .....	66
3.3.3 Photovoltaic Array Equations:.....	67
<b>CHAPTER 4 Control System Design .....</b>	<b>70</b>
4.1 Import.....	70
4.2 Voltage Boosting Inverter Control of Photovoltaic Array.....	70
4.3 Load Side Control.....	71
4.3.1. Phased-LockedLoop: .....	72
4.3.2. Internal Current Control Loop:.....	73
4.3.3. External Voltage Control Loop: .....	75
<b>CHAPTER 5: Experimental Arrangement .....</b>	<b>79</b>
5.1 Import.....	79
5.2 Real Time Typhoon Hardware in the Loop .....	79
5.3 Circuit System Model in Typhoon Hardware In the Loop .....	91
5.4 System Power Converters Control Schemes .....	94
5.5 The C2000 Launchpad XL tms320f28379d Microcontroller .....	98
5.5.1. Import.....	98
5.5.2. Features .....	98
5.5.3. Applications: .....	99
5.5.4. Advantages.....	100
5.5.5. Detailed use of the C2000 Launchpad XL in the PV experiment .....	100
<b>CHAPTER 6: Simulations .....</b>	<b>101</b>

6.1 Import.....	101
6.2 Photovoltaic Array without Shading.....	101
6.2.1 Photovoltaic Array without Shading, radiation change scenario.....	108
6.3 Photovoltaic Array under Partial Shading Conditions:.....	110
CHAPTER 7: Results .....	114
7.1 Results of Simulations under normal shading conditions.....	114
7.1.1 Perturb and Observe without losses.....	114
7.1.2 Perturb and Observe with losses.....	117
7.2 Results of Simulations under partial shading conditions:.....	122
7.2.1 Perturb and Observe without losses.....	122
7.2.2 Particle Swarm Lossless Optimization .....	125
7.2.3 Particle Swarm Optimization with Losses.....	128
7.3 Results of Experiments .....	134
7.3.1 Perturb and Observe without Shading .....	134
7.3.2 Particle Swarm Optimization without Shading .....	135
7.3.3 Perturb and Observe partial shading .....	136
7.3.4 Particle Swarm Optimization Partial Lossless Shading.....	137
7.3.5 Particle Swarm Optimization partial shading with losses .....	138
Bibliography .....	140



# CHAPTER 1: Electricity Systems

## 1.1 Import:

Electricity is one of the most basic needs not only in all modern societies, but also in developing countries. It is used for the operation of industries, residential, transport, infrastructure and many other basic needs that make it beyond important and very critical. The above was confirmed by the recent geopolitical turbulences which led to an energy crisis, uncertainty and intense concern. The effects have been immediate and painful not only in terms of electricity production and costs but also in many other sectors such as industry, resulting in inflation skyrocketing and the need for alternative forms of energy becoming greater than ever.

Electricity systems are the systems that produce, transmit and distribute electricity. They are complex systems that consist of various parts, such as Power Stations, Transmission Lines, Distribution Networks , etc.

More specifically, Generating Stations are the units that produce electricity. There are several types of generating stations, depending on the energy source they use. The main types are fossil fuel plants, such as steam power plants, gas turbine plants, and combined-cycle plants. Wind turbines and photovoltaic panels belonging to RES, as well as hydroelectric power plants and nuclear power plants, which produce electricity from the kinetic energy of water and the fission of uranium respectively.

Transmission lines carry electricity from power stations to consumers, at various levels such as low, medium, high, super-high and with the use of appropriate transformers are used in households. With high voltage showing greater efficiency, as it has the ability to carry more electricity in a shorter route.

Distribution networks distribute electricity to consumers, with the networks Distribution Low Voltage to Meet Often. It is

worth noting that in recent years there have been intense efforts to decarbonize the SEAs. The reason for this effort is to address the ever-increasing levels of greenhouse gas emissions (mainly CO<sub>2</sub>) and the constant increase in the average temperature. Achieving energy security is also of major importance, i.e. avoiding dependence of production on fossil fuels fuels, which are known to exhibit, constantly decreasing availability and they come from countries with geopolitical tensions, such as Russia's example with natural gas. Finally, the economy, since the production of energy from Renewable Energy Sources basically costs less than that of conventional fuels.

In Greece, the transmission lines and electricity distribution networks belong to the Hellenic Electricity Distribution Network Operator (HEDNO) and constitute a natural monopoly. HEDNO is a private entity established in 2013, following the liberalization of the electricity market in Greece. It is the only entity that can construct, operate and maintain these networks.

There are several reasons why electricity distribution networks are monopolistic. One reason is that building and operating a distribution network is a very expensive investment. Another reason is that it is important to have a single body responsible for the operation of the network in order to ensure its security and reliability.

The monopoly of distribution networks has a number of advantages and disadvantages. On the one hand, monopoly can lead to lower prices for consumers, as the monopoly entity has the ability to exploit economies of scale. On the other hand, monopoly can lead to reduced innovation, as the monopoly operator does not have to compete with other operators to attract customers.

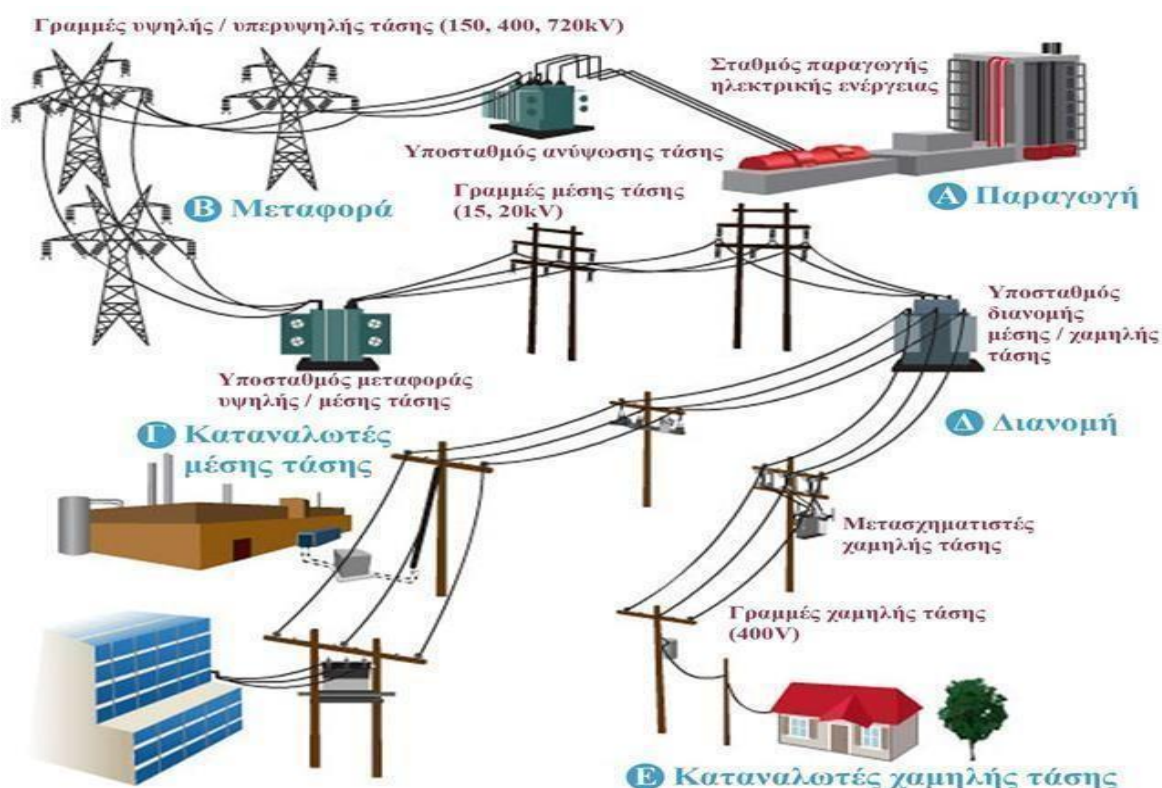


Figure 1. Electricity Systems

In addition to their strengths, however, electricity systems also face a number of challenges. For example, increasing the penetration of renewable energy sources (RES) is a major challenge for electricity systems (RES). RES, such as wind and solar, are more volatile than conventional energy sources, such as fossil fuels. This means that electricity generation from renewables can be more difficult to predict and predict. Checked. For this reason, bodies have been established that are solely responsible for the forecasting of electricity production from RES. Furthermore, the safety of the network, as the RES, must be safe and reliable, in order to be able to meet the needs of consumers. The safety of the network includes the protection of consumers from electric shock and damage to the electrical installation, while the reliability of the grid includes its ability to provide electricity to consumers without interruptions. Finally, the stations

The production of fossil fuels contributes to air pollution and climate change by influencing phenomena such as the greenhouse effect. On the contrary, renewable energy sources are more environmentally friendly than conventional ones, and the shift towards consolidating them seems a one-way street.

## **1.2 Microgrids-Dispersed Productions-RES:**

Household loads, i.e. the common appliances used by consumers in their daily lives, such as refrigerators, kitchens, washing machines, etc., are usually AC and are powered by home power supplies. In Greece, as in many other countries, most households are powered by the main conventional electricity grid. It is transported from power plants to distribution centers via high-voltage transmission lines. The construction of such projects is costly, but it is justified by the fact that they serve a large number of consumers. However, what happens when a load is located in a remote area and the demand for electricity is not large enough to justify the construction of new transmission lines?

There are several solutions to this problem. One solution is to use independent electricity generators, such as photovoltaic panels or wind turbines. These generators can generate electricity close to the load and feed it directly.

Another solution is the use of microgrids. Microgrids are small, local electricity grids consisting of dispersed generation, consumers and storage systems. Distributed generation is small power plants that are located close to consumers. These units can be based on various energy sources, such as wind, solar, biomass and fossil fuels and have the ability to operate independently of the main electricity grid.

Microgrids and distributed generation systems represent important aspects in the field of electrical energy systems. For example, microgrids seek autonomy and high reliability, while providing the possibility of local energy production. The aim is to make efficient use of energy resources at local level. Technological aspects such as renewables and Energy storage systems play a central role. Economic factors have also had significant impacts. The reduction in the cost of renewable technologies, as well as the increase in the cost of conventional energy sources, has made microgrids and distributed generation systems economically competitive. The promotion of research and development in this field has enabled the creation of advanced technologies such as smart energy management platforms , energy-efficient appliances and sophisticated control algorithms.

To increase the participation of renewable energy sources in RES, dispersed production can help, as they can be placed in areas where it is not possible to build large RES plants. For example, wind turbines can be installed in remote areas with strong

winds, while photovoltaic panels can be installed on roofs and other spaces. They help reduce dependence on large grids, as they can operate independently of them, which can be useful in the event of a major grid outage, and at the same time they can act as a support to it by offering a backup in the event of a failure of a large production plant.

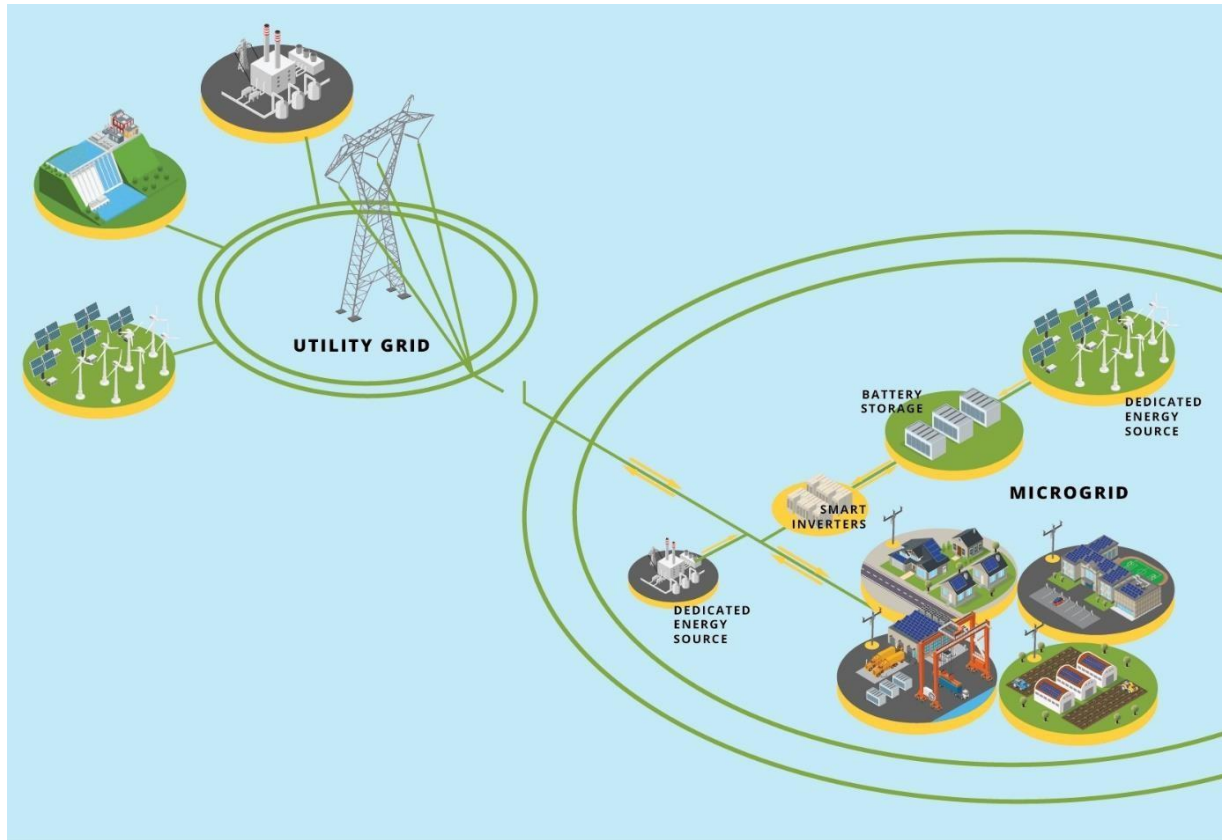


*Figure 2.Main Grid-Microgrids*

In conclusion, microgrids and dispersed generation provide an increase in the participation of renewables, a reduction in dependence on large grids, increased grid security, improved grid reliability and reduced energy losses. On the contrary, they also present some disadvantages such as higher installation and operation costs, difficulties in regulation and control, and increased probability of downtime.

### **1.3 Power Converters:**

### 1.3.1 Introduction:

What we have mentioned above has become possible in recent years with the development of other technologies and more specifically power converters, which play a vital role in microgrids. The rapid evolution of others is the one that now allows us to integrate such systems as Generating Stations and to take others seriously into account in the intraday electricity market. In particular, scattered generation units, such as photovoltaics and wind turbines, produce electricity with different characteristics. Photovoltaics produce continuous voltage, while wind turbines generate alternating voltage. In order for these sources to be able to be connected to a common grid, it is necessary to convert other voltage and current into a form compatible with the grid. It is clear, then, that power conversion is a basic function of microgrids, as it allows other electricity from different sources to be adapted into a common form. Power conversion devices used in microgrids can be divided into three main categories:

- 3) Alternating Voltage to DC (AC-DC) Inverters: These inverters are used to convert other AC voltage from other sources such as wind turbines to DC voltage, which is the form that photovoltaics produce.

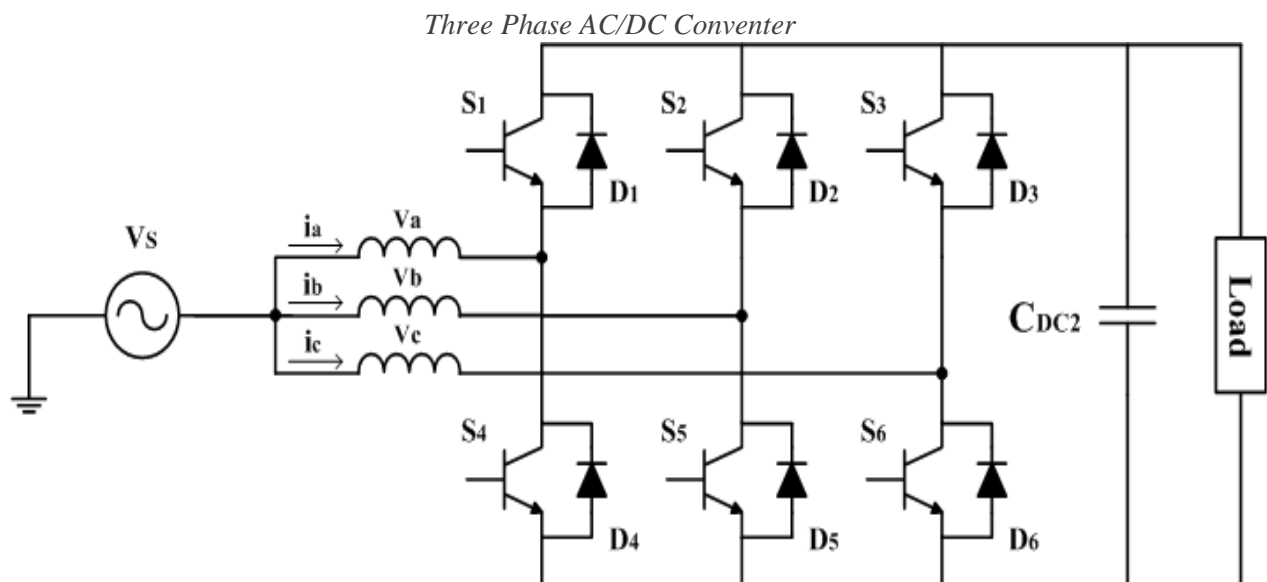


Figure 3. Three Phase AC to DC Voltage Converter

Other than other ones of AC converters are for powering electronic devices, as most electronic charges, other computers, televisions, mobile phones, etc., require constant voltage to operate others. Also AC/DC inverters can be used to reduce other voltage from a higher level to a lower one. This is useful in some

Applications, others the charging of batteries or the power supply of loads which can operate with lower voltage and to protect others from surges. This avoids possible damage to other electronic devices, where it is important to take measures to protect others.

2) Direct Voltage to AC (DC-AC) Inverters: These inverters are used to convert other DC voltage from sources other than photovoltaics to AC voltage, which is the form required to supply and transport electricity to residential and commercial loads.

*Three Phase DC/AC Inverter*

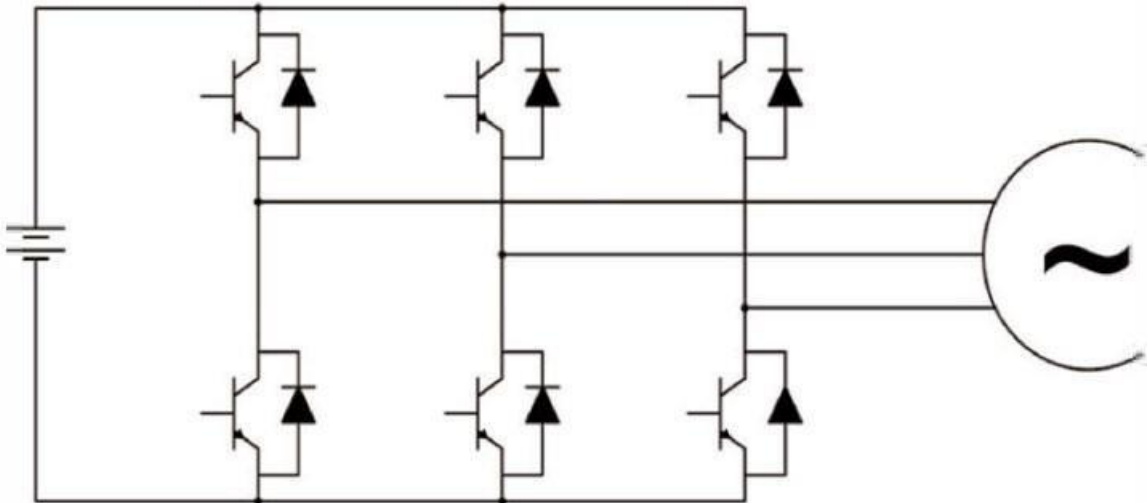


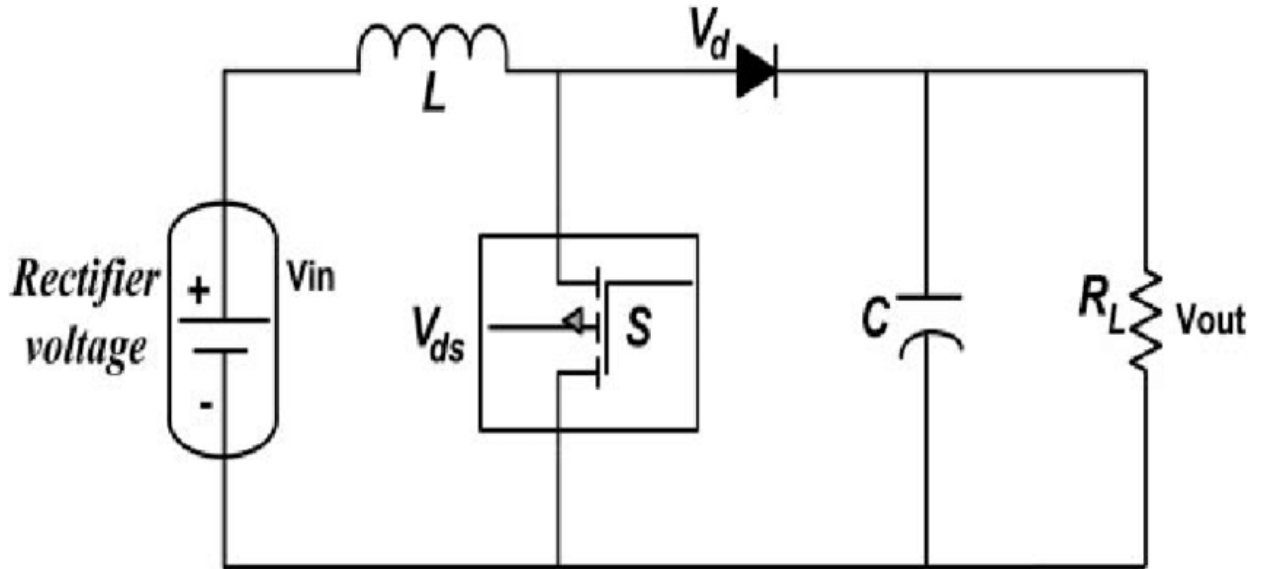
*Figure 4.Three Phase Voltage Inverter*

Direct current to AC (DC-AC) inverters are used in a variety of applications, others to generate AC voltage with different parameters. Some of these other parameters may be voltage, frequency, and waveform. This is useful in some applications, others powering industrial loads or generating electricity to transport others. In stand-alone solar energy systems, DC-AC inverters are used to convert other DC voltage generated by photovoltaics into alternating voltage that can be used by home appliances or connected to the electrical grid.

Correspondingly in energy storage systems, they are used to convert other DC voltage stored other batteries into alternating voltage.

Another application is in industrial facilities, where DC-AC inverters are used to generate alternating voltage with different parameters for the operation of industrial loads, other motors and lighting equipment. Finally, in telecommunication systems, they are used to convert other direct voltage produced by photovoltaics in alternating voltage that can be used to transmit data, which will inform for example with signals received from sensors or other electronic devices.

3) Direct Voltage to DC (DC-DC) Converters: DC-DC converters can be used to convert a DC voltage to another DC voltage with various characteristics. For example, they can be used to convert a high voltage to a lower voltage, or to convert a voltage with a specific shape to another voltage with a different shape. The right DC-DC converter for a particular application depends on a number of factors, such as the power required, the input and output voltage, and the characteristics of the output voltage.



5.DC-DC Power Converter Figure

DC/DC converters are widely used, some of the many applications are as follows:

- Photovoltaic systems: Photovoltaic panels produce a direct current voltage, which can be too high or too low to be used directly by the electrical systems of a building or appliance. DC-DC inverters are used to adjust the voltage of photovoltaic panels to match the voltage of the batteries or load.
- E-vehicles: E-vehicles use batteries to store energy. DC-DC converters are used to convert voltage from batteries into voltage that can be used by the vehicle's electrical systems, such as the engine, electrical appliances, and safety systems.
- Security systems: Security systems, such as fire detection systems and industrial plant security systems, must operate continuously, regardless of the power supply. DC-DC converters are used to supply safety systems with voltage stored in batteries, in order to ensure their proper and continuous operation.

However, power conversion devices in microgrids must also meet a number of requirements, such as:

- High efficiency: That is, no energy is lost during the conversion process either from alternating to continuous or vice versa.
- Resistance to disturbances: To be resistant to disturbances, such as surges and short circuits. Phenomena that are often encountered, especially in industrial applications where large currents and consequently intense electromagnetic interference are developed.
- Good control characteristics: Have good control characteristics, so that they can be adjusted to ensure the stability of the network, either in terms of frequency or voltage and current.

Choosing the right power conversion devices for a microgrid is crucial for the network to run efficiently. They must be selected based on the requirements of the grid, such as its size, voltage level and the nature of the energy sources connected to it. In fact, some aspects of the microgrids that power converters apply are:

- The management of the balance between production and consumption in a microgrid. For example, DC-AC converters can be used to charge batteries from excess electricity, which can then be used to meet the needs of the grid in the event of a power outage.
- To improve the reliability of the electricity supply in a microgrid. For example, AC-DC converters can be used to create local backup energy sources in the event of a power outage.
- Reducing greenhouse gas emissions from a microgrid. For example, DC-AC converters can be used to connect photovoltaics to a fossil fuel-backed grid.

All the aforementioned features of inverters and the features they provide us, have made today's reality capable. Where we can now operate and plan the future based on RES and dispersed production, improving the efficiency of RES, reducing operating costs and protecting not only the grid and supply from possible damage, but also our planet from phenomena such as that of the greenhouse.

### 1.3.2 Comparison with Old:

As it has been understood, the use of power converters has dramatically changed the way we view Modern Electricity Systems. Compared to the past, where

Electromechanical devices or linearly controlled electronic devices were used, electronic power devices have a number of advantages:

- Lower volume, weight and purchase cost, for corresponding power prices.
- Less power losses, resulting in a high degree of efficiency, which can exceed 90%.
- Minimal maintenance needs, as they have no moving parts, do not require strong support bases and are additionally characterized by quiet operation
- Due to the electronic control, they offer greater accuracy and faster response to the adjustment of output quantities (voltage, current, torque, revolutions, etc.).

However, it is worth noting that with their use there are superior harmonics both on the supply side and on the load side, which causes the existence of Electromagnetic interference, an increase in Reactive Power as well as losses.

### 1.3.3 Semiconductors In POWER FISH:

Power semiconductors are the basic building block for all power converters. They consist of layers of semiconductors that contain impurities and are divided according to their control capacity into three main categories:

- 1) Uncontrolled (e.g. Diodes)



Figure 6. Diode

- 2) Partially controlled (e.g. thyristors)



Figure 7.Thyristor

3) Fully Controlled (e.g. transistors)



Figure 8.Various Types of Transistors

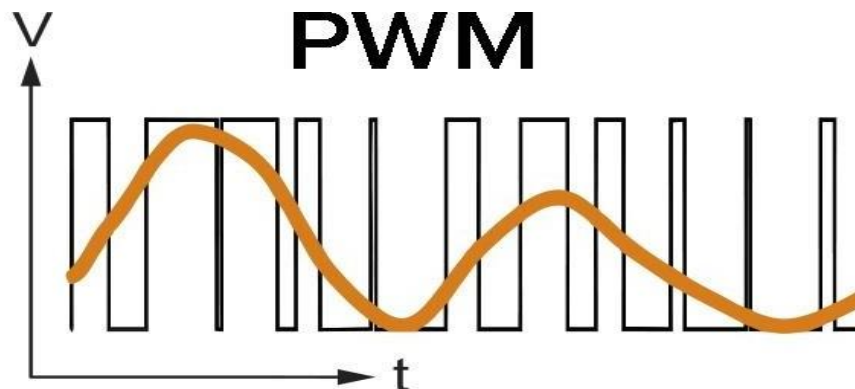
The structure of semiconductor power cells is complex, especially when compared to that of low-voltage cells, however they exhibit a number of electrical characteristics that make them particularly useful. First, high resistance to decay voltages ensures the safe operation of semiconductor cells under increased electrical charges. This is crucial for power applications that require high performance. Second, The ability to pass through high current values allows semiconductors to operate efficiently even under intense loads, offering stable and reliable performance. In addition, small voltage drops during the conduction state, low conduction resistances and small leakage currents help to minimize power losses and ensure efficient operation. The short switching times during start-up and shutdown promote safe operation and are a significant advantage in applications that require rapid changes of situations. The ability to withstand high temperatures ensures stable performance even in environments with elevated temperatures. Finally, the low power requirements in the control circuit and the low total implementation costs make the power semiconductors cost-effective and flexible for various applications.

### 1.3.4 Pulse:

The use of semiconductor power cells, as mentioned above, requires proper control. Pulsing of semiconductor power cells is the process of controlling the operation of semiconductor power cells using sinusoidal (Sinusoidal Pulse Width Modulation) or non-sine pulses (Pulse Width Modulation). It usually drives transistors, IGBTs (Insulated Gate Bipolar Transistors) or MOSFETs (Metal- Oxide-Semiconductor Field-Effect Transistors) and is used in a variety of applications, including power supplies, motors, transformers, and electronic power systems. Its purpose is to regulate the amount of energy supplied to the load. This is achieved by controlling the duration of the pulses by adjusting the time at which the semiconductor is switched on or off. This pulse allows efficient control of the power and voltage supplied to the load, reduces losses from heat generation and allows for rapid change of power levels. During each pulse, the semiconductor element is activated, thus allowing the passage of current. The frequency of the pulses is determined by the application in which the power converter is placed. The combination of all of the above achieves both a reduction in energy consumption and a reduction in noise, as it allows the use of higher operating frequencies. It is therefore easy to understand that pulsing semiconductor power elements is a complex process that requires careful planning and implementation. However, the advantages of pulsation can be significant, making it an attractive option for a variety of power applications.

#### Pulse Width Modulation ( PWM):

PWM is a method of controlling the average power provided by an analog signal through the digital output of a microcontroller. The average value of the voltage or current supplied to the load is controlled by switching the supply between 0 and 100% at a faster rate than needed to change the load significantly. The longer the switch is on, the greater the total power delivered to the load.



9.Pulse Width Modulation Figure

Variants of PWM configuration are based on the format of reference and driving signals. The most common variations are:

- Delta PWM: The pulse duration is equal to the difference between the reference signal and the driving signal.
- Delta-sigma PWM: The duration of the pulse is equal to the logarithm of the difference between the reference signal and the driving signal.
- Space vector modulation (SVM): The duration of the pulse is equal to the percentage of carrier space occupied by the reference signal.
- Direct torque control: The duration of the pulse is equal to the force required to control the motor.

PWM is used in a variety of applications, including:

- Servos: PWM is used to control the position, speed, and torque of servos.
- Telecommunications: PWM is used to transmit digital signals.
- Energy transfer: PWM is used to control voltage and current in power transmission systems.
- Power electronics: PWM is used to control voltage and current in power converters.
- Sound effects and amplification: PWM is used to create different forms of waveforms, such as square, triangular, semi-sided, or even random waveforms.
- LED Indicator: PWM is used to create different brightness levels on LEDs.

PWM is a non-linear process, which means that the recovery of a low-pass filter signal is not perfect. However, the PWM sampling theorem shows that PWM conversion can be perfect, provided that the sampling frequency is greater than 2 times the bandwidth of the reference signal.

The sampling frequency determines the number of pulses in the PWM waveform. The higher the sampling frequency, the smaller the amplitude of each pulse, and the closer the PWM waveform is to the original reference signal.

PWM is an effective method of controlling the average power provided by an electrical signal. It's simple to apply and offers a range of benefits, including energy savings, noise reduction, and improved performance.

### Sinusoidal Pulse Width Modulation (SPWM):

In the technique of Sinusoidal Pulse Modulation (SPWM), a triangular-shaped signal, known as a high-frequency carrier signal, is compared to a sinusoidal signal, which represents the desired frequency at the transducer output and is called a reference signal. When the value of the reference signal exceeds the bearing signal, a positive pulse is produced by the comparator. Conversely, when the value of the reference signal is less than the bearing signal, a negative pulse is produced. The diagram below first shows the signals being compared and then the pulses produced.

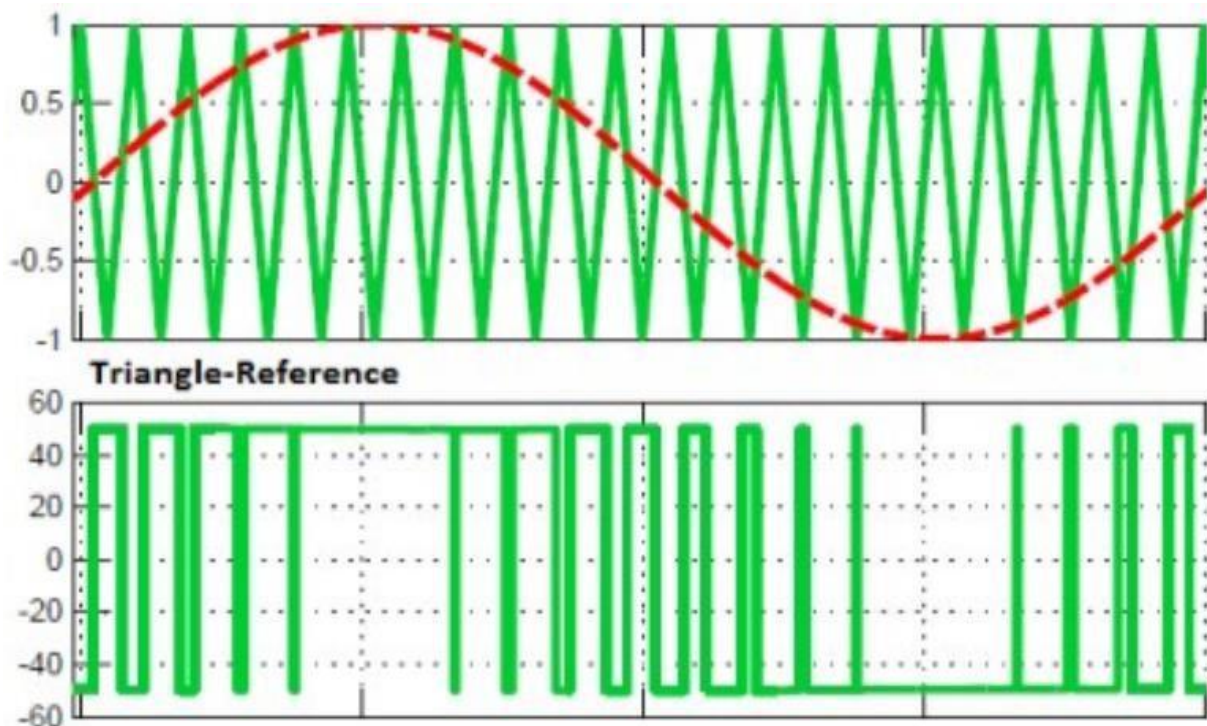


Figure 10. Sinusoidal Pulse Width Modulation

By adjusting the amplitude and frequency of the reference signal, we control the frequency and the active value of the output voltage of the inverter. At the same time, with the change in the initial phase of the reference signal, there is a change in the phase of the alternating current at the input of the inverter, thus controlling the power factor of the device. The pulsation of the transistors occurs in the upper branch using the corresponding triangle signal, while in the lower branch its reverse waveform is used. To pulse the three-phase inverter, three reference signals are generated, one for each phase, with a different phase 120 degrees apart. These signals are compared with the same triangular signal and are applied to each branch of the inverter. The corresponding reference signals feed into the corresponding lower branches. The waveforms of phased and polar trends are shown in the diagram below.

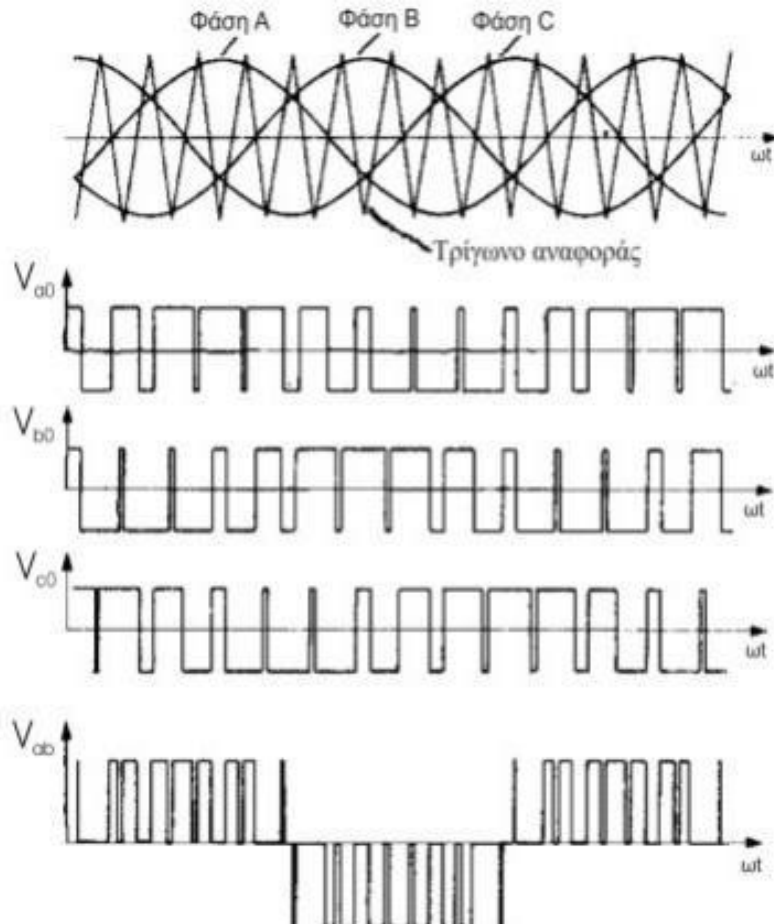


Figure 11. Waveforms of Phased and Polar Trends

#### 1.4 Objectives of the Diploma Thesis:

The purpose of this thesis is to improve the performance of a photovoltaic system connected to the grid, in the particular case of partial shading. More specifically, we create the scenario where photovoltaic arrays receive different solar radiation and show the responses they have through the Power-Voltage (P-V) characteristics. Then, we observe these graphics and how they are approached by algorithms for finding the maximum point Maximum Power Point. By comparing the above, we manage to show some weaknesses presented by one of the most widespread heuristic algorithms, Perturb and Observe. The Perturb and Observe (P&O) algorithm is one of the simplest and most effective algorithms for detecting the maximum power point (MPP) in photovoltaic (PV) systems. It works by sequentially modifying the output voltage of the system and monitoring the change in the output power. If the output power increases, the algorithm continues to increase the output voltage until it reaches the MPP. If the output power decreases, the algorithm reduces the output voltage until it finds the MPP again. Thus, it stops at the first power peak it encounters, which may be the local maximum of the characteristic resulting in our system not working in MPP under some cases of partial shading. Instead, using the heuristic Particle Swarm Optimization algorithm, where each particle

In the algorithm represents a possible solution to the optimization problem and the particles move in the solution space, learning from their own previous experiences and the experiences of other particles, we show that finding MPP is always possible. We therefore conclude that it is more efficient in the shading scenarios of photovoltaic systems. Clearly all of the above take place in a system where the PV is connected to an inverter Boost, which in turn connects to the Reverse Voltage Converter (Inverter) and finally the network. We must therefore take into account the losses generated in the inverters and the wiring used to raise the voltage (Boost Converter) produced by the PV as well as its reversal from continuous to alternating (Inverter). In this way, the change in the Maximum Power point and the inability of the P&O to find the Global MPP becomes apparent.

In order for this system to be feasible, careful design of the control system and the interface between the inverters is required. That is, it is important to design the internal control loops so that the Boost works properly and its pulsation leads to the desired voltage rise. The same applies to the Inventor, and it is also important to synchronize with the network as well as to drive the d,q components to the desired reference levels.

The final goal of the work is of course what we mentioned to be proven in the laboratory, where with the use of the Typhoon Hardware In the Loop Simulator, both the Schematic Editor, and its Scada Environment, and in combination with the C2000 microcontroller of Texas Instruments, we pulse the Boost and the Inverter, we take the measurements, i.e. how the voltage and current of the photovoltaic system responds and we observe with the use of each algorithm that the system It leads us to different points of equilibrium which are recognized by them as maximum points of power production.

## **1.5 Steps and Implementation:**

In this section we will describe in turn the steps we followed in order to be able to initially build the photovoltaic system and connect it appropriately to the power converters in MATLAB Simulink and then transfer this model to the Hardware in the Loop Schematic Editor, as well as all the next steps until the final implementation of the system in the laboratory, consisting of microcontroller, and HIL.

Initially, we started with the step-by-step study of the system and algorithms. In the first stage, we created a model in Simulink's MATLAB that contained a photovoltaic system connected to a Boost inverter. We appropriately designed the internal control loop of the voltage booster on the side of the PV array and confirmed that the system is indeed driven to the desired reference current. the correct functioning of the algorithms we intended to introduce, we proceeded to extract the P-V and I-V characteristics. These characteristics are what show us exactly the point (MPP) to which the algorithms should lead the control system

and by extension the operation of the photovoltaic system. To achieve this, we connected in series to the photovoltaic array, Controlled Power Source, to which we set as an input signal a ramp from 0 to the short circuit current of the photovoltaic array. So we were able to find the characteristic and consequently the MPP, in which Will must to our

Lead The Algorithms. The next step, of course, was the algorithms we wanted to use in our system. Initially, we studied the more widespread Perturb and Observe algorithm, we saw the philosophy it follows and applied it to our own system, with the difference that we relied on the change of the reference current, instead of that of the power as is usual in such systems. After completing the algorithm, we placed it in a MATLAB Function Block in a common Simulink file with the original PV array and confirmed that it works correctly. We then added the Inverter to the system and therefore the appropriate control required. This control consists of the external control loop of the Vdc, i.e. the voltage after the Boost and before the Inverter (DC bus), which in our case we want to be 1200 Volts, the control on the load side and the Phased-Locked Loop. While the control on the load side, it makes sure that the voltage and frequency are kept constant and on the one hand that the voltage on the Q-axis is zeroed

, on the other hand, to be driven to a desired value on the D-axis of the network side. With the These three control circuits we achieve:

- The outer loop of the voltage produces a current reference signal for the d-axis and the inner loop free of nonlinearities produces the appropriate trigger variable of the power converter through the S.P.W.M. technique.
- The PLL produces the desired operating frequency while zeroing the voltage on the q-axis on the load side.
- The current flow on the q-axis is reduced to zero in order to reduce power losses and reactive power more specifically.

After completing these and making sure that the system and algorithms are working properly, we applied the partial shading effect. To achieve this, instead of one photovoltaic array with common radiation, we placed three with different radiation each in a row. We also placed a Bypass Passage in each of them, which allows the current to bypass the shaded cell, thus maintaining the flow of the current to the rest of the circuit and dealing with phenomena such as that of the Hot Spot. This helps minimize shading losses and maintains high efficiency of the solar system.

Once again and in the same way as before, we extracted the characteristics of the system and confirmed the correct functioning of the algorithms in the case of of partial shading, with the main difference that in this case the characteristic P-V has 2 maximums, one local and one total. This is where the inability of Perturb and Observe to separate these two becomes apparent, resulting in the local maximum rather than the MPP. Unlike using Particle Swarm Optimization, finding MPP is correct, thus concluding that it is a more efficient algorithm at scenario this.

So, after we had completed our system in Simulink, we transferred this model to the corresponding HIL environment, the Schematic Editor, without including the control part. For the control and pulsation of the converters, we created a new Simulink file, in which we placed Blocks that insert the analog inputs, and the appropriate control that we had designed, as well as the Particle Swarm Optimization algorithm and we received as output the pulses needed for the Boost converter and which we set as input to the HIL device. So, by properly connecting the microcontroller to the HIL and the computer, after loading the Simulink control and signal file to the C2000 and having created a SCADA model in the HIL at the same time, we were able to confirm experimentally what we mentioned earlier. That is, using the 2 algorithms in the photovoltaic system that we had built, and observing the measurements through Code Composer Studio and SCADA, we found that indeed the Particle Swarm Optimization algorithm is optimal and leads the PV to MPP as opposed to Perturb and Observe which stops at the first local maximum. This is how we completed the experimental study and we are now confident in our conclusions.

## CHAPTER 2: Photovoltaic Systems

Photovoltaic systems are an innovative technology that converts solar energy into electricity. This technology has redefined the way

energy generation, offering a sustainable and clean alternative. In this chapter, we will examine the history, construction, operation, and various categories of photovoltaic systems as well as analyze the losses presented in them and algorithms suitable for their maximum efficiency.

## 2.1 Theory:

The concept of converting solar energy into electricity began in the 19th century, when physicist Alexandre-Edmond Becquerel discovered the photoelectric phenomenon. However, it was in 1954 that American physicists Daryl Chapin, Calvin Fuller, and Gerald Pearson built a photovoltaic cell that could generate electricity with an efficiency of 6%. Subsequently, the efficiency of photovoltaic cells increased significantly, thanks to advances in materials technology and manufacturing processes. Today, photovoltaic cells have an efficiency of up to 25%. Their commercial use began in the 1970s. Initially, they were used in small appliances, such as radios and computers, and later in larger applications, such as lighting, telecommunications systems, and power generation systems.

Photovoltaic cells, which are the heart of photovoltaic systems, are usually made of semiconductor materials. The most commonly used materials include silicon and gallium, while the process of building cells consists of multiple stages. In the first stage, the semiconductor from which the photovoltaic cell will be made is manufactured. The most common material used to make the semiconductor is silicon, which can be manufactured by various methods, such as crystallization, printing and chemical coating. In the second stage, the photovoltaic cell is manufactured from the semiconductor selected in the first stage. The photovoltaic cell consists of two regions with different electrical Properties. These regions are called the p region and the n region. The p region has an excess of electrons, while the n region has a lack of electrons. This difference in electrical properties creates an electric voltage between the two regions. To create this difference in electrical properties, the p and n regions are connected between with a metal electrode. The metal electrode attached to the region is called the reducing electrode, while the metal electrode attached to the n region is called the oxidizing electrode. The construction of the photovoltaic cell is completed by applying a protective layer to the surface of the cell that protects the cell from external influences, such as moisture and dust. This structure allows photovoltaic cells to absorb sunlight and create photoelectric current. The diversity of manufacturing processes results in various photovoltaic cell technologies, making them suitable for various applications.

The operation of photovoltaic systems, therefore, is based on the photoelectric phenomenon, which is a natural phenomenon that involves the displacement of electrons in semi-conductive materials under the influence of sunlight. Let's break down the steps of this process:

- Light Absorption:** Photovoltaic cells comprise a semiconductor material. When photons from sunlight encounter this material, they activate the electrons in the semiconductor.
- Electron Release:** Photons by their incidence transfer energy to the semiconductor's internal electrons, allowing certain electrons to detach from the atoms of the material. This process creates electrically charged electrons and holes (gaps where electrons were previously located).
- Charge Transfer:** The electrons released from the outer layer of the semiconductor can move inside the semiconductor, creating a current of electric charge. This electric current is the result of the flow of electrons to the output of the photovoltaic cell.
- Current Collection and Use:** Inductive collectors on both sides of the photovoltaic cell collect electrons and transfer the generated electrical current to the external circuit. This current can be used to power electrical appliances or stored for later use.

This process of shifting electric charging using the photoelectric effect explains how photovoltaic systems convert solar energy into electricity, offering a clean and sustainable energy source.

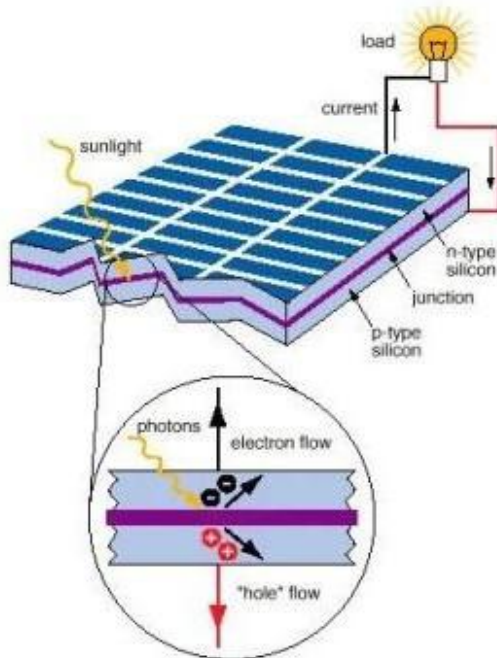


Figure 12. Photoelectric Effect

Photovoltaic cells are divided into three main categories:

- 1) **Silicon Solar Cells:** They are the most common of all on the market and are made of crystalline silicon. In fact, they consist of three subcategories:

- a) Monocrystalline Silicon Solar Cells (Sc-Si): They have high efficiency and efficiency, but their production process is more expensive. Their thickness ranges from about 0.3 millimeters. In industry, their efficiency ranges between 15% - 18% for the frame. Under laboratory conditions, even higher yields have been achieved, reaching as high as 24.7%.
  - b) Polycrystalline Solar Cells (mc-Si): These are more economical, but present a slightly lower efficiency compared to monocrystalline ones. In laboratory applications, yields of up to 20% have been achieved, while in the commercial market, polycrystalline elements are available with yields from 13% to 15% for photovoltaic panels (panels).
  - c) Silicon Film (Ribbon-Si): It is a relatively new photovoltaic cell technology. One of their advantages is a reduction of up to 50% in the use of silicon compared to the classic techniques of manufacturing monocrystalline and polycrystalline silicon photovoltaic cells. Their yield has reached about 12-13%, with their thickness ranging around 0.3 millimeters. In the laboratory, yields of 18% have been achieved.
- 2) Minutes Pavers (Thin-Film Solar Cells): These photovoltaic cells are made with thin layers of various materials, are lightweight and flexible, and can be used in a variety of applications. However, they typically exhibit lower efficiency compared to crystalline silicon photovoltaic cells. Construction materials include copper diselenide dioxide ( $\text{CuInSe}_2$  - with an efficiency of up to 11%), amorphous silicon (a-Si - with an efficiency of 6 to 8%), cadmium telluride ( $\text{CdTe}$  - with an efficiency of around 6-8%) and gallium arsenide ( $\text{GaAs}$ ), which exhibits an efficiency of up to 29%. However, the biggest drawback of this technology is the excessive cost of the monocrystalline  $\text{GaAs}$  substrate.
- 3) Hybrid Photovoltaic Cells: A hybrid photovoltaic cell includes layers of materials from various technologies. HIT (Heterojunction with Intrinsic Thin- layer). The most common consists of two layers of amorphous silicon (one at the top and one at the bottom) while between them there is a layer of monocrystalline silicon. The significant advantage of this technology is the high degree of efficiency of the panel, which reaches 17.2% in commercial applications. This means that a smaller surface area is required to achieve the same installed power compared to other photovoltaic systems.

### **2.1.1 Equivalent Circuit:**

The equivalent circuit of a photovoltaic cell is a simplified electrical circuit, which is used to describe the function of the cell during the

exposure to solar radiation. This circuit helps to calculate the electrical efficiency of the photovoltaic cell and to predict its behavior during its operation.

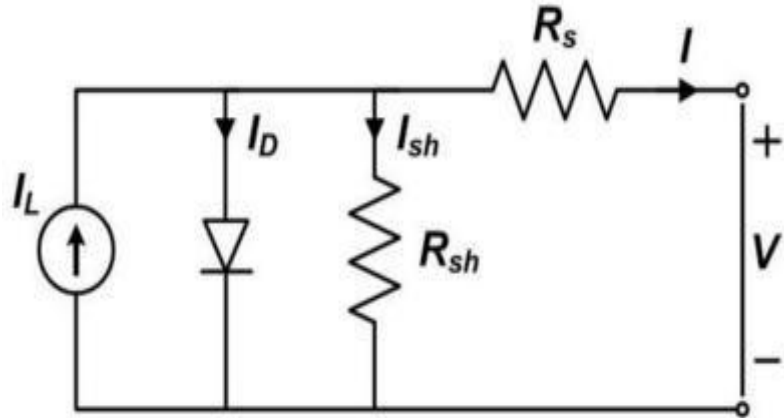


Figure 13. Equivalent Photovoltaic Circuit

The basic equation that describes the cell is:

$$I = IL - I_0 * \left( e \frac{qV}{kT} - 1 \right)$$

In the above type,  $I_0$  is the current of the diode and  $IL$  is the light current, i.e. the current that is responsible for the incident radiation received by the solar cell. The types of calculation of these quantities are:

$$I_0 = A_{Cell} * \left( \frac{q * De * ni^2}{L * e * NA} + \frac{q * Dh * ni^2}{L * h * ND} \right)$$

$$IL = q * A * G * (Le + W + Lh)$$

Where:

- q: The electron charge)
- T: The absolute temperature of the cell
- k: The Boltzmann constant ( $1.38 \times 10^{-23}$  J/K)
- $A_{Cell}$ : The cross-section of the cell
- V: The voltage at the exit of the cell
- $Le$ : The electron diffusion length =  $\sqrt{De * \tau_e}$
- $Lh$ : The hole diffusion length =  $\sqrt{Dh * \tau_h}$
- $\tau_e, \tau_h$ : The lifetime of electrons (holes) as minority carriers
- W: The Scope of Contact (Depletion Region)
- G: The Rate of Production for Solar Radiation

The basic equation of the solar cell is the Shockley-Queisser equation, which describes the function of a solar cell as a p-n diode. This equation is a good approximation of the actual behavior of the solar cell, but it is not accurate in all cases.

Experimental observations have shown that the basic equation of the solar cell does not accurately reflect the actual I-V characteristic curve of a cell for practical purposes. This is because it does not take into account certain factors that affect the actual behavior of the solar cell, such as:

- The outer short circuit: The basic equation of the solar cell assumes that the outer circuit is open. In fact, the outer circuit is usually attached to a charge, which affects the I-V curve of the solar cell.
- Losses in the outer circuit: Losses in the outer circuit, such as resistance losses and capacitance losses, also affect the I-V curve of the solar cell.
- Internal losses: Internal losses, such as losses due to the liquefaction of photovoltaic voltage (the photovoltaic voltage begins to decrease as the current intensity increases) and losses due to thermal flow, also affect the I-V curve of the solar cell.

To improve the accuracy of the solar cell's basic equation, the researchers have introduced three additional parameters:

- $R_s$ : The in-line resistance of the cell represents the resistance encountered by carriers during their flow within the cell. This resistance comes from various sources, such as the resistance of the main semiconductor, the resistance of the surface layer, and the resistance of the atomic contact (the area where two different materials, such as the semiconductor and the metal electrode of the photovoltaic cell) meet.
- $R_{sh}$ : The parallel resistance of the cell represents the resistance encountered by the vectors that leak the cell. This resistance comes from various sources, such as the reconnection of carriers to the contact area, the leakage of carriers to the outer surface of the cell, and the leakage of carriers into crystal abnormalities.
- $A$ : The constant  $A$  represents the reconnection phenomena that occur in the contact area. The value of  $A$  ranges between 1 and 2, depending on the type of material from which the cell is made and its operating conditions.

Based on the above, the final formula emerges:

$$I = I_L - I_0 * \left( e^{-\frac{q(V+I*R_s)}{A*kT}} - 1 \right) - \frac{V}{R_{sh}}$$

The I-V, P-V characteristic curves at the output of a cell are represented as follows :

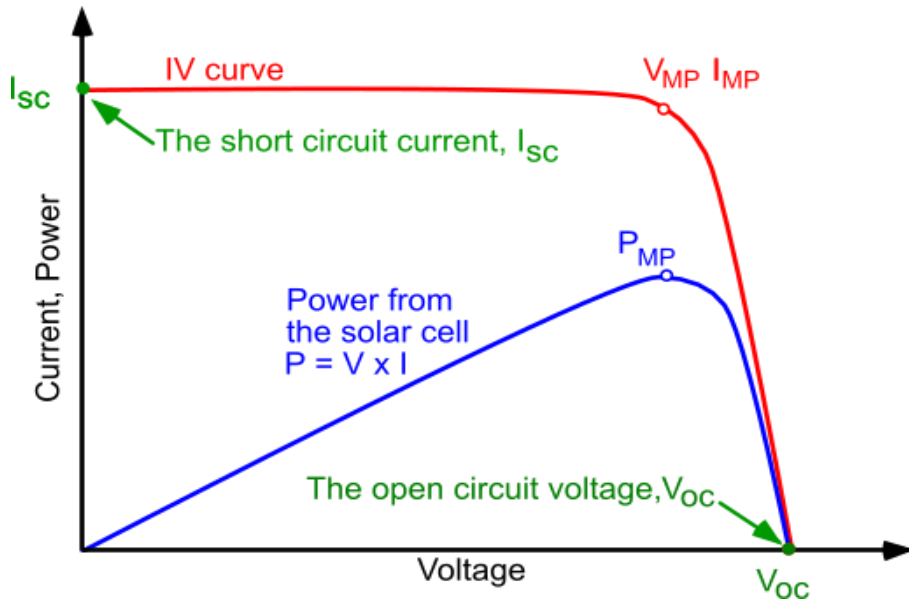


Figure 14.P-V and I-V Photovoltaic Characteristics

- Open Circuit Voltage (VOC ): Open circuit voltage is the voltage generated by a photovoltaic panel when no current is drawn from it. Under ideal conditions, it is relatively stable under varying brightness. However, As the temperature increases, the cell voltage at the open circuit point decreases.
- Short Circuit Current (ISC): Short circuit current is the maximum current generated by a photovoltaic panel when its terminals are short-circuited. Under ideal conditions, it is also relatively stable under Changing brightness. However, as the temperature rises, the short-circuit current increases.
- Maximum Power Voltage (VMP): The maximum power voltage is the voltage at which a photovoltaic panel produces the maximum electrical power. This voltage is less than the open circuit voltage and greater than the short-circuit voltage.
- Maximum Power Current (IMP): Maximum power current is the current at which a photovoltaic panel produces the maximum electrical power. This current is less than the short-circuit current and greater than zero.
- Maximum Output Power Point (PMP ): The maximum output power point is the point at which the power-voltage curve of a photovoltaic panel reaches its maximum. This point corresponds to the maximum power voltage and the maximum power current.

### 2.1.2 Photovoltaic Efficiency:

The I-V curve of a solar cell depends on two main factors: the intensity of the incident radiation and the temperature. As the intensity of the incident radiation increases, so does the number of photons absorbed by the

This leads to an increase in the number of carriers in motion, i.e. current. The Voc voltage also decreases slightly, as the intensity of the incident radiation increases. When the temperature of the solar cell increases, the mobility of the carriers in motion increases. This leads to an increase in the Isc current and the Voc voltage. It also increases slightly as the temperature of the solar cell increases. The fast response of the I-V curve to the intensity of incident radiation makes the solar cells suitable for applications where the power supply needs to be quickly adapted to changing radiation conditions.

The degree of efficiency of a photovoltaic cell is defined as the ratio of the maximum electrical power PMP produced by the cell to the product of the cell surface A and the radiation intensity G. The formula for calculating the degree of efficiency is as follows:

$$n = \frac{P_M}{\frac{P_i}{n}} = \frac{V_{MP} * I_{MP}}{A * G}$$

- n is the degree of performance
- PMP is the maximum electrical power
- A is the surface area of the photovoltaic cell
- G is the radiation intensity

The radiation intensity G is expressed in watts per square meter (W/m<sup>2</sup>). The maximum electrical power is expressed in watts (W). The surface area of the photovoltaic cell A is expressed in square meters (m<sup>2</sup>).

The efficiency rating of commercial solar cells is in the range of 14% to 20%. The highest degrees of efficiency are achieved by using specialized technologies, such as the use of materials with a low energy gap, the use of anti-reflection layers, and the use of solar radiation concentration technologies. However, these technologies are more expensive than conventional technologies, resulting in an increase in the cost of a solar cell. It is worth noting that the degree of efficiency of a photovoltaic element is not stable and is changed by various factors, such as:

#### ***External factors:***

- Solar radiation intensity
- Temperature

- Shading
- Reflection
- Resistance

***Internal factors:***

- The Construction Material
- The build quality of the item
- His age

It is worth mentioning the Hot Spot phenomenon, since this particular scenario will play an important role in this thesis.

***Hot Spot:***

The hotspot effect is a major problem that can occur in photovoltaic systems. It is due to the existence of one or more photovoltaic (PV) elements that produce lower current (due to shading, material failure, opposite polarity, etc.) than the other elements that are connected in series. This results in an increase in the voltage in these elements, resulting in their overheating. The most common causes that cause the hotspot effect are the following:

- Shading: Shading one or more PV elements can lead to a decrease in power generation from them. This is because the shadow reduces the amount of light that reaches the specific elements and therefore the current.
- Hardware failure: Hardware failure, such as a crack in a PV element, can also lead to a decrease in current output from that element.
- Reverse polarity: Reverse polarity occurs when the two electrodes of a PV element are connected in opposite directions. This can happen during the installation or maintenance of the photovoltaic system.

The hotspot effect can have serious effects on photovoltaic systems. The most important are the following:

- Reducing system efficiency: The hotspot effect can lead to a decrease in the efficiency of the photovoltaic system by 10% or more.

- Damage to PV elements: Overheating of PV elements can cause damage to them, resulting in a shortened service life.
- Fire: In extreme cases, the hotspot effect can even lead to a fire.

For the above reasons, it is therefore necessary to take measures to prevent and deal with the Hot Spot phenomenon. The most effective methods are:

- Scheduled maintenance: Scheduled maintenance of the PV system can help detect and troubleshoot problems that may be causing the hotspot phenomenon in a timely manner.
- Use of special components: There are special devices that can help deal with the hotspot effect, such as voltage balancing resistors.
- Changing the layout of PV elements: In some cases, changing the layout of PV elements can help avoid the hotspot effect.

## ***2.2 Algorithms Find Maximum Point Power (MPPT Algorithms) :***

MPPT (Maximum Power Point Tracking) methods are used to monitor and search for the maximum power point (MPP) of a photovoltaic panel. The MPP is the operating point of the panel where the maximum power is generated and therefore the PV system works optimally.

MPPT methods are divided into three main categories:

1. Direct MPPT Methods
2. Indirect MPPT Methods
3. MPPT Methods Using Artificial Intelligence

### ***Direct MPPT Methods:***

Direct MPPT methods detect MPP by directly studying the power curve (P-V) of the photovoltaic panel. The power curve is a graph of the power output of the panel versus the voltage of the panel. The MPP is the point on the curve where the power is maximum. Direct MPPT methods are usually more accurate than indirect methods, but also slower. That's because they have to look at the entire

power curve to find the MPP. Some of the most well-known direct MPPT methods are:

- Perturb and Observe: This method starts with an initial voltage value and then increases or decreases the voltage until the MPP is found. As we mentioned in a previous section, in this thesis we changed the reference current of the internal control loop instead of the voltage.
- Sequential Search: This method tests a range of possible trend values until it finds the MPP.
- Divide-and-Conquer: This method splits the power curve into smaller segments, then uses a direct MPPT method to find the MPP in each segment.

#### *Indirect MPPT methods:*

Indirect MPPT methods detect MPP using a parameter that is bound to MPP. For example, the open-circuit voltage ( $V_{oc}$ ) and short-circuit current ( $I_{sc}$ ) of the photovoltaic panel are connected to the MPP. They are usually faster than direct methods, but also less accurate. That's because they don't have to look at the entire power curve to find the MPP.

- P&O with Exponential Smoothing: This method is a variation of the ascent method that uses an exponential smoothing to improve accuracy.
- P&O with Pulse Width Modulation: This method uses the duty cycle as a variable to control the voltage of the photovoltaic panel.

#### *AI-powered MPPT methods:*

Artificial Intelligence (AI) MPPT methods use machine learning and artificial intelligence techniques to detect the MPP of a photovoltaic panel. These methods have the potential to learn and adapt to changing

operating conditions of the photovoltaic panel, offering greater accuracy and speed than traditional MPPT methods.

There are several types of AI-powered MPPT methods that have been developed, some of the most well-known are:

- Neural network-based methods: Neural networks are a form of machine learning that mimics the functioning of the human brain. Neural networks can be used to train a model that can predict the output power of a photovoltaic panel for a given voltage.

- Machine learning-based methods: Machine learning is a broader field of artificial intelligence that includes various techniques, such as classification, irregularity detection, and prediction. Machine learning techniques can be used to develop models that can detect the MPP of a photovoltaic panel.

AI-powered MPPT methods are still under development, but they have the potential to change the way photovoltaic systems are designed and manufactured. These methods have the potential to improve the efficiency of photovoltaic systems, reduce their costs and make them more reliable.

Some specific advantages of MPPT methods with AI are as follows:

- They can be adapted to changing operating conditions, such as temperature, solar radiation intensity, and shading.
- They are more accurate than traditional MPPT methods, resulting in greater output power.
- They can be used to create simpler and more cost-effective MPPT systems.

The disadvantages of MPPT methods with AI are as follows:

- They are more complex than traditional MPPT methods and require more training time.
- They may be more susceptible to data errors.

Overall, AI-powered MPPT methods have the potential to offer significant advantages over traditional MPPT methods. However, they are still under development and further research is needed to improve their reliability and performance.

### **2.2.1 Perturb and Observe algorithm:**

The Perturb and Observe (P&O) algorithm is an MPPT method used to monitor and search for the maximum power point (MPP) of a photovoltaic panel. It is a simple algorithm that is subsidized by its ease of implementation and efficiency in a variety of operating conditions. The algorithm works by observing the power response of the photovoltaic system when small perturbations occur in voltage or current. If the

Conversely, if the response shows a decrease in power, the algorithm changes the disturbance in the opposite direction.

The P&O algorithm works in the following way:

1. Initially, the algorithm starts with an initial trend value.
2. The algorithm then increases or decreases the voltage by a small amount.
3. The algorithm calculates the output power of the photovoltaic panel for the new voltage.
4. If the output power is greater than the output power in the previous voltage, then the algorithm increases the voltage. Otherwise, the algorithm decreases the voltage.
5. The algorithm keeps repeating these steps until the MPP is found.

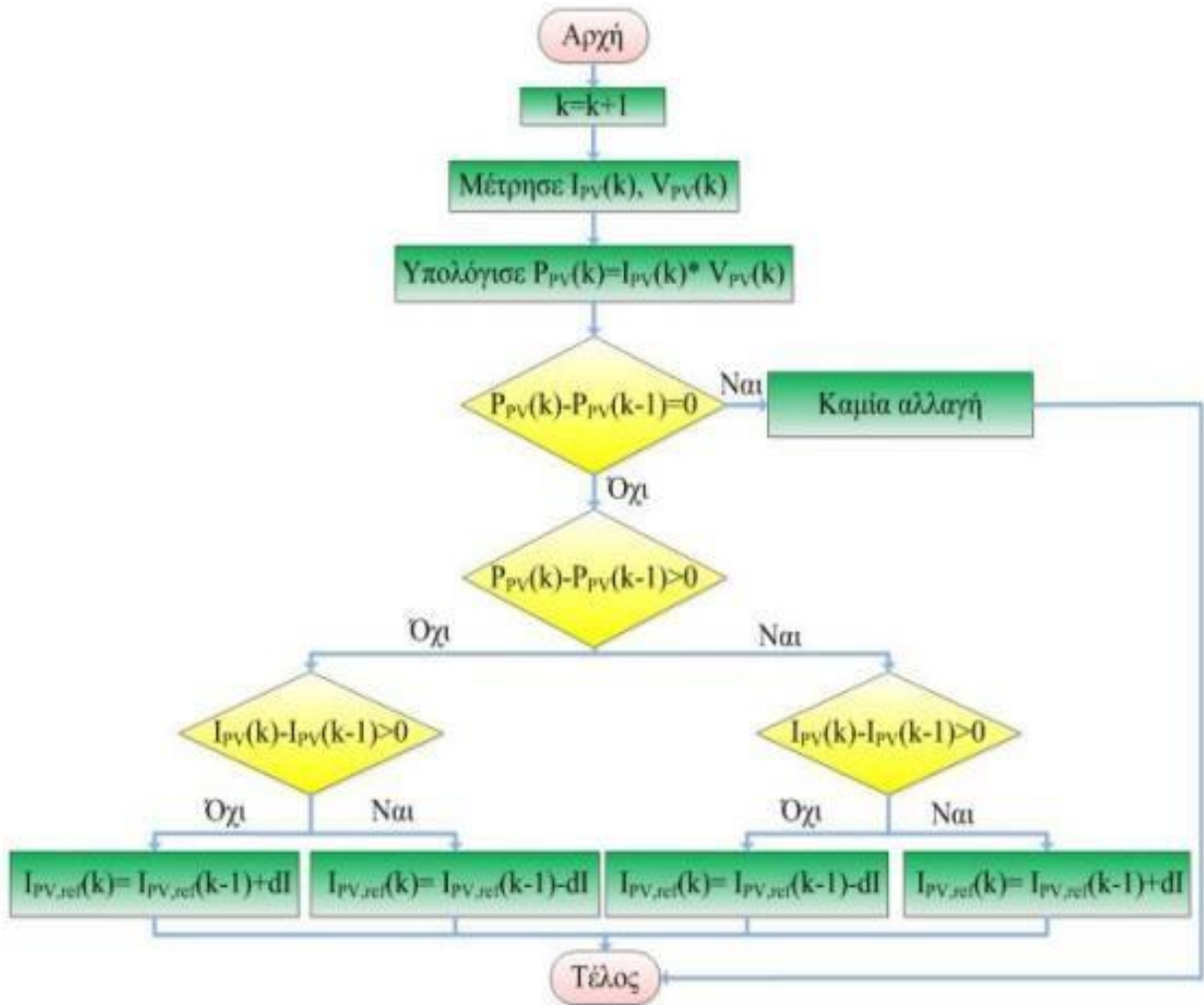


Figure 15.Perturb and Observe Flow Chart

In our case, as we have already mentioned, we used a modified form of Perturb and Observe as shown in the above figure. More specifically, the change we make when a difference in power is observed is in the desired reference current and not in the voltage. This is how the following algorithm written in MATLAB was derived:

```

function iref = P_and_O(Vpv, Ipv)
persistent Vold Pold iref_old Ipv_old;
if isempty(Vold) % Initialize Vold, Pold, and iref_old with isempty
    Vold = 0;
    Pold = 0;
    iref_old =0;
    Ipv_old=0;
end
P = Vpv * Ipv;
dP = P - Pold;
dVpv = Vpv -
Vold; dI = Ipv -
Ipv_old; d = 0.02;
if dP ~= 0
    if dP > 0
        if dI > 0
            iref = iref_old + d; % Change iref directly inside the if loop
        else
            iref = iref_old - d;
        end
    else
        if dI > 0
            iref = iref_old - d; % Change iref directly inside the if loop
        else
            iref = iref_old + d;
        end
    end
else
    iref = iref_old;
end
Vold = Vpv;
Pold = P;
iref_old = iref;
Ipv_old=Ipv;
end

```

## 2.2.2 Particle Swarm Optimization Algorithm :

The particle flock optimization algorithm (PSO) is a simulation algorithm designed to mimic the behavior of flocks of birds during the search for food. It has proven effective in solving many optimization problems, including peak power point (MPP) detection problems in photovoltaic systems. It starts with an initial particle flock, where each particle represents a potential solution to the problem. Each particle has two components: its position and its velocity. The position of the particle represents the value of the parameter being improved, while the speed of the particle represents the tendency to change the parameter.

At each step of the algorithm, each particle calculates its distance from the best particle it has found so far, as well as its distance from the position of the world's best particle. The particles then adjust their velocities based on these distances and the positions of their best neighbors.

Adjusting the velocity of each particle is determined by a mathematical function that takes into account the behavior of the cluster as a whole. The algorithm continues to repeat these steps until a solution is found that meets the accepted criteria.

It has been successfully used to solve peak power point (MPP) detection problems in photovoltaic systems and has been shown to be able to detect MPP more accurately than traditional MPPT methods, such as the Perturb and Observe (P&O) algorithm. Some of the advantages and disadvantages it presents are the following:

Advantages of PSO algorithm:

- It is a flexible algorithm that can be adapted to various operating conditions of photovoltaic systems.
- It is efficient and can detect MPP accurately.
- It can be run quickly and easily on software.

Disadvantages of the PSO algorithm:

- It may be susceptible to measurement errors.
- May need more time to detect the MPP in changing operating conditions.

The PSO is mathematically represented as follows:

Let  $x_i(t)$  be the position of the i-th member of the cluster at time t, and  $v_i(t)$  its velocity. Each member attempts to find the optimal point  $p_i$  to which it has reached so far, as well as the general optimal point  $g$  that has been detected by the whole cluster. The position is updated as follows:

$$x_i(t+1) = x_i(t) + v_i(t+1)$$

And the speed is updated as follows:

$$v_i(t+1) = w \cdot v_i(t) + c_1 \cdot r_1 \cdot (p_i - x_i(t)) + c_2 \cdot r_2 \cdot (g - x_i(t))$$

The parameters  $w$ ,  $c_1$ ,  $c_2$  are important as they affect how the members of the cluster inform their position and velocity.  $w$  is the inertia weight that determines the effect of the previous velocity.  $c_1$ ,  $c_2$  are the acceleration constants that divide the effects of the local and general optimal position. The random numbers  $r_1$ ,  $R_2$  are used to randomize the update, while  $p_i$  is the member's current local optimal position and  $g$  is the overall optimal position in the cluster as a whole. The iterations continue until some termination criterion is reached, such as the desired number of repetitions or the achievement of a satisfactory value of the cost function.

The general PSO structural diagram for finding MPP is as follows:

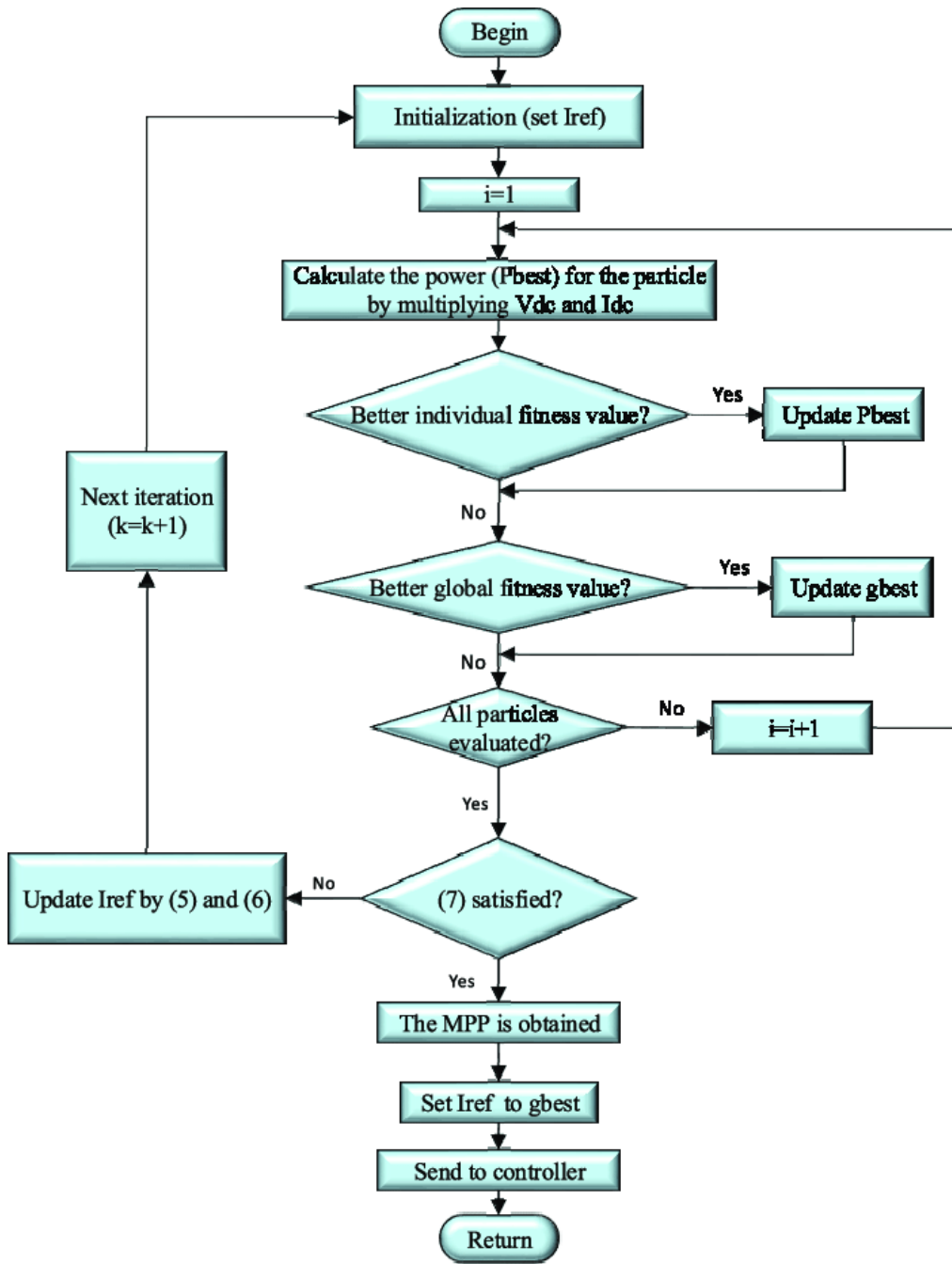


Figure 16. Particle Swarm Optimization Flowchart

Using the above we developed the following code in MATLAB and which we used in this thesis:

```

function I_pso = PSO(Vpv,Ipv,Ppv,n,Isc,Control)

persistent u; % current particle
persistent Icurrent; % current I
persistent p; % power
persistent pbest;
persistent I; % current
persistent v; % velocity (delta I)
persistent counter;
  
```

```

persistent gbest;
if Control==1
    L_pso=37;
    counter = 0;
    Icurrent = 0.7*Isc;
    gbest = Icurrent;
    p = zeros(n,1);
    for j = 1:n
        p(j) = -100000000;
    end
    v = zeros(n,1);
    pbest = zeros(n,1);
    u = 0;
    I = zeros(n, 1);
    for j = 1:n
        I(j) = 15 + rand() * (Isc - 15); % Generate a random value between 20 and Isc
    end
    return
else
    if isempty(counter)
        counter = 0;
    end

    if isempty(Icurrent)
        Icurrent = 0.7*Isc;
    end

    if isempty(gbest)
        gbest = Icurrent;
    end

    if isempty(p)
        p = zeros(n,1);
        for j = 1:n
            p(j) = -100000000;
        end
    end

    if isempty(v)
        v = zeros(n,1);
    end

    if isempty(pbest)
        pbest = zeros(n,1);
    end

    if isempty(u)
        u = 0;
    end

    if isempty(I)
        I = zeros(n, 1);
        for j = 1:n
            I(j) = 15 + rand() * (Isc - 15); % Generate a random value between 20 and Isc
        end
    end

% if (counter >= 1 && counter < 500)
%     L_pso = Icurrent;
%     counter = counter + 1;

```

```

%      return;
% end

counter = 0;

if (u >= 1 && u <= n)
    p(u)
    if ((Ppv) > p(u))
        p(u) = Ppv;
        pbest(u) = Icurrent
    end
end

u = u + 1;

if u == (n+2)
    u = 1;
end

if (u >= 1 && u <= n)
    L_pso = I(u);
    Icurrent = L_pso;
    counter = 1;
    return;
elseif u == (n+1)
    [m,i] = max(p);
    pbest
    gbest = pbest(i)
    L_pso = gbest;
    Icurrent = L_pso;
    counter = 1;
    for j = 1:n
        v(j) = updatevelocity(v(j), pbest(j), I(j), gbest);
        I(j) = updateI(I(j), v(j));
    end
    v
    I
    return
else
    L_pso = 30;
end
end
end

function vfinal = updatevelocity(vel, pobest, I, gwbest)

w = 0.9;
c1 = 1;
c2 = 1;

vfinal = w*vel + c1*(pobest-I) + c2*(gwbest-I);

end

function Ifinal = updateI(I, vel)

```

Ifinal = I + vel;

End

### 2.3.1 Photovoltaic Array Losses:

In photovoltaic systems, the dc/dc power converter (Boost) is the main power interconnection instrument. It usually operates in continuous conductivity (CCM) mode, due to the high currents that leak through the photovoltaic panels, which means that the inverter current is never reduced to zero. The Boost power converter can operate in two circuit conditions: when the transistor is open and when the transistor is closed. conditions are independent of each other and can be analyzed separately.

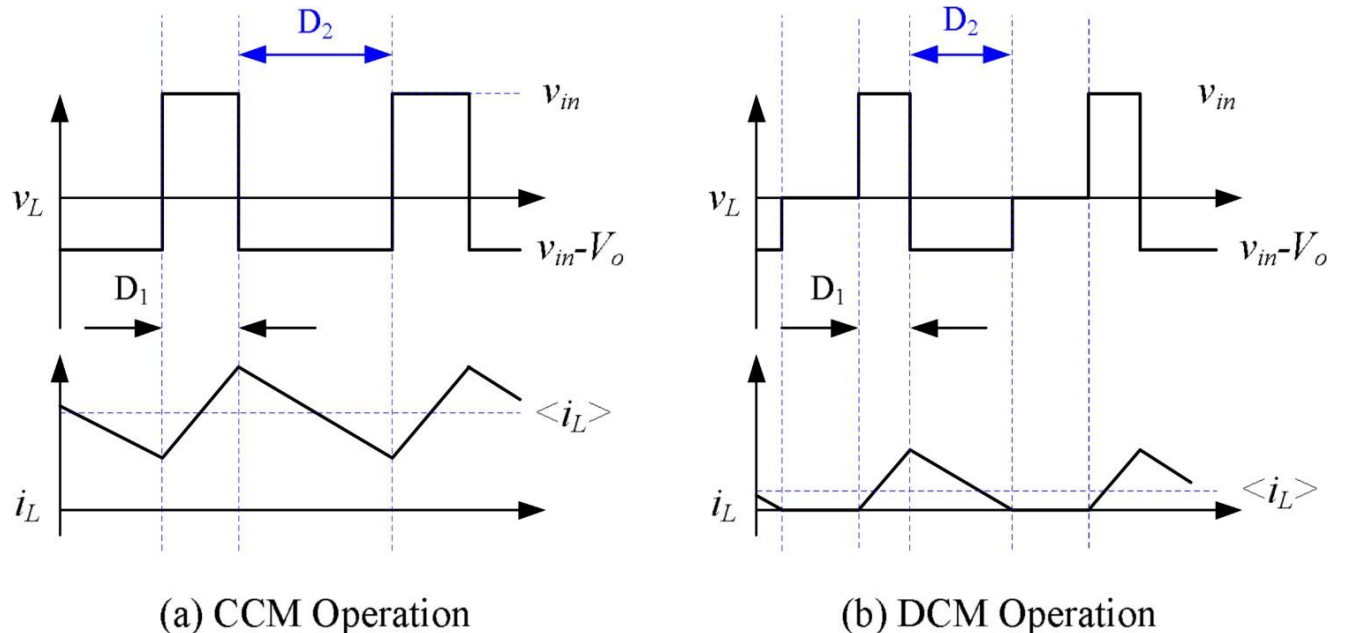


Figure 17. Continuous-Discontinuous Operation Boost Converter

For simplification, the accumulated resistance due to the wires can be considered as part of the induction resistance of the Boost inverter. In addition, the equivalent circuit of the transistor with forward polarity can be considered as a small resistor, while the diode can be replaced by a resistor accompanied by a voltage drop of close to 0.7 Volts.

The duty cycle, denoted by d, represents the period of time during which the transistor is active, i.e. conducts, divided by the period T. Correspondingly, the diode operates for the rest of the period, i.e. for (1-d)T, where T is the period of the waveform and results from the inverse of the frequency transistor opening/closing using pulse (PWM). The frequency of the PWM signal is selected depending on the application.

When the transistor is active, the current of the photovoltaic collector flows through the semiconductor, avoiding the branch of the diode. In this case, the induction current increases at a rate equal to:

$$\frac{VPV - IPV_{,tr}(Rtr_{,on} + Req)}{LH}$$

As the input of the Boost comes from the voltage of the photovoltaic panels, the calculation of the coil current is easy, as the resulting circuit is a classic R-L. The equation describing the corresponding current is listed below.

$$IPV_{,tr} = \frac{1}{LH} \int_0^D (VPV - IPV_{,tr}(Rtr_{,on} + Req)) dt$$

Where VPV is simultaneously the output voltage of the PV and the input voltage of the Boost inverter, IPV<sub>,tr</sub> corresponds to the current leaking the transistor, Req is the equivalent resistance of the wiring harness and coil, and finally  $\frac{d}{T}$ . It is equal to the duty cycle  $d$ .

The above relationship is a common first-degree differential equation similar to that of a conventional R-L circuit, and the analytical solution can be easily calculated.

When the transistor is in the shutdown state, the current from the PV passes through the diode and enters the capacitor at the output. Unlike the previous case, now the coil current will decrease to the initial value of the previous stage to increase the output voltage. The reduced current will have a slope equal to:

$$\frac{VPV - IPV_{,di}(Rdi_{,on} + Req) - Vdi_{,on} - Vout}{LH}$$

In the same way, the final circuit can be considered as a conventional R-L ending On Following Equations:

$$IPV_{,di} = \frac{1}{LH} \int_D^T (VPV - IPV_{,di}(Rdi_{,on} + Req) - Vdi_{,on} - Vout) dt$$

Where IPV<sub>,di</sub> is the current flowing from the diode when the transistor is not conducting, V<sub>di, on</sub> is the voltage of the diode and V<sub>out</sub> is the voltage at the output the Boost. To simplify the calculation, the current will be considered stable and equal to the average value of the photovoltaic. In practice, the root of the inverter's average square value of current is about 0.5% larger than that of photovoltaics. To calculate the actual power generated by the photovoltaic system, we will use the average power equation. Since the incoming current and voltage are fixed values, the final power equation will be:

$$PPV = \frac{1}{T} \int_0^T (VPV \cdot IPV) dt = \frac{1}{T} (VPV \cdot IPV) T = (VPV \cdot IPV)$$

For the calculation of induction losses, we have:

$$P_{Loss,con} \stackrel{1}{=} \frac{1}{T} \int_0^T V_{con} I_{PV,tr} dt$$

Applying Ohm's law to this equation, it follows:

$$P_{Loss,con} = R_{tr, on} \frac{1}{T} \int_0^T I_{PV,tr}^2 dt = R_{tr, on} I_{PV,tr} \cdot RMS$$

$$\text{Where } I_{PV,tr,RMS} = \sqrt{\frac{1}{T} \int_0^T I_{PV,tr}^2 dt} = I_{PV} \sqrt{d}$$

Based on the above, it therefore follows that the losses of the transistor and the diode are :

$$P_{Loss,con} = R_{tr, on} I_{2} d \quad P_{Loss,con,di} = R_{di, on} I_{2} (1 - d)$$

Now, calculating the heat loss due to the resistances of the cables connecting the PV to the conversion amplifier is simple. This is mainly due to the fact that the coil operates under CCM and therefore there is always a current flowing through the same coil and its corresponding resistance. Therefore, following the same steps taken previously, the losses can be found to be:

$$P_{Loss,cables} = R_{cable} I_{PV}^2$$

We also need to calculate the loss that occurs during the correct polarization of the diode where there is a voltage drop. The voltage drop of the diode occurs only when it is anterior polarization, and this only occurs when current flows through the diode. In order to do this,  $V_{di, on}$  should not be considered constant, but the duration of the corresponding signal is equal to that of  $I_{PV, di}$   $1-d$ , resulting in the following expression:

$$P_{Loss,fw} = \frac{1}{T} \int_0^T V_{di, on} I_{PV, di} dt = (1 - d) V_{di, on} I_{PV}$$

Losses can also be attributed to the interruptive nature of semiconductors. There are many ways to reduce them, but minimizing through current regulation has little effect in terms of optimization.

Transistors are semiconductors that are considered to do the reverse conduction, that is, if the input voltage is high, their output will be low. Changing the state of a transistor cannot be carried out instantaneously, due to the fact that capacitive elements are inserted between the input and output. Therefore, when the transistor input is high, a certain amount of time must pass for the capacitors to be fully charged and their output voltage to change, resulting in the transistor being activated. For this purpose, the power from the input voltage source at the Gate is injected into the transistor. The same applies when the transistor is about to be turned off, but in this case it is a matter of discharging the capacitors. The power that needs to be injected into the transistor gate is considered not to be significantly affected by the current flowing into the transistor. Consequently, the input voltage losses of the

transistors will not be included in this analysis. An accurate approximation of intermittent losses is as follows:

$$PSW = V_{PV} I_{fsw} \frac{QGS + QGD}{G}$$

Where  $fsw$  is the switching frequency,  $IG$  is the current at the transistor gate and  $QGS + QGD$  are the time frames needed for the capacitive elements in the portal and the source for to Charge.

Summing up all of the above, the final formula of power results as follows:

$$P_{true} = P_{PV} - P_{Loss,con} - P_{Loss,con.di} - P_{Loss,cables} - P_{Loss,fw} - PSW$$

It is clearly observed that system losses not only affect the P-V curve under normal shading conditions, but also under partial shading. Depending on the interconnection of the PV panel cells, the shape of the P-V curve changes significantly, especially under partial shading conditions. If the power function corrections are incorporated into the previous power equation used, then an increase in the output power by 5% can be expected. In particular, due to the existence of many local MPPs under partial shading conditions, this correction could prove crucial when selecting the Global MPP.

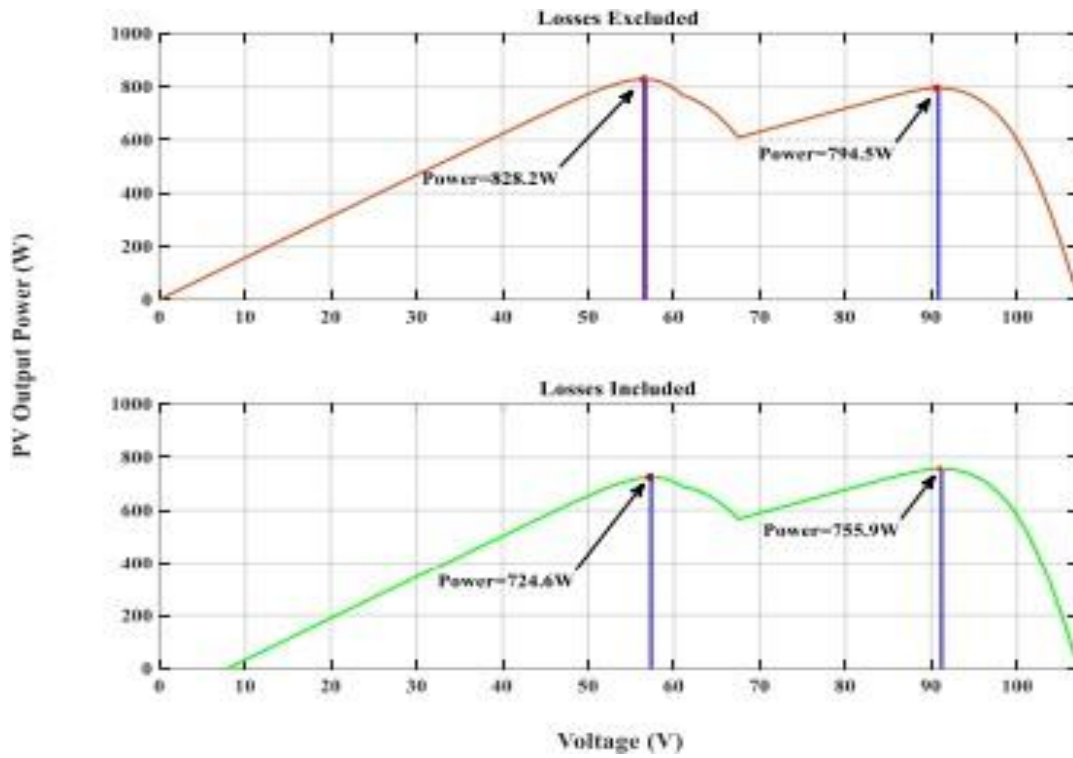


Figure 18. Global Maximum Power Point Shift

This is exactly what the above images show, where, in the first scenario, the calculation of Power does not take into account the losses mentioned above, unlike in the second. It is therefore observed that the addition of losses can be decisive

and bring about a shift in the Global MPP. This is exactly the scenario that we have invoked in this diploma thesis, proving the importance of correcting the formulas for calculating Power. This change is mainly due to large currents that are created and consequently Large Losses because of Heat. It is very important to

mention that the change in the type of Power can be proved problematic for the use of heuristic algorithms. This is because such Algorithms such as Perturb and Observe are based on the instantaneous response of the system and its derivative. Thus, an inaccuracy in the measurement could cause the controllers to function incorrectly. The measurement of instantaneous power at the output, due to variability in the state of the inverter, will result in an intermittent current waveform. Therefore, for a valid calculation of the power, It is necessary to use the RMS value of the electricity, which, however, as is expected adds higher harmonics and oscillations to the system. One solution would be to use filters and curve smoothing equipment, but this would result in a dramatic increase in costs. So a new solution emerges, which instead of maximizing  $P_{pv}$ , maximizes the  $P_{true}$  mentioned above. There is no longer a need for separate power measurements since a P-V curve that includes losses and has no harmonics is easy to construct. Simplifying the power equation and preserving its most important parts, i.e. the losses of transistors, diodes and cables, we end up with the final formula:

$$P_{MPP} = P_{PV} - [R_{tr,ond} + R_{req} + R_{di,on}(1 - d)]I^2$$

Therefore, we conclude that based on the more detailed and accurate power ratio, it is more efficient and correct to use metaheuristic algorithms instead of heuristics as they find the Global MPP more efficient.

### 2.3.2 Modified P&O and PSO:

Based on what we reported above, we converted the Perturb and Observe and Particle Swarm Optimization algorithms, so that there is a better approach to Global Maximum Power Point. This, as it is understood, was achieved by modifying the formula for calculating Power. Thus, the new algorithms are as follows:

#### Perturb and Observe:

```

function iref = P_and_O(Vpv,Ipv)
    persistent Vold Pold iref_old Ipv_old;
    if isempty(Vold) % Initialize Vold, Pold, and iref_old with isempty
        Vold = 0;
        Pold = 0;
        iref_old = 0;
        Ipv_old = 0;
    end
    P = Vpv * Ipv - (0.001 * d + 1 + 0.001 * (1 - d)) * Ipv * Ipv;
    dP = P - Pold;
    dVpv = Vpv - Vold;
    dI = Ipv - Ipv_old;
    d = 0.02;
    if dP ~= 0

```

```

if dP > 0
    if dI > 0
        iref = iref_old + d; % Change iref directly inside the if loop
    else
        iref = iref_old - d;
    end
else
    if dI > 0
        iref = iref_old - d; % Change iref directly inside the if loop
    else
        iref = iref_old + d;
    end
end
else
    iref = iref_old;
end
Vold = Vpv;
Pold = P;
iref_old = iref;
Ipv_old=Ipv;
end

```

### Particle Swarm Optimization:

Essentially, in the PSO Block the power value was entered as input, so we didn't have to change anything in the body of the code, but we calculated the correct power value with blocks . This connection is as follows:

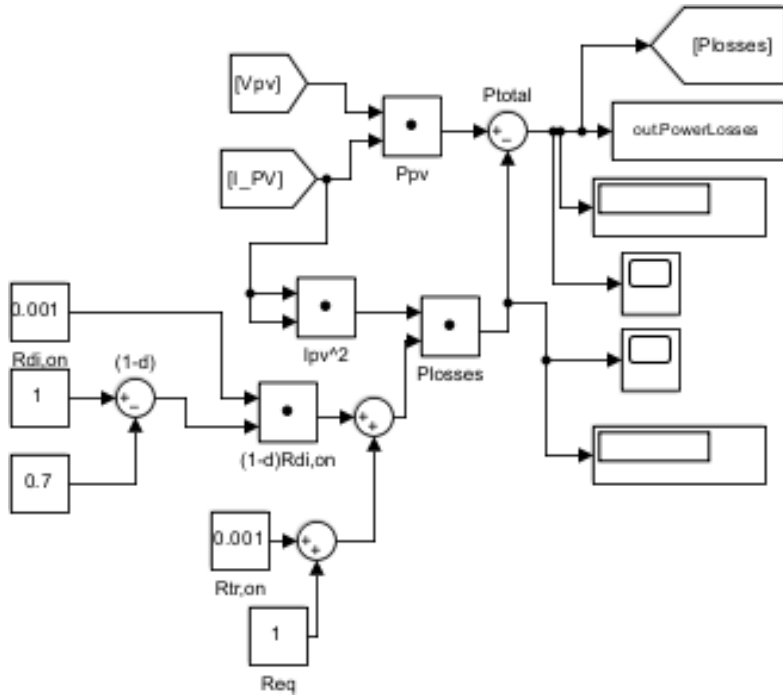


Figure 19. Calculation of Actual Power

An important role is also played by the speed of response of the control system, which is affected by the selection of the algorithm, the settings of the parameters and the processing time of the system. Also, the existence of harmonics can affect the accuracy of the Maximum Power Point Tracker algorithms. A solution to this problem is provided by the integration of filters to remove them. The selection of the filter must be done carefully as it affects the speed and accuracy system and a wrong approach could have the opposite of the desired results.

## CHAPTER 3: Modeling

### 3.1 Import:

In this chapter we will deal with the extensive analysis and extraction of mathematical models for the systems that make up our microgrid. More specifically, these systems are:

- 1) The photovoltaic array
- 2) Boost Conventer
- 3) Voltage Inverter ( Inventer )
- 4) DC Bus
- 5) Filter and Network

The topology we created is shown in the image below:

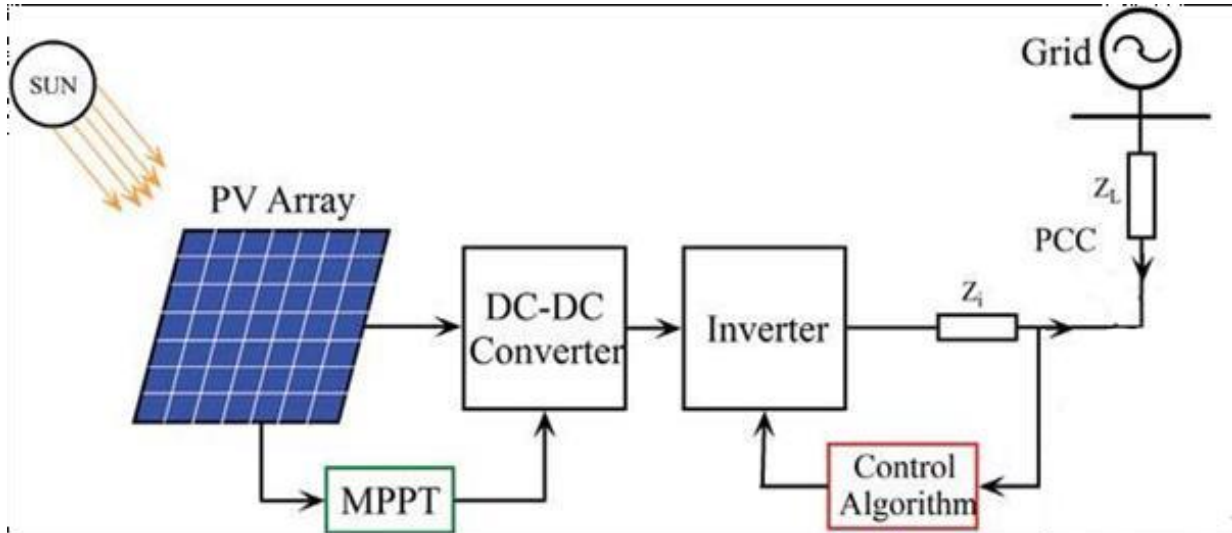


*Figure 20. System Presentation*

On the left side of the image we have the photovoltaic array which receives radiation from the sun and then is connected to the DC bus through the voltage lifting converter. From the DC bus there is a flow of power to the grid. Then passing to the side of the grid, to the right of the DC bus we have the Voltage Inverter (Inventer) and then the RL filter and finally the Grid. AC voltage and indeed of the desired amplitude and frequency, while at the same time the higher harmonic frequencies are cut off, improving the overall operation of the network. To extract the necessary models, we used a number of mathematical tools, such as the Park transform.

#### Transformation Park:

To simplify the control of certain electronic power systems with a reverser, the well-known Clarke and Park transforms are used. With them, we can convert the reactions of three-phase alternating voltages and currents from the fixed three-phase reference frame of  $120^\circ$  to a two-phase reference frame (Clarke) or even better to two rotating rectangular constant-value components (Park). The calculations in the reference frame of the three components a-b-c are complex due to the number of the three variables and their temporal change. The Clarke and Park transformations in time and in vector form are shown below.

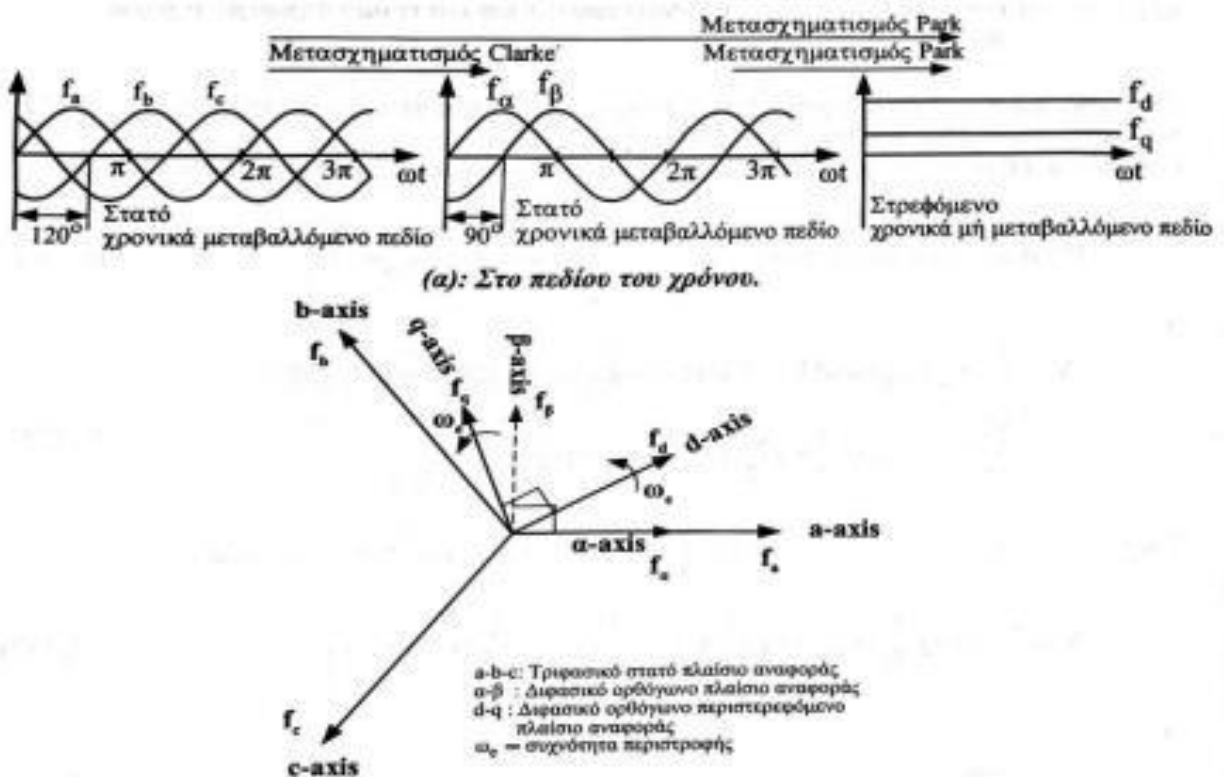


Figure 21. Graphic representation of Clarke-Park transformations

Due to the use of Sinusoidal Pulse Width Modulation for the Inventor, we will prefer Park's direct analysis. Through this transformation, we can transfer from the three-phase reference frame a-b-c to three fixed vectors d<sub>q0</sub>. These vectors rotate around the imaginary coordinate system at a speed equal to the frequency of the seminoid quantities. However, to achieve the final form of two modern rotating vectors, instead of three, the existence of a purely symmetrical sequence is required. The Park transformation is given by the following relationship:

$$\begin{bmatrix} f_d \\ f_q \\ f_0 \end{bmatrix} = \frac{2}{3} \begin{bmatrix} \cos(\omega_e * t) & \cos(\omega_e * t - 120^\circ) & \cos(\omega_e * t - 240^\circ) \\ -\sin(\omega_e * t) & -\sin(\omega_e * t - 120^\circ) & -\sin(\omega_e * t - 240^\circ) \\ \frac{1}{2} & \frac{1}{2} & \frac{1}{2} \end{bmatrix} * \begin{bmatrix} f_a \\ f_b \\ f_c \end{bmatrix}$$

And vice versa:

$$\begin{bmatrix} f_a \\ f_b \\ f_c \end{bmatrix} = \frac{2}{3} \begin{bmatrix} \cos(\omega_e * t) & -\sin(\omega_e * t) & \frac{1}{2} \\ \cos(\omega_e * t - 120^\circ) & -\sin(\omega_e * t - 120^\circ) & \frac{1}{2} \\ \cos(\omega_e * t - 240^\circ) & -\sin(\omega_e * t - 240^\circ) & \frac{1}{2} \end{bmatrix}^* \begin{bmatrix} f_d \\ f_q \\ f_0 \end{bmatrix}$$

Where  $f_0$  is the zero component and  $\omega_e$  is the rotating frequency. For a three-phase symmetric system the above relation becomes:

$$\begin{bmatrix} f_d \\ f_q \end{bmatrix} = \frac{2}{3} \begin{bmatrix} \cos(\omega_e * t) & \cos(\omega_e * t - 120^\circ) & \cos(\omega_e * t - 240^\circ) \\ -\sin(\omega_e * t) & -\sin(\omega_e * t - 120^\circ) & -\sin(\omega_e * t - 240^\circ) \end{bmatrix}^* \begin{bmatrix} f_a \\ f_b \\ f_c \end{bmatrix}$$

when:  $f_a + f_b + f_c = 0$  And also the Park transform from the a-b frame of reference to d-q is given by the following relation when again it is true that  $f_a + f_b + f_c = 0$  :

$$\begin{bmatrix} f_d \\ f_q \end{bmatrix} = \frac{2}{3} \begin{bmatrix} \cos(\omega_e * t) & \sin(\omega_e * t) \\ -\sin(\omega_e * t) & \cos(\omega_e * t) \end{bmatrix}^* \begin{bmatrix} f_\alpha \\ f_\beta \end{bmatrix}$$

and vice versa:

$$\begin{bmatrix} f_\alpha \\ f_\beta \end{bmatrix} = \frac{2}{3} \begin{bmatrix} \cos(\omega_e * t) & -\sin(\omega_e * t) \\ \sin(\omega_e * t) & \cos(\omega_e * t) \end{bmatrix}^* \begin{bmatrix} f_d \\ f_q \end{bmatrix}$$

### 3.2 AC Side:

### 3.2.1 Import:

On the side of our system, where it is characterized by alternating voltage, belongs the inverter and the representation of the electricity network. The voltage source inverter belongs to the semiconductor elements of our system and is one of the most important parts of it, as well as in modern SUVs in general. Its role, as its name suggests, is the reversal of the voltage from continuous to alternating. There are various ways to control this power converter, the most prevalent being the Sinusoidal Pulse Modulation (S.P.W.M), which we use in this thesis. We will then analyze the operation of the inverter, as shown in the image below:

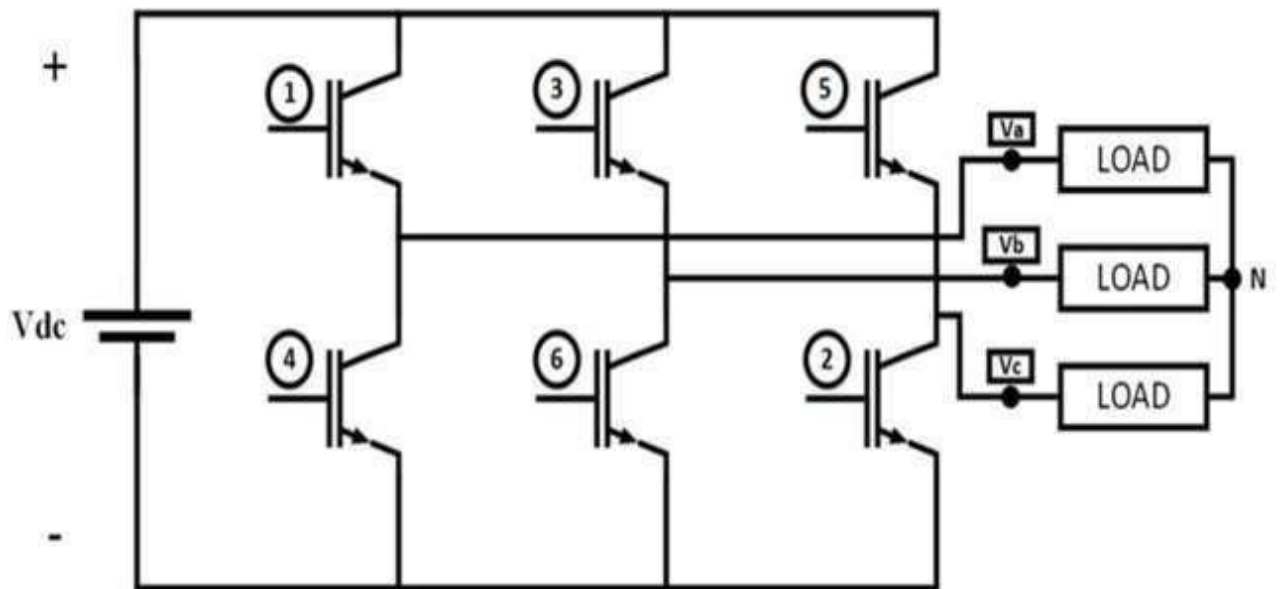


Figure 22. Three Phase Inverter

In this case, for the mathematical description of the inverter, the mean value model is used, according to which we have the following partition ratios on the d-q axes:

$$mid = \frac{V_{ld}}{v_{dc}} \quad miq = \frac{V_{lq}}{v_{dc}}$$

Where  $V_{ld}$ ,  $V_{lq}$  : the voltages on the d-q axes at the output of the inverter.

Next, we will analyze the technique of S.P.W.M. Sinusoidal pulse amplitude modulation (SPWM) is a signal shape modulation technique that is widely used in power electronics applications, such as motor control, transformers, and generators. In SPWM, a sinusoidal reference signal with amplitude

$A_R$  and frequency  $f_R$  is compared to a triangular carrier signal with AC amplitude and frequency

$fC$ . This comparison produces a pulse range with a width that is proportional to the difference between the two signals.

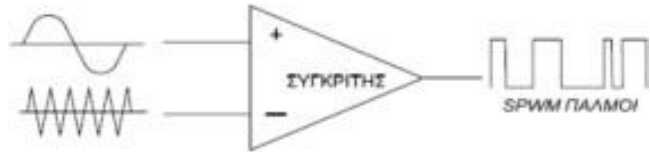


Figure 23. Creating SPWM Pulses

The operating principle of SPWM is as follows:

1. The reference signal goes through a low-frequency filter to remove its contents at high frequencies.
2. The filtered reference signal is compared to a triangular carrier signal.
3. This comparison produces a logic signal that is reasonable "1" when the reference signal is greater than the carrier signal and reasonable "0" when the reference signal is smaller than the carrier signal.
4. The logic signal goes through an amplifier to increase its power.
5. The amplified logic signal is used to turn on or off a inverter's semiconductor switches.

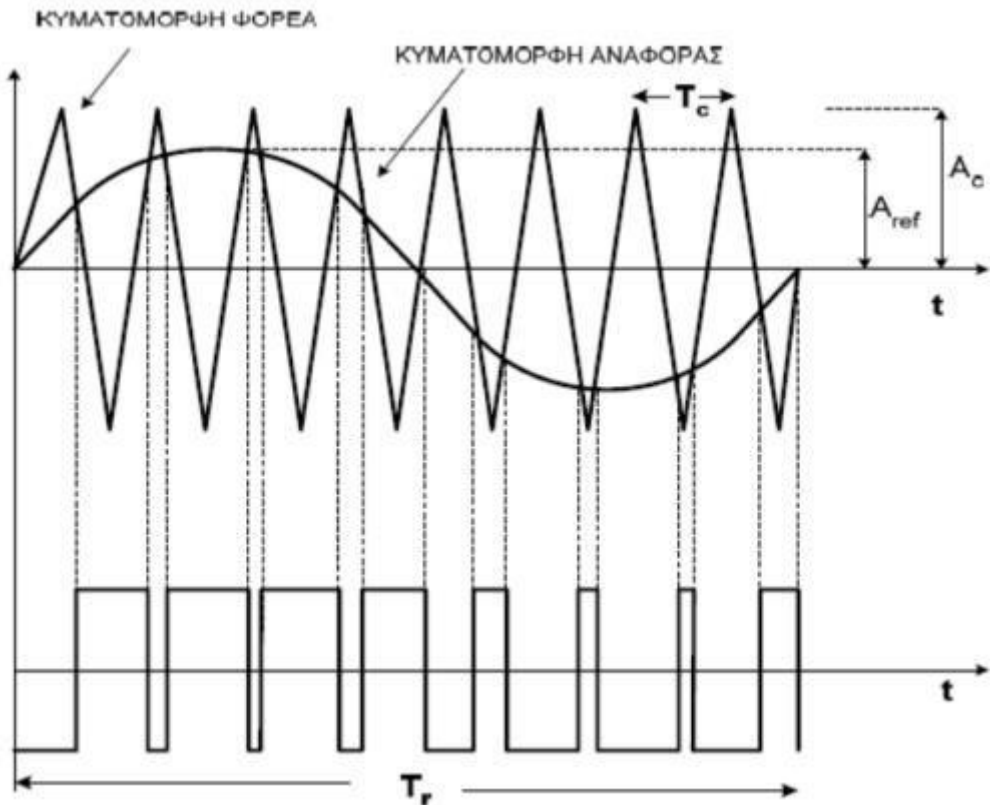


Figure 24. SPWM Function

Thus, when the alternating voltage is produced at the output of the inverter, we observe the presence of harmonics due to the process of SPWM. These harmonics occur in specific frequency bands close to integer multiples of the interruptive frequency, i.e. the frequency of the carrier.

The good thing is that these harmonic frequencies can be relatively easily isolated and cut off using filters. This allows unwanted harmonics to be eliminated or reduced, thus providing a cleaner alternating voltage to the load. In the case of three-phase inverters, the SPWM method is applied with similar logic, but with the difference that we now have three reference sines. Each of these sine has a different phase, where each of them is compared to the same triangular carrier waveform.

Specifically, the three reference semitons have a phase difference between them equal to  $120^\circ$ . These sines are then compared to the triangular waveform of the carrier. In the figure below, the function of the SPWM technique for the three-phase inverter is shown in detail, with the production of the trigger pulses for the semiconductors, as well as the way the output voltage is produced.

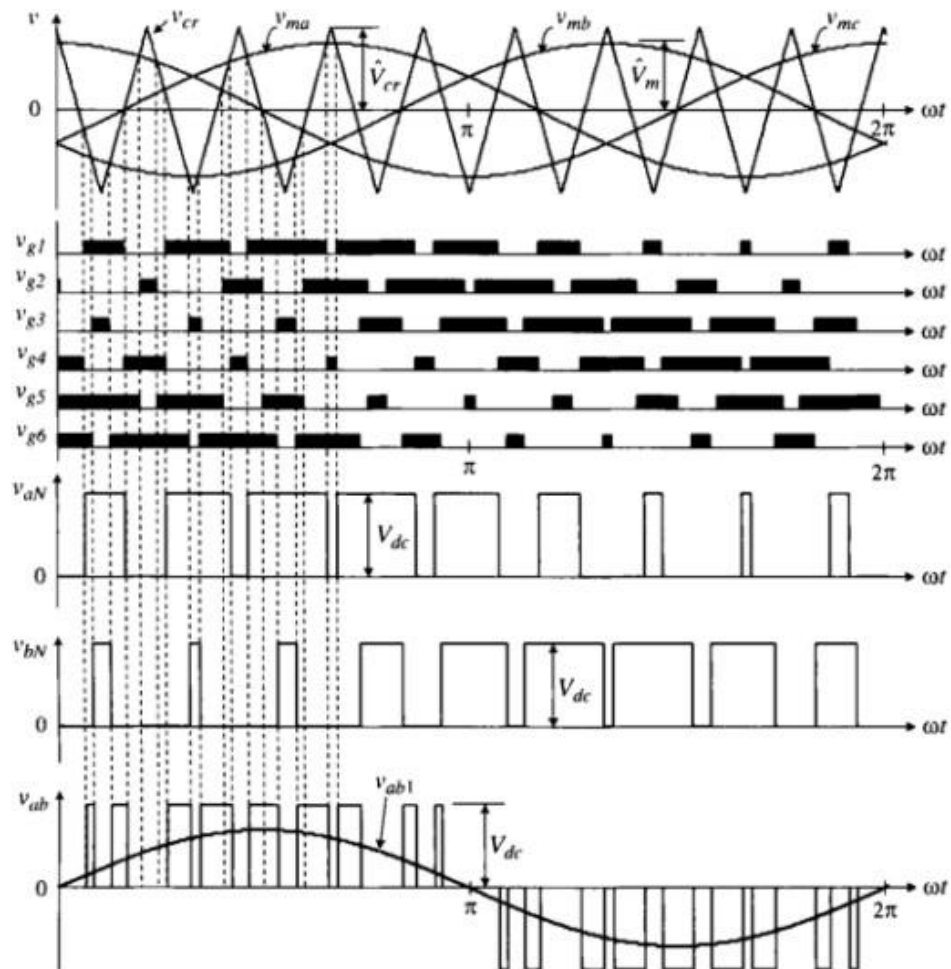


Figure 25. Representation from Sine to Pulses

For convenience, we can adopt the approach that, if a transistor of the upper branch is turned on, the alternating voltage at the output is equal to VDC /2. Correspondingly, if the transistor of the lower branch is turned on, the voltage will be -VDC /2 So, with this approach, we can represent switching function as follows:

$$V_{ou}(t) = \frac{V_{DC}}{2}, \text{ when the top transistor is enabled}$$

$$V_{ou}(t) = -\frac{V_{DC}}{2}, \text{ when the lower transistor is enabled}$$

$V_{ou}$

$t$

This simplification allows for an easier description of the switching operation of the system.

$$va = \frac{MaV_{DC}}{2} \cos(\omega_s t)$$

Where Ma is the state for transistors of the same branch, if the bottom branch transistor is active then we have Ma=-1, while if the upper branch transistor is active we have Ma=1. This representation, which uses the values 1 and -1 instead of the actual voltage values, is more suitable for modeling a mean value system .

However, in the calculation of the control variables of the voltage inverter, the variables are used, which represent the consonants of the saw triangular periodic function with width  $m$ . These variables are taken from

-1 to 1, replacing the corresponding values of the real function in the mean value model applies to:

$$\tilde{m}_i = m_i \cos (\omega_s t)$$

Where i determines the phase.

Using the Park transform, in the DQ0 system we have:

$$vsd = m_{sd} \frac{V_D}{C}$$

$$vsq = m_{sq} \frac{V_D}{C}$$

- **VSD, VSQ** the alternating voltages at the input of the inverter
- **VDC** the DC bus capacitor continuous voltage.
- **MSD** are the DQ0-transformed, synsinitoid quantities and are the control variables of the inverter.

### **3.2.2 LC Filter and Coil Coupling:**

The use of LC underpass filter and coupling coil in a topology where Inventer is used to interface with the network, can offer multiple benefits. Some of them are the following:

1. It protects the grid from the harmonics produced by the inverter. Harmonics are frequencies that are multiples of the base frequency of the grid. When an inverter is operating, it produces harmonics that can cause problems in the grid, such as rising cable temperatures, loss of power, and electromagnetic interference to other devices. The LC underpass filter removes the harmonics from the grid, protecting it from damage.
2. Improves the quality of the Inventer's output voltage. The output voltage of the inverter also contains harmonics, which can cause problems in the loads connected to the inverter, such as a decrease in power and an increase in temperature. The LC underpass filter reduces the harmonics of the output voltage, improving the quality of the voltage.
3. It limits the energy returning from the grid to the system. The output voltage of the inverter also contains harmonics, which can cause problems in the loads connected to the inverter, such as reducing power and increasing temperature. The LC underpass filter reduces the harmonics of the output voltage, improving the quality of the voltage.

The LC underpass filter consists of a coil and a capacitor. The coil has high resistance to low frequencies, while the capacitor has high resistance to high frequencies. The combined action of these two elements creates a downpass filter that allows the base frequency of the network to pass through and removes harmonics.

The coupling coil is connected between the inventor and the network and has two functions:

1. It creates a magnetic field that connects the inverter to the grid. This magnetic field allows power to be transferred from the inverter to the grid.
2. Protects the inverter from power leaks from the grid. Power leaks can cause damage to the inverter. The coupling coil limits current leaks, protecting the inverter.

The topology of the LC filter and coupling coil is as follows:

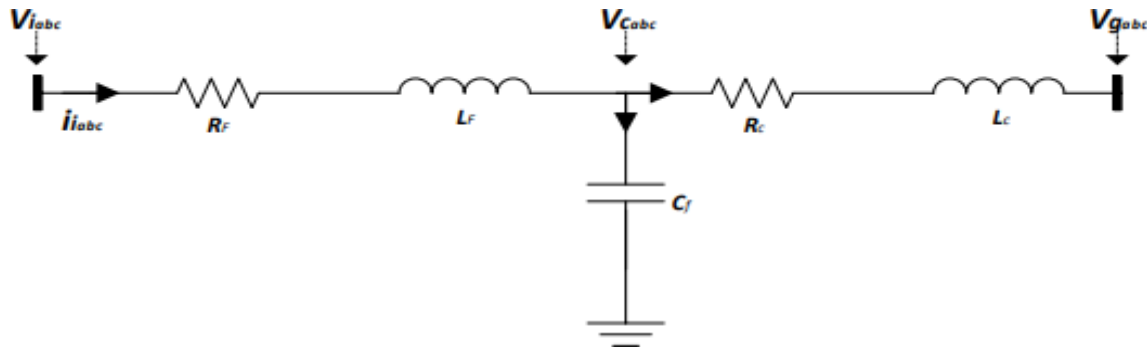


Figure 26. LC Filter and Coil Coupling

At the output of the inverter we have:

$$\begin{bmatrix} v_{ia} \\ v_{ib} \\ v_{ic} \end{bmatrix} = \begin{bmatrix} R_F & 0 & 0 \\ 0 & R_F & 0 \\ 0 & 0 & R_F \end{bmatrix} \cdot \begin{bmatrix} i_{ia} \\ i_{ib} \\ i_{ic} \end{bmatrix} + \begin{bmatrix} L_F & 0 & 0 \\ 0 & L_F & 0 \\ 0 & 0 & L_F \end{bmatrix} \cdot \frac{d}{dt} \begin{bmatrix} i_{ia} \\ i_{ib} \\ i_{ic} \end{bmatrix} + \begin{bmatrix} v_{ca} \\ v_{cb} \\ v_{cc} \end{bmatrix}$$

At the outlet of the underpass filter assembly we have:

$$\begin{bmatrix} v_{ca} \\ v_{cb} \\ v_{cc} \end{bmatrix} = \begin{bmatrix} R_c & 0 & 0 \\ 0 & R_c & 0 \\ 0 & 0 & R_c \end{bmatrix} \cdot \begin{bmatrix} i_{ca} \\ i_{cb} \\ i_{cc} \end{bmatrix} + \begin{bmatrix} L_c & 0 & 0 \\ 0 & L_c & 0 \\ 0 & 0 & L_c \end{bmatrix} \cdot \frac{d}{dt} \begin{bmatrix} i_{ca} \\ i_{cb} \\ i_{cc} \end{bmatrix} + \begin{bmatrix} v_{ga} \\ v_{gb} \\ v_{gc} \end{bmatrix}$$

It is true that:

$$\begin{bmatrix} i_{ca} \\ i_{cb} \\ i_{cc} \end{bmatrix} = \begin{bmatrix} i_{ia} \\ i_{ib} \\ i_{ic} \end{bmatrix} - \begin{bmatrix} C_F & 0 & 0 \\ 0 & C_F & 0 \\ 0 & 0 & C_F \end{bmatrix} \cdot \frac{d}{dt} \begin{bmatrix} v_{ca} \\ v_{cb} \\ v_{cc} \end{bmatrix}$$

Where:

$v_{ia}$ ,  $v_{ib}$  and  $v_{ic}$  are the voltage at the output of the inverter directed to the mains side, in the three phases a,b,c respectively.

$V_{CA}$ ,  $V_{CB}$  and  $V_{CC}$  are the voltage at the output of the LC underpass filter, in the three phases a,b,c respectively.

$V_{GA}$ ,  $V_{GB}$  and  $V_{GC}$  are the voltage at the output of the device, in the three phases A,B,C respectively.

$I_{IA}$ ,  $I_{IB}$ , and  $I_{IC}$  are the currents that come out of the inverter and enter the downstream filter, in the three phases A,B,C respectively.

$i_{ca}$ ,  $i_{cb}$  and  $i_{cc}$  are the currents at the output of the RC filter, in the three phases a,b,c respectively.

$R_F$ ,  $C_F$  and  $L_F$  constitute the parasitic resistance of the coil, the capacitance of the capacitor and the inductance of the filter respectively.

RC and LC constitute the parasitic resistance and inductance of the coupling coil

Using the Park transform, the final relationships for the LC underpass filter are as follows:

$$L_F \cdot \frac{d I_{id}}{dt} + R_F \cdot I_{id} = v_{id} - v_{cd} + \omega_s \cdot L_F \cdot I_{iq}$$

$$L_F \cdot \frac{d I_{iq}}{dt} + R_F \cdot I_{sq} = v_{iq} - v_{cq} - \omega_s \cdot L_F \cdot I_{id}$$

$$L_C \cdot \frac{d I_{cd}}{dt} + R_C \cdot I_{cd} = v_{cd} - v_{gd} + \omega_s \cdot L_C \cdot I_{cq}$$

$$L_C \cdot \frac{d I_{cq}}{dt} + R_C \cdot I_{cq} = v_{cq} - v_{gq} - \omega_s \cdot L_C \cdot I_{id}$$

$$C_F \cdot \frac{d V_{cd}}{dt} = i_{id} - i_{cd} + \omega_s \cdot C_F \cdot V_{cq}$$

$$C_F \cdot \frac{d V_{cq}}{dt} = i_{iq} - i_{cq} - \omega_s \cdot C_F \cdot I_{id}$$

Where:

$v_{id}$  and  $v_{iq}$  are the voltages at the output of the inverter directed to the mains side, on the two D and Q axes respectively.

$v_{cd}$  and  $v_{cq}$  are the voltage at the output of the LC downward filter, on the two d and q axes respectively.

$V_{GD}$  and  $V_{GQ}$  are the voltage at the output of the device, on the two D and Q axes respectively.

$I_{id}$  and  $I_{iq}$  are the currents that come out of the inverter and enter the underpass filter, on the two D and Q axes respectively.

$i_{cd}$  and  $i_{cq}$  are the currents at the output of the RC filter, on the two d and q axes respectively.

as we call the frequency of the voltage regulated through the inverter and coincides with the frequency used for the Park matrix, i.e. the frequency of the inverter voltage is equal to the eigenfrequency of the rotating frame DQ0.

### **3.3 DC Side:**

The DC side of the system that we are developing in this thesis consists of the following devices:

1. The photovoltaic array where solar energy is converted into electricity
2. The DC/DC Boost Converter, which is responsible for raising the voltage to the desired value, so that it is properly connected to the Inventor and consequently to the grid.

#### **3.3.1 Model DC/DC Boost Converter :**

The use of this inverter in our system, as we saw above, is done between the photovoltaic array and the Inventor. Its presence is essential as it offers the system some basic advantages such as:

- Increase the voltage of the photovoltaic array to the level required by the inverter. Photovoltaic panels produce energy at low voltage. The DC/DC Boost Converter increases this voltage to levels that can be more efficient for the inverter.
- Maximizing the power generated by the photovoltaic array. The power of a photovoltaic array depends on the voltage and current it produces. The DC/DC Boost converter can be used to move the PV array to the point of maximum power (MPP), where it produces the maximum possible power.
- Performance Optimization: The Inverter requires a high input voltage to operate efficiently. The Boost Converter ensures that the voltage from the photovoltaics is at the desired level, thus optimizing the performance of the system.
- Surge Protection: The Boost Converter can also act as surge protection, protecting the Inverter from high voltages that could be caused by brightness changes or other abnormalities.

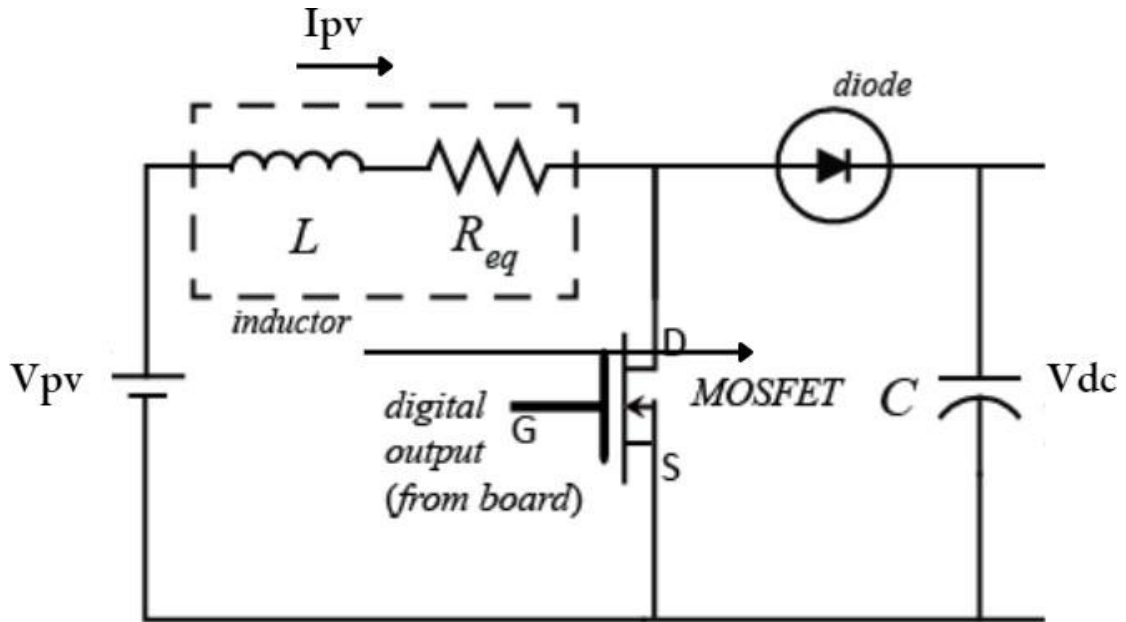


Figure 27. Boost Converter

In a voltage lift inverter, the lifting function is achieved by using a semiconductor element, such as a MOSFET transistor or a diode. The semiconductor is turned on or off to control the flow of current from the DC source to the inverter output. A suitable way to trigger the transistor is the conventional PWM method. PWM uses a control signal that oscillates between values 1 and 0. When the control signal is 1, the semiconductor is activated and current flows from the DC source to the output of the inverter. When the control signal is 0, the semiconductor is switched off and no current flows from the DC source to the output of the inverter. Being a switch element, the transistor distinguishes this arrangement into two states, i.e. depending on whether the middle branch of the transistor Q conducts or not.

In the case of a MOSFET transistor, the average branch of the transistor is active when the transistor is enabled. In the case of a single diode, the middle branch of the diode is active when the diode is forward biased. So, we have a control variable  $i$ , which will get values of 1 or 0 when the MOSFET is enabled or not respectively.

The control variable  $i$  is a continuous variable that takes values in space (0,1). The value  $i=1$  corresponds to the transistor activation state, and the value  $i=0$  corresponds to the transistor's off state. Replacing the discrete  $u$  with the continuous variable  $m$ , which takes values in space (0,1), we arrive at the model of the average value of the voltage lift converter and it is represented by the following equation.

The equation describing the average value model of the voltage lifting inverter is as follows:

$$L \frac{d}{dt} i_{PV} + R_{eqiPV} = V_{PV} - (1 - m)V_{dc}$$

where  $R_b$  is the parasitic resistance of the inverter,  $L_b$  is the inductance of the inverter coil, and  $m$  is the ratio of the inverter segmentation (duty cycle).

If we consider parasitic resistance negligible, then in the permanent state the following arises:

$$V_{dc} = \frac{V_{PV}}{1 - m}$$

### 3.3.2 DC Bus Model (DC Link):

Electricity systems are connected to each other via the most important nonlinear element, the DC Bus. In essence, all devices are connected to each other through a capacitor and in this way they can interact. In our system the DC Bus connects the Boost Voltage Booster Converter to the Inventor.

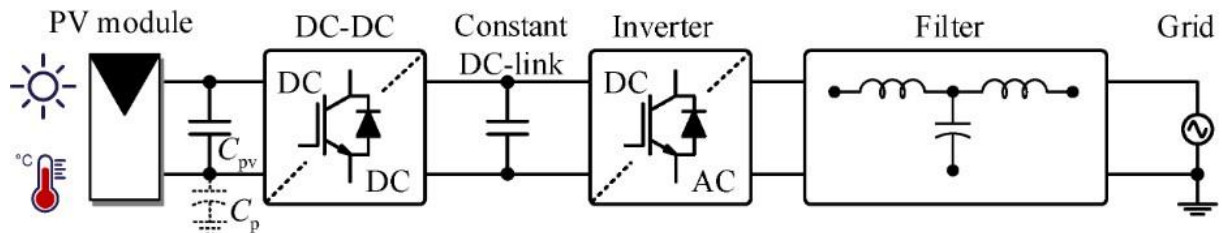


Figure 28. Integrated System

$$\frac{dV_{DC}}{dt} = \frac{(1 - \frac{I_{PV}}{V})IP + I_{Grid}}{C_{DC}}$$

Where:

- CDC the capacitor capacity.
- VDC the voltage induced in the capacitor armatures.
- IPV the current at the output of the photovoltaic array.
- IGrid is the current coming from the inverter that is directed to the grid .

### 3.3.3 Photovoltaic Array Equations:

The equivalent circuit of a photovoltaic cell is a simplified electrical circuit, which is used to describe the function of the cell during its exposure to solar radiation. This circuit helps to calculate the electrical efficiency of the photovoltaic cell and to predict its behavior during its operation.

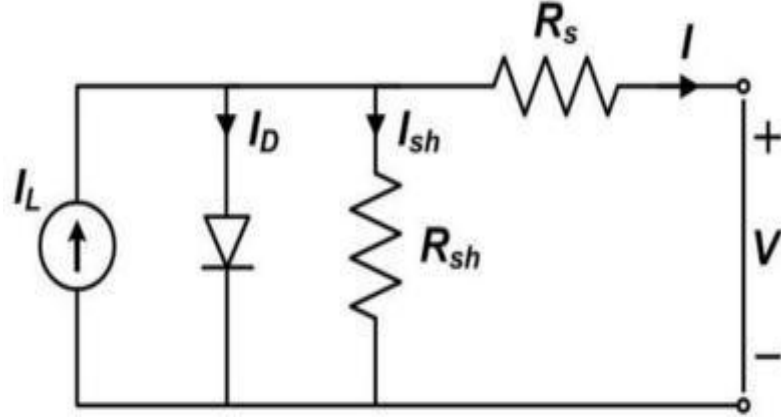


Figure 29. Equivalent Photovoltaic Array Circuit

The basic equation that describes the cell is:

$$I = I_L - I_0 * \left( e^{\frac{qV}{kT}} - 1 \right)$$

In the above type,  $I_0$  is the current of the diode and  $I_L$  is the light current, i.e. the current that is responsible for the incident radiation received by the solar cell. The types of calculation of these quantities are:

$$I_0 = A_{Cell} * \left( \frac{q * D_e * n_i^2}{L * e * N_A} + \frac{q * D_h * n_i^2}{L * h * N_D} \right)$$

$$I_L = q * A * G * (L_e + W + L_h)$$

Where:

- $q$ : The electron charge)
- $T$ : The absolute temperature of the cell
- $k$ : The Boltzmann constant ( $1.38 \times 10^{-23}$  J/K)
- $A_{Cell}$ : The cross-section of the cell
- $V$ : The voltage at the exit of the cell
- $L_e$ : The electron diffusion length =  $\sqrt{D_e * \tau_e}$
- $L_h$ : The hole diffusion length =  $\sqrt{D_h * \tau_h}$
- $\tau_e, \tau_h$ : The lifetime of electrons (holes) as minority carriers
- $W$ : The Scope of Contact (Depletion Region)
- $G$ : The Rate of Production for Solar Radiation

The basic equation of the solar cell is the Shockley-Queisser equation, which describes the function of a solar cell as a p-n diode. This equation is a

good approximation of the actual behavior of the solar cell, but it is not accurate in all cases.

Experimental observations have shown that the basic equation of the solar cell does not accurately reflect the actual I-V characteristic curve of a cell for practical purposes. This is because it does not take into account certain factors that affect the actual behavior of the solar cell, such as:

- The outer short circuit: The basic equation of the solar cell assumes that the outer circuit is open. In fact, the outer circuit is usually attached to a charge, which affects the I-V curve of the solar cell.
- Losses in the outer circuit: Losses in the outer circuit, such as resistance losses and capacitance losses, also affect the I-V curve of the solar cell.
- Internal losses: Internal losses, such as losses due to the liquefaction of photovoltaic voltage (the photovoltaic voltage begins to decrease as the current intensity increases) and losses due to thermal flow, also affect the I-V curve of the solar cell.

To improve the accuracy of the solar cell's basic equation, the researchers have introduced three additional parameters:

- $R_s$ : The in-line resistance of the cell represents the resistance encountered by carriers during their flow within the cell. This resistance comes from various sources, such as the resistance of the main semiconductor, the resistance of the surface layer, and the resistance of the atomic contact (the area where two different materials, such as the semiconductor and the metal electrode of the photovoltaic cell) meet.
- $R_{sh}$ : The parallel resistance of the cell represents the resistance encountered by the vectors that leak the cell. This resistance comes from various sources, such as the reconnection of carriers to the contact area, the leakage of carriers to the outer surface of the cell, and the leakage of carriers into crystal abnormalities.
- $A$ : The constant  $A$  represents the reconnection phenomena that occur in the contact area. The value of  $A$  ranges between 1 and 2, depending on the type of material from which the cell is made and its operating conditions.

Based on the above, the final formula emerges:

$$I = IL - IO * \left( \frac{q(V+I*RS)}{A*kT} - 1 \right) - \frac{V}{R_{sh}}$$

The I-V, P-V characteristic curves at the output of a cell are represented as follows:

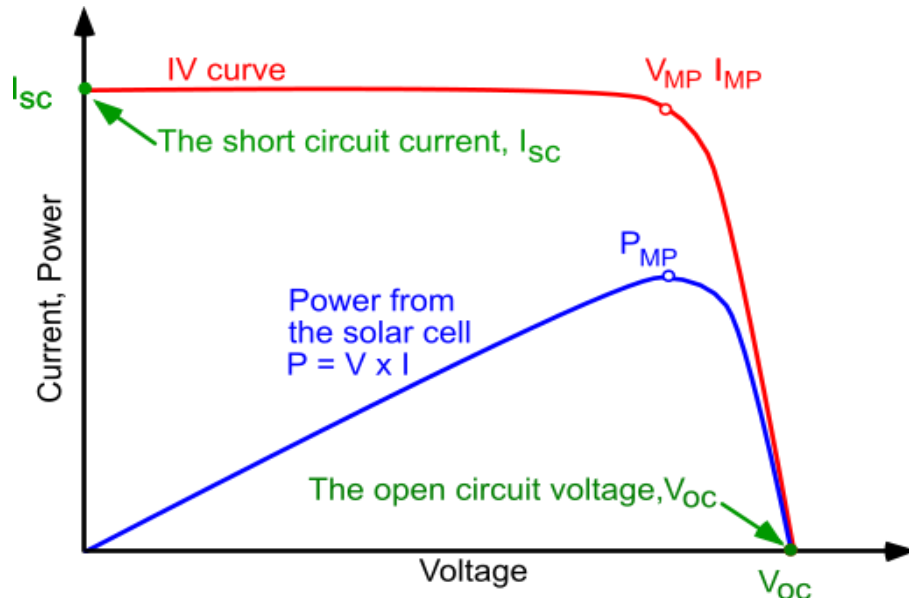


Figure 30. I-V, P-V Photovoltaic Cell Characteristics

- Open Circuit Voltage (VOC ): Open circuit voltage is the voltage generated by a photovoltaic panel when no current is drawn from it.  
Under ideal conditions, it is relatively stable under varying brightness. However, as the temperature increases, the cell voltage at the open circuit point decreases.
- Short Circuit Current (ISC): Short circuit current is the maximum current generated by a photovoltaic panel when its terminals are short-circuited. Under ideal conditions, it is also relatively stable under  
Changing brightness. However, as the temperature rises, the short-circuit current increases.
- Maximum Power Voltage (VMP): The maximum power voltage is the voltage at which a photovoltaic panel produces the maximum electrical power. This voltage is less than the open circuit voltage and greater than the short-circuit voltage.
- Maximum Power Current (IMP): Maximum power current is the current at which a photovoltaic panel produces the maximum electrical power. This current is less than the short-circuit current and greater than zero.
- Maximum Output Power Point (PMP ): The maximum output power point is the point at which the current-voltage curve of a photovoltaic panel reaches its maximum. This point corresponds to the maximum power voltage and current maximum power.

# CHAPTER 4: Control System Design

## 4.1 Import:

The modules discussed in the previous chapters require proper control for their proper functioning. This includes a number of tricks and techniques to implement it. For electronic power converters, the control modes differ in terms of how semiconductors are switched on and off. Semiconductors are not ideal and, therefore, The start/off frequency must remain within certain limits. Excessively high frequencies can cause damage to semiconductors. With these inverters, we mainly aim to control the photovoltaic array, the operating frequency of the load voltage after the LC filter, as well as the voltage at the capacitor ends of the DC bus. With the appropriate initiation method for each inverter, we can achieve a controlled operation of the power generation system. Of course, the main element of our control will be the use of the widely used PI controllers.

## 4.2. Voltage Boosting Inverter of the PV Array SC/SC Control:

The equation by which the voltage lifting inverter is characterized is nonlinear, so in order to be able to control it, we will feed the PI controller the error between the reference current and the actual current flowing by the photovoltaic. Then we subtract from the output of the controller the voltage  $V_{pv}$  that you are counting from the voltmeter at the ends of the photovoltaic system and divide by the  $V_{dc}$ . We end up getting the Duty Cycle ratio for the Check the DC/DC Boost Converter from the following relationship:

$$mPV = \frac{1}{V_{DC}} \cdot [KpIPV \cdot (IPV_{Ref} - IPV) + KiIPV \cdot \int (IPV_{Ref} - IPV) - VPV]$$

Now to determine the K coefficients we need to extract the closed-loop transport functions for the  $IPV_{Ref}$ ,  $IPV$  streams. Replacing it with the Boost formula results in the following:

$$L \frac{d}{dt} iPV + R_{eqiPV} = [KpIPV \cdot (IPV_{Ref} - IPV) + KiIPV \cdot \int (IPV_{Ref} - IPV) dt]$$

Using the Laplace transform we will arrive at the following first-order system for the transport function:

$$\frac{IPV}{PV,Ref} = \frac{1}{\left( \frac{L \cdot s + Req}{Kp \cdot s + Ki} \right) \cdot s + 1}$$

Thus, with the right choice of winnings, it results that:

$$Kp_{IPV} = \frac{L}{T_{i,PV}}$$

An  
d

$$Ki_{IPV} = \frac{Req}{T_{i,PV}}$$

The following image shows the structural diagram of the internal control loop of the voltage lifting inverter:

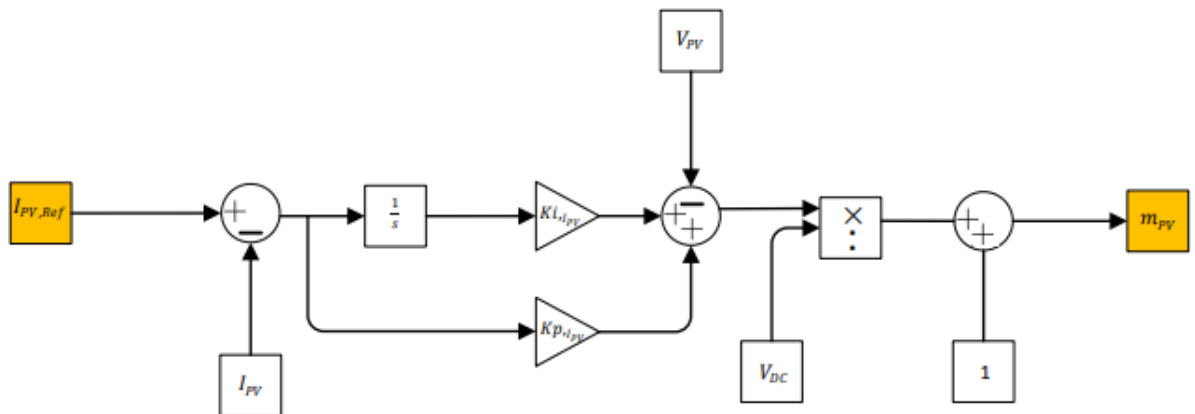


Figure 31. Internal Control Loop Boost Converter

### 4.3 Control on the load side:

The main objective of the control circuit applied to the inverter is to maintain a constant voltage and frequency throughout the operation of the system, regardless of changes in the sources of power generation. The voltage and frequency refer to the network, which is followed by the L-C underpass filter. This filter removes the upper harmonics of the voltage generated by the inverter, providing an almost pure sine signal.

The control tactic is based on Voltage Oriented Control and is applied to the two-phase rotating frame dq0 using PI controllers.

The operating frequency is also used for various Park transformations in the control, but it is also the operating frequency on the load side. Serial control is used to achieve the stable operation of the control system and ensure its asymptotic stability. With serial control, we use an internal and an external control loop. The internal loop is responsible for producing the appropriate signal that relates to the segmentation ratio corresponding to the PWM pulse of the voltage reversal inverter. This signal drives the inverter to produce the desired output voltage. The Outer Loop

The controller is responsible for monitoring the desired DC voltage on the bus and adjusting it as needed. This is achieved through the regulation of the internal current loop, which undertakes to manage the output of the voltage lifting converter, while the external voltage loop monitors the DC voltage and adjusts the internal current loop accordingly. Stabilization of the DC bus voltage at the desired level is achieved. The control is designed so that the voltage on the q-axis of the grid side is zeroed, minimizing losses and the presence of reactive power. While on the d-axis the voltage we want to be driven to the value of the reference voltage, which in our case is at 1200 Volts. The above control is implemented using a Phased-Locked Loop, a conventional PI controller that takes the voltage to zero as a reference and adds the desired operating frequency as an error to the output.

Therefore, based on the above, three control circuits are required for the inverter:

1. Voltage control circuit on the d-axis on the load side:
  - a. The outer loop of the voltage produces a current reference signal for the d-axis.
  - b. The inner loop, free from non-linearities, produces the appropriate actuation variable of the power converter through the S.P.W.M. technique.
2. Phased-Locked-Loop: Produces the desired operating frequency and at the same time zeros the voltage on the q-axis on the load side.
3. Loop that zeros current flow on the q-axis: Used to reduce power losses.

#### **4.3.1. *Phased-Locked Loop:***

The function of the phase lock loop (PLL) is important for the proper operation of the inverter. The main role of the PLL is to orient the rotating frame through the angular frequency at which it is rotated. Specifically, the control objective of the unit is to orient the voltage frame in the two-phase rotating frame  $dq0$  in the direction of zero voltage  $v_{gq}$ . The purpose of the controller is to maintain the angle  $i$  at the desired value, so that the trend is zeroed, thus allowing the safe orientation of the trend frame. The controller is described by the following relationship:

$$\omega_{PLL} = \omega_n - K_p,PLL \cdot (v_{gq},Ref - v_{gq}) - K_i,PLL \cdot \int (v_{gq},Ref - v_{gq})dt$$

We set  $v_{gq},Ref = 0$ , but we can use PLL to achieve a desired power angle for each even between the stresses of the d and q axes.

It is worth noting that the input to the Blocks of the Park transform is an angle and not a frequency, hence the integration at the output of the controller with respect to the angle  $\theta$  :

$$\theta = \int \omega_{PLL} dt$$

The structural control diagram of PLL is as follows:

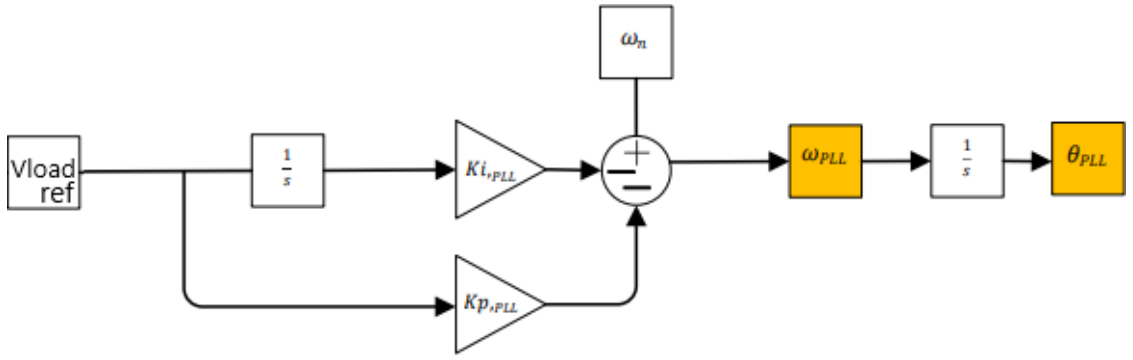


Figure 32. Phase Locked Loop

#### 4.3.2. Internal Current Control Loop:

The equations describing the currents in the line after the inverter on the load side are nonlinear, and the successful deletion of their nonlinear terms from the two control loops enables us to arrive at a first-order transfer function, including the mathematical expression for analog and integral gains. The control system will consist of PI controllers, one for each d and q axis. These controllers will receive as input the difference between the current reference value and the actual current ( $i_{q,ref} - iq$ ), thus making use of the closed feedback system to improve the stability of the system. The electrical system after the inverter is described by the following equations:

$$L \cdot \frac{Id}{dt} + R \cdot Id = Vin_d - Vout_d + \omega_s \cdot L \cdot Iq$$

$$L \cdot \frac{Iq}{dt} + R \cdot Iq = Vin_q - Vout_q + \omega_s \cdot L \cdot Id$$

Simplifying the above relationships and replacing the voltages at the output of the inverter results in:

$$md = \frac{2}{V_{DC}} \cdot [K_{p,Id} \cdot (I_{d,Ref} - I_d) + K_{i,Id} \cdot \int (I_{d,Ref} - I_d) dt - \omega_s \cdot L \cdot I_q]$$

$$mq = \frac{2}{V_{DC}} \cdot [K_{p,Ig} \cdot (I_{q,Ref} - I_q) + K_{i,Ig} \cdot \int (I_{q,Ref} - I_q) dt + \omega_s \cdot L \cdot I_d]$$

By applying the Laplace transform, we arrive at the transport function from which the following proportional and integer gains of the PI controller are derived:

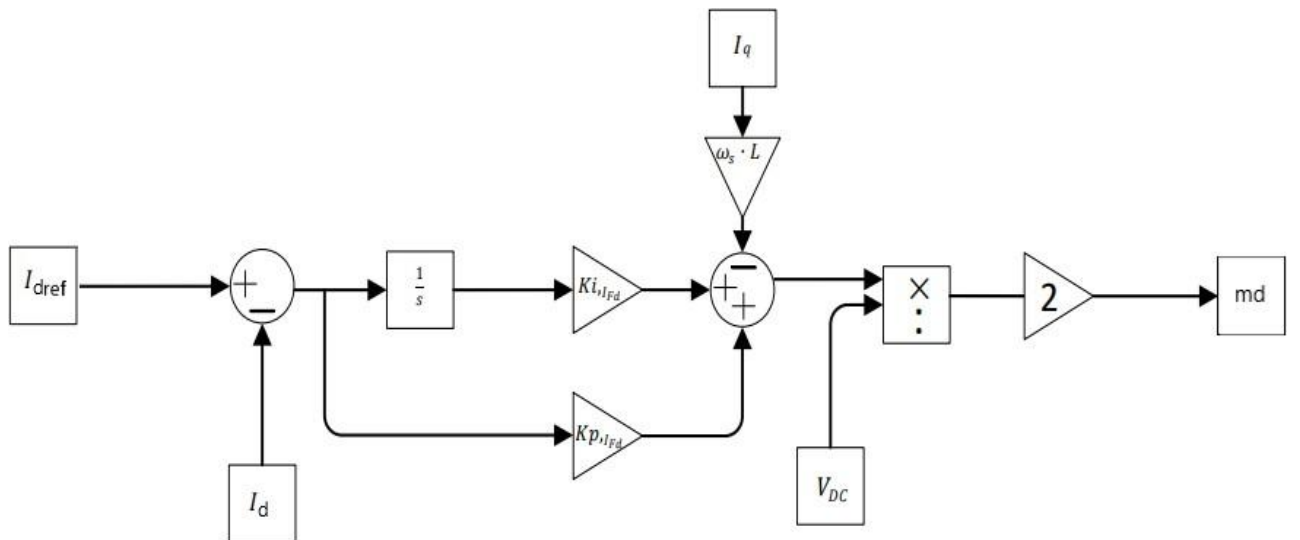
$$K_{p,Id} = K_{p,Ig} = \frac{L}{T_i}$$

$$K_{i,Id} = K_{i,Ig} = \frac{R}{T_i}$$

Consequently

$$\frac{I}{I_{Ref}} = \frac{1}{(K_p \cdot s + K_i) \cdot s + 1}$$

Based on the above, the structural diagram of the internal loop control system is as follows:



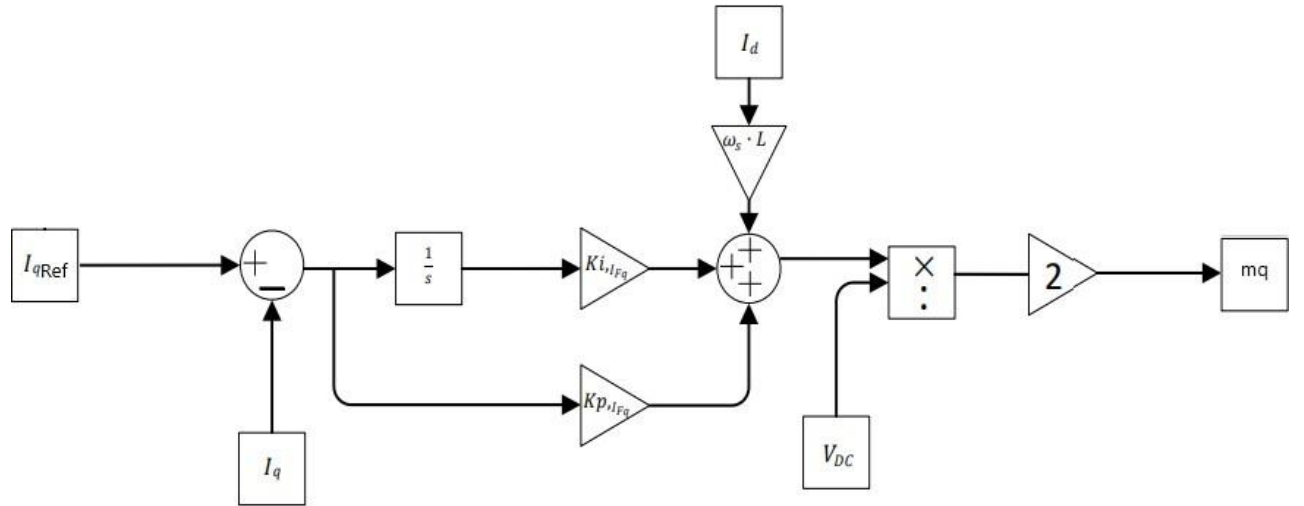


Figure 33. Internal Current Control Loops on the Load Side

#### 4.3.3. External Voltage Control Loop:

The load voltage refers to the potential difference applied to the load. In this case, the load is placed behind an LC underpass filter. For the design of the external negative voltage feedback loop, a PI controller is used , with input the error between the reference value and the measured voltage of the load.

In this case, extracting a transport function for the load voltage requires extensive analysis and nonlinear control tricks. Therefore, the trial and error method is used to determine the proportional and integral factors. This means that the controller's gains are systematically altered until the desired response is achieved.

Finally, the output of the controller is the reference current used as an input to the internal control loop of the d,  $I_{q, \text{Ref}}$  axis in order to form the coefficient  $m_d$ . The mathematical expression of this description is presented below.

$$Id_{,\text{Ref}} = [Kp_{,VLOAD} \cdot (VLOAD_{,\text{Ref}} - VLOAD) + Ki_{,VLOAD} \cdot \int (VLOAD_{,\text{Ref}} - VLOAD) dt]$$

Based on the above, the structural diagram of the external loop voltage control system is as follows:

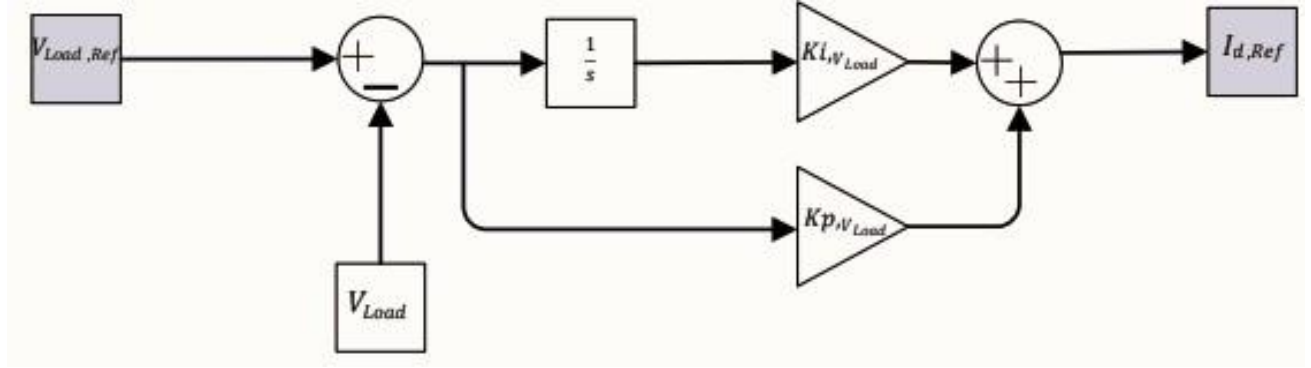


Figure 34. External Voltage Control Loop on the Load Side

Based on the above analyses, the gains we come to for PI controllers are the following:

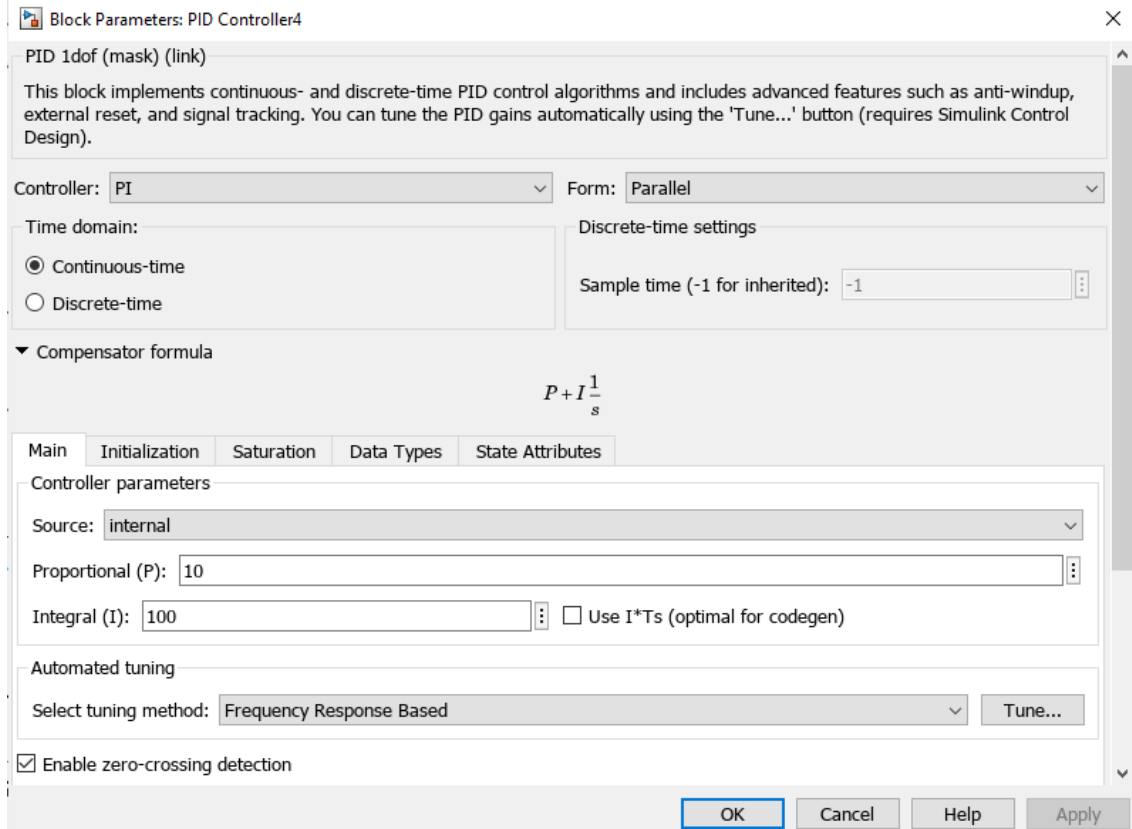


Figure 35.PI Gains Internal Loop Controller Boost Converter

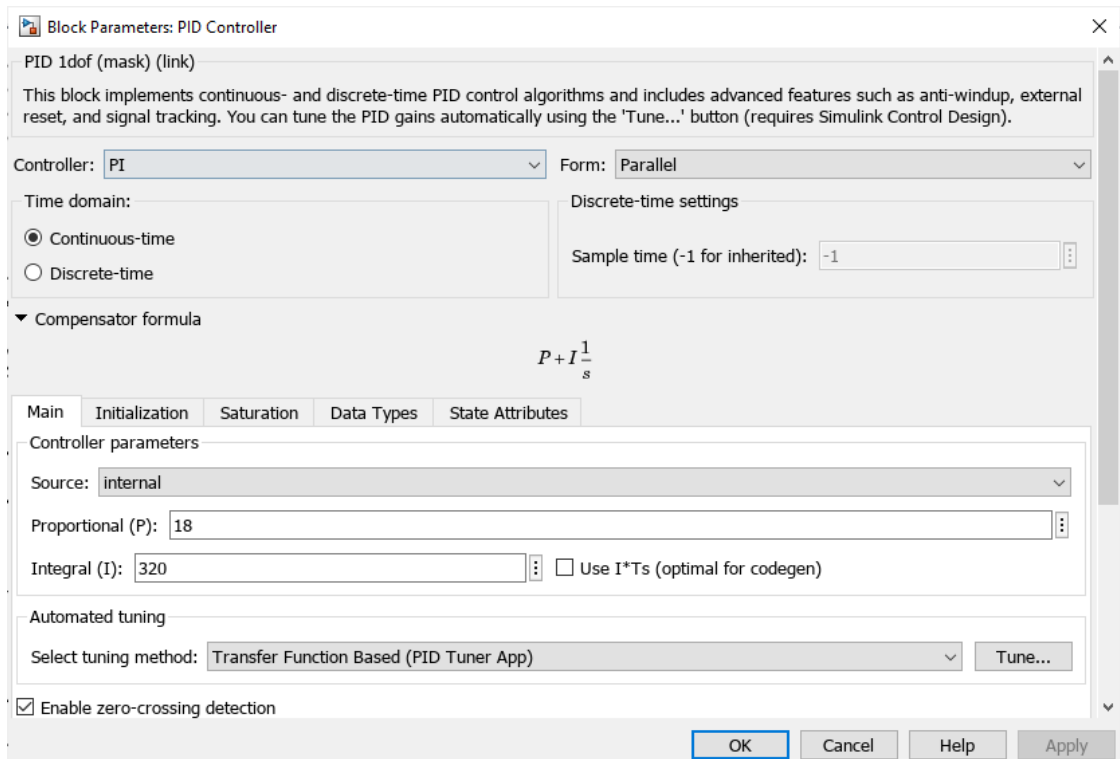


Figure 36.PLL Controller PI Gains

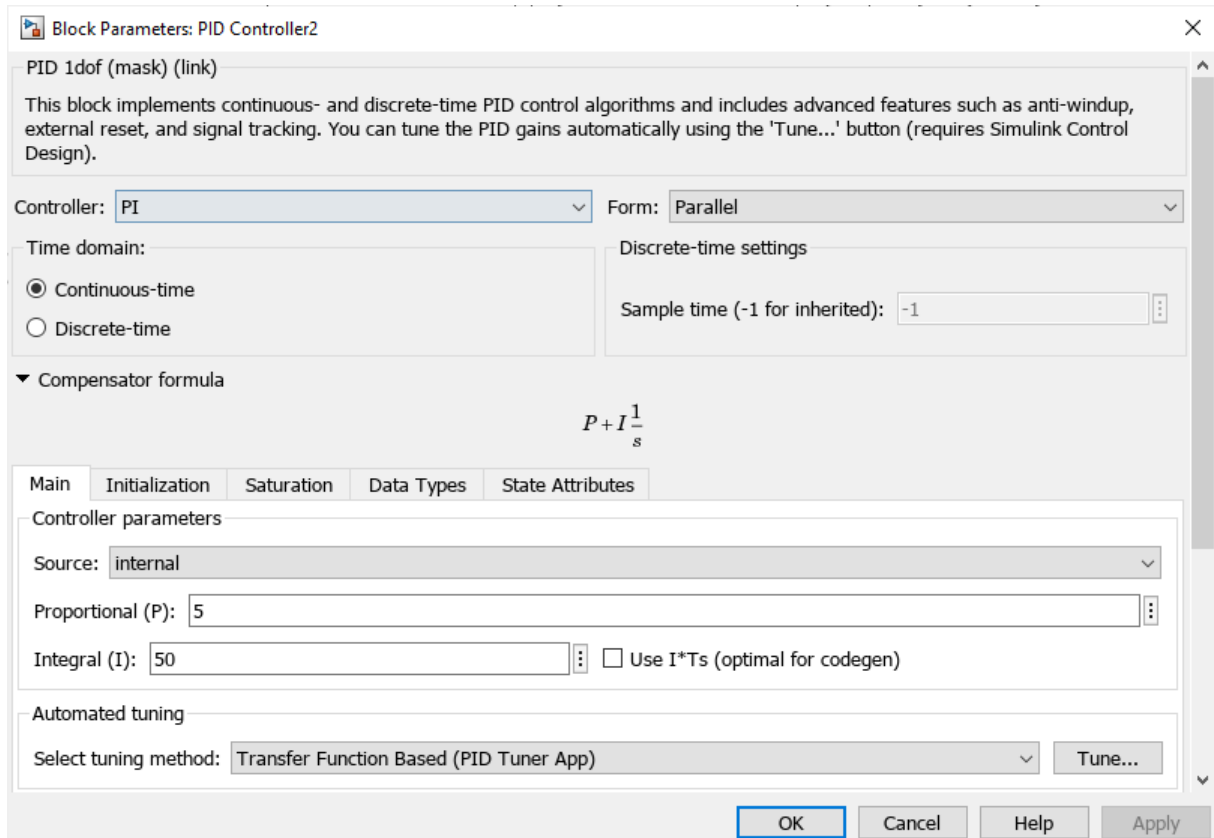


Figure 37.PI Gains Internal Current Loop Tester on the Load Side.

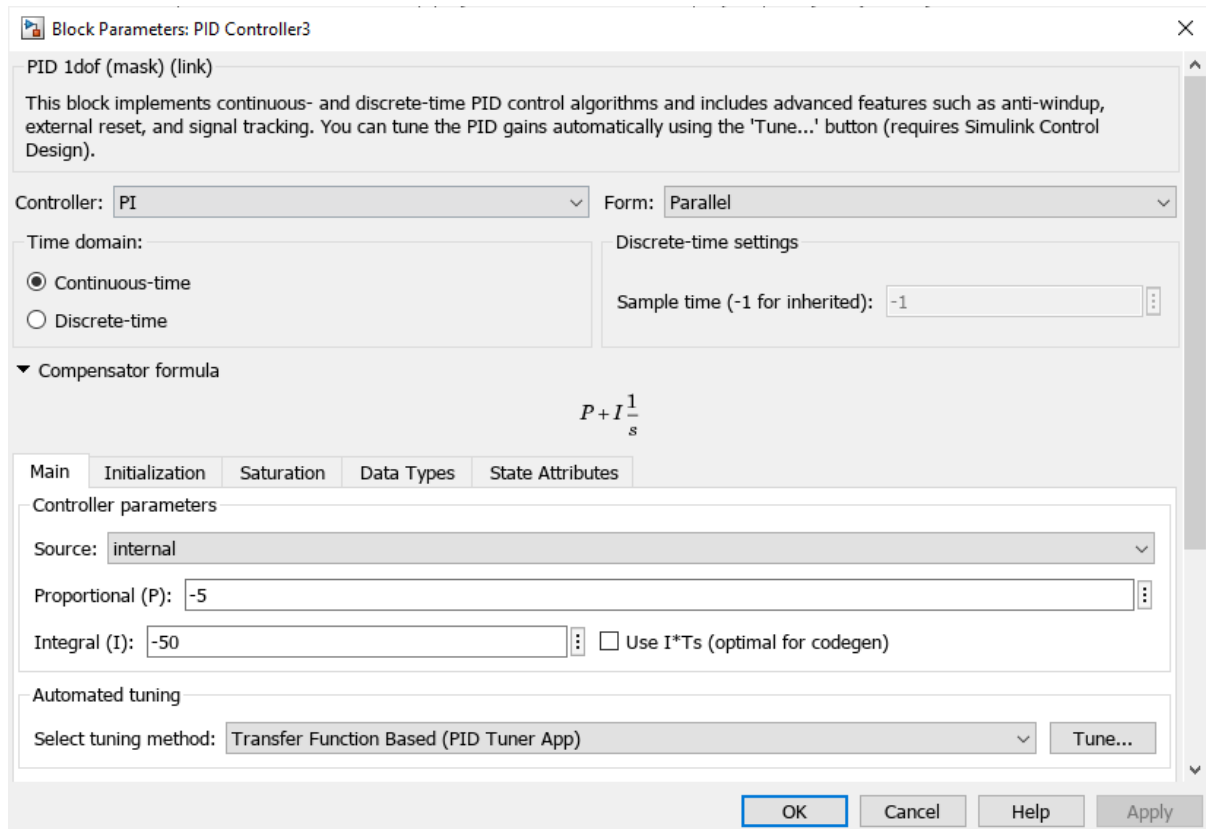


Figure 38.PI Gains External Voltage Control Loop Tester on the Load Side.

# CHAPTER 5: Experimental Arrangement

## 5.1 Import:

In this chapter we will analyze the system we have created, using the above mathematical tools and control techniques. More specifically, we will present the Hardware In the Loop real-time simulator as well as how we built the system in it, and more specifically in the Schematic Editor. We will also show the operation of the Scada environment and the way in which we checked its various characteristics in real time and observed measurements from a series of measuring instruments of the simulator. Finally, we will show the use of the environment of the Texas Instruments C2000 microcontroller that we used to pulse the HIL and measure the currents and voltages produced by the model, as well as the connection of analog and digital inputs and outputs to complete their interconnection.

## 5.2 Real Time Typhoon Hardware In the Loop:

Real-Time Hardware-in-the-Loop (HIL) refers to a controller consisting of both hardware and software. The hardware part is programmed with the appropriate parameters for any real-time problem that a simulation through software, such as Simulink, cannot address.

Specifically, in HIL, mathematical equations and models that describe each real-time problem in detail and satisfactorily are introduced separately. Thus, the system under study may behave like a real real-time system when operating within the HIL. Through this process, the emulation and evaluation of the performance of a control system or device is achieved before its actual application.



Figure 39. HIL Device

The key components that make up a HIL system include the Electronic Control Unit (ECU), communication channel between ECUs, software and support tools, system interface, battery, sensors, and actuators

(sensors and actuators), microprocessor, memory, timers and I/O ports. The I/O ports can be digital or analog, depending on the type of data exchanged with the HIL. The associations and exchange of signals between the elements are shown in Figure 4.3.

The basic controls applied at HIL include hardware control, where it is circuitously checked if there are problems with the equipment (sensors, actuators, memory, I/Os), ground-to-ground, where component behavior is checked, power voltage switch-off, where the system's signal transmission behavior is checked, open-circuit controls, the surge checks, the RAM check, and the EEPROM check, as well as the WDG timer check.

HIL's applications are important in many areas, including automotive systems control, radar, robotics, power systems, and offshore systems.

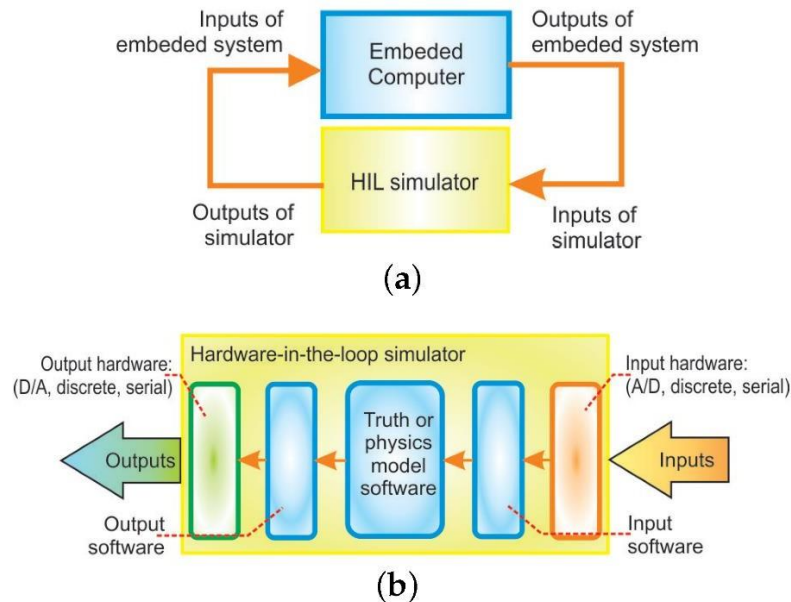


Figure 40. Hardware Structure of HIL

The system under study, whether it is an electronic control unit (ECU), a fully autonomous digital electronics controller (FADEC), or a programmable logic controller (PLC), sends the desired size signals to the HIL's signal control unit. These signals are passed to the HIL's I/O module, adapted to real-time signals, and sent to the user interface for processing and control. Thus, through these signals, it is possible to carry out the necessary system automation tests.

The process of simulating a HIL is as follows: On a computer, the model of the system is constructed into software, including the control scheme, and through I/O devices it communicates with the HIL. In the HIL, the system is adapted in real time through a real-time microprocessor , which receives control commands from an external real controller that implements a software model of this in our case has the Laptop.

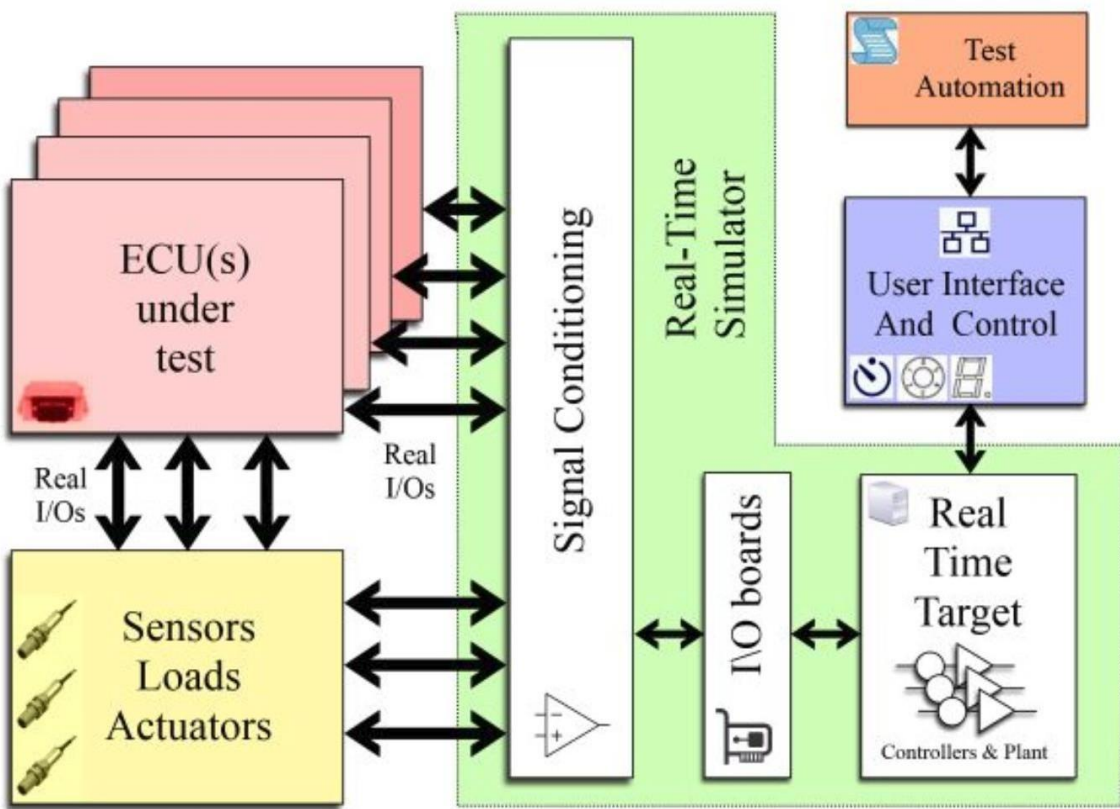


Figure 41. System Hardware Connection Representation

The HIL can function either as a closed loop or as an open loop with the system under study. In fact, open loop is mainly used in electrical system control and protection applications

Closed-loop is used in systems operation monitoring applications.

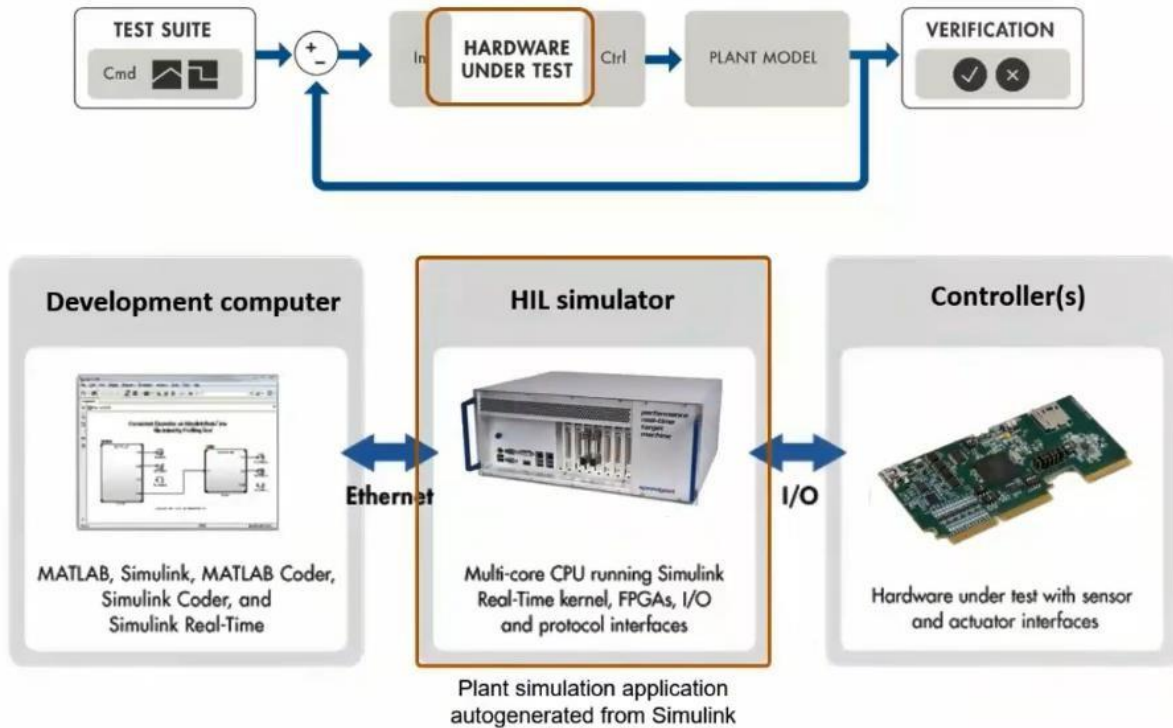


Figure 42. System Interface-Communication and Feedback

Communication between the central processing unit (CPU) of the computer and the HIL can be done either by physical wired interface or by telecommunication interface. There are various real-time HIL simulation (RTHIL) software, known as Virtual HILs, which operate in time increments smaller than real-time. Some of them are the RTDS, Typhoon HIL, and OPAL-RT.

In large industrial facilities  
systems with multiple I/O ports.

and control laboratories

Used larger HIL



Figure 43.HIL Industrial Model

The Typhoon HIL 606 is a high-performance hardware-in-the-loop (HIL) simulator designed to meet the demanding requirements of power electronics and network modernization applications. It is the company's trademark product and offers unparalleled performance, flexibility, and scalability.

#### Main Specifications:

- Analysis time: Up to 200 ns, allowing accurate simulation of real-time control systems
- Analog Signal Input Channels: 160 Channels
- Analog Signal Output Channels: 128 Channels
- Digital Signal Input Channels: 128 Channels
- Digital Signal Output Channels: 64 Channels
- Modelability: Supports a wide range of physical models, including electronic power devices, machines, and control systems
- Communication Interfaces: Ethernet, USB, CAN, and LIN

The Typhoon HIL 606 is a high-performance hardware-in-the-loop (HIL) simulator designed to meet the demanding requirements of applications

It is the company's flagship product and offers unparalleled performance, flexibility and scalability.

#### Main Specifications:

- Analysis time: Up to 200 ns, allowing accurate simulation of real-time control systems
- Analog Signal Input Channels: 160 Channels
- Analog Signal Output Channels: 128 Channels
- Digital Signal Input Channels: 128 Channels
- Digital Signal Output Channels: 64 Channels
- Modelability: Supports a wide range of physical models, including electronic power devices, machines, and control systems
- Communication Interfaces: Ethernet, USB, CAN,

#### and LIN Features:

- Hardware-in-the-loop (HIL) testing: Simulates the real-world environment of a system, allowing developers to test and fix problems in their control software without connecting it to the actual system.
- Power-HIL Test: Simulates the dynamic response of power electronics systems, including inverters, motors, and batteries.
- Modeling and simulation: Allows developers to create and test custom physical models of their systems.
- Real-time data acquisition and analysis: Collects and analyzes data from the simulated system to evaluate performance and troubleshoot.
- Scripting and automation: Enables the creation of automated sequences of tests and simulations.



Figure 44. Model HIL 606

The interface cards that are most commonly used in a HIL system are:

Let's add more details about Typhoon's interface cards for HIL systems:

#### 1. **DSP 180 Interface:**

- It has a bus with 24 analog outputs or 24 digital inputs and 16 digital outputs.
- It provides high performance for power electronics applications.
- It is used for fast application development.

#### 2. **Launchpad:**

- It is connected to a bus of 16 analogue outputs and 4 analogue inputs.
- It is used for communications and power delivery.
- It offers fast development of communications applications.

#### 3. **HIL Breakout:**

- It is used as a terminal board for the inputs and outputs of the HIL.
- Allows easy connection of control devices and sensors.

#### 4. **HIL dSPACE:**

- There are two types: type-A and type-B.

- The Type-A interface offers a direct interface between HIL devices.
- The Type-B interface does not provide a direct interface between HIL devices.

## 5. HIL Connect:

- It provides realistic simulation for inverters, control conditions, and sensors.
- It offers flexible connection to HIL.

Each interface card offers unique features and adapts to different HIL application needs. They are connected to the corresponding HIL I/O ports via DIN connections. In addition, each card has a USB port that is used to communicate between the microprocessor hosted on the card and the host. The model of the system under study is implemented on the host computer, and communication with the HIL is done through this USB port. In this way, the computer can control and monitor the operation of the HIL system and interact with it for various purposes, such as developing, validating, and auditing the system being tested.

Typhoon's Hardware In the Loop, as we understand it, covers a wide range of applications and offers the user multiple possibilities. When using this system firmware, two main environments are provided which we used during the laboratory experiments and implementation of our system.

### 1. Schematic Editor :

Schematic Editor HIL is a software that allows users to create and modify graphical circuits for HIL simulations. It is a powerful tool that can be used to:

Creating Circuits:

- Circuit design with drag & drop Accessories from a library of pre-built components.
- Add and modify component parameters.
- Connecting components with cables.
- Define trends, currents, and other metrics.

Circuit Modification:

- Changing the arrangement of the components.
- Processing of component parameters.
- Adding and removing components.

- Change cable connections.

Running Simulations:

- Run HIL simulations to see how the circuit works.
- Real-time measurement tracking.
- Analysis of simulation results.

Pros of Schematic Editor HIL:

- Ease of use: The graphical user interface (GUI) makes it easy to create and modify circuits.
- Flexibility: It can be used to create a wide range of circuits.
- Accuracy: Provides accurate simulation of circuit behavior.
- Time-saving: Helps save time and effort when developing and testing circuits.

Applications of Schematic Editor HIL:

- Education: It can be used for educational purposes to teach students how circuits work.
- Research: It can be used for research purposes to develop and test new circuits.
- Industry: It can be used in industrial applications to develop and test circuits for products.

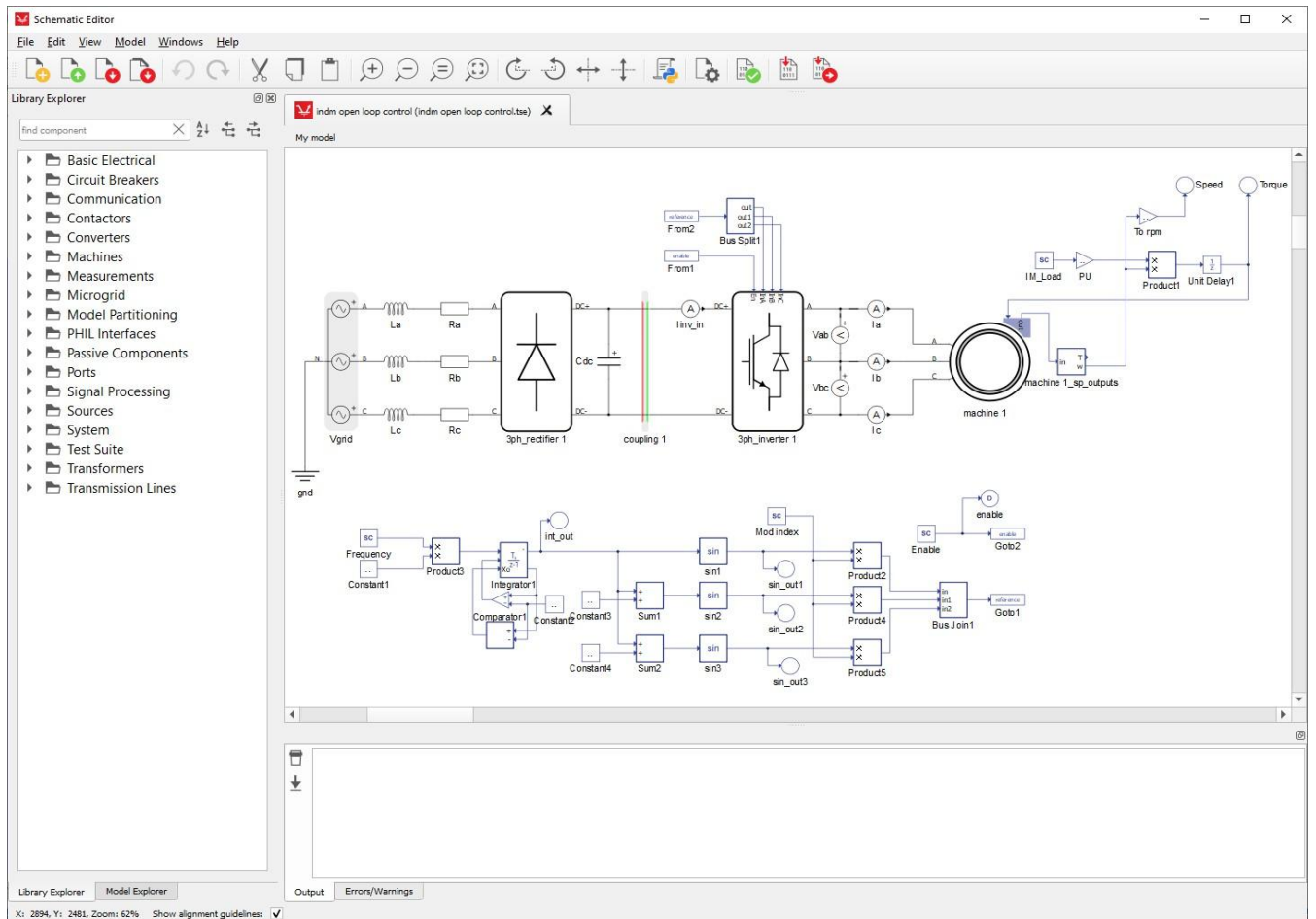


Figure 45. SCADA Environment

## 2. HIL SCADA :

HIL SCADA (Supervisory Control And Data Acquisition) is a graphical user interface (GUI) software that allows users to control and monitor Hardware-in-the-Loop (HIL) simulations. It provides an easy-to-use interface for:

- Control:
  - Configuration of the circuit.
  - Turning components on and off.
  - Insert control signals.
- Monitoring:
  - Real-time measurement display.
  - Visualization of circuit behavior.
  - Record simulation data.

## Advantages of HIL SCADA:

- Ease of use: The GUI makes it easy to control and monitor HIL simulations.
- Interactivity: Allows users to interact with the circuit in real-time.
- Flexibility: It can be customized to meet the needs of different applications.
- Powerful features: Provides a host of features for auditing, monitoring, and analysis.

## Applications of HIL SCADA:

- Education: It can be used for educational purposes to teach students how to control and monitor circuits.
- Research: It can be used for research purposes to develop and test new methods of control and monitoring.
- Industry: It can be used in industrial applications to control and monitor circuits in real-world systems.

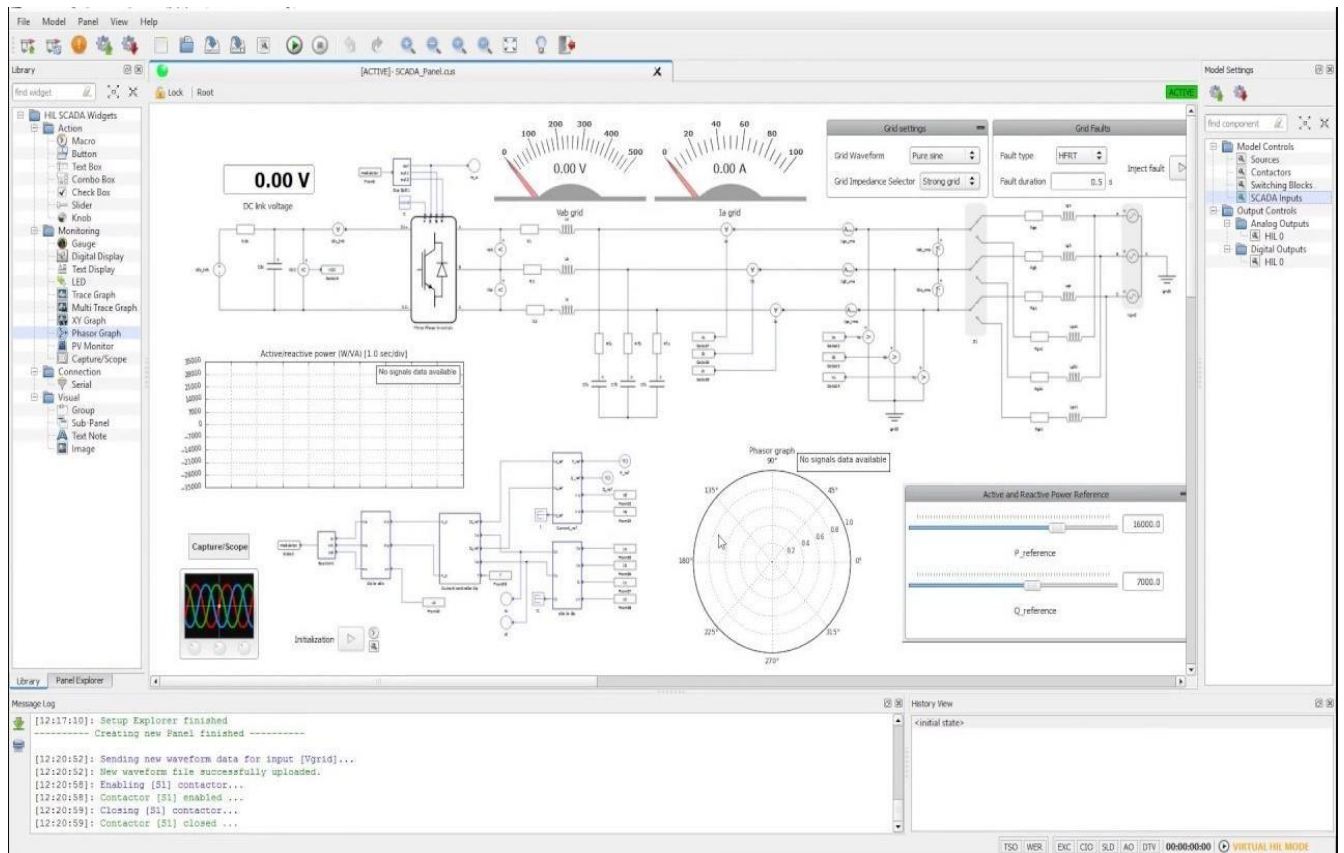


Figure 46. Environment and Gadgets Scada

In addition to the easy-to-use interface and the basic control and monitoring features, the HIL SCADA offers a number of specialized features that enhance its flexibility and efficiency. We can use a range of gadgets depending on what we want to analyze, We will look at some examples below to make it easier to understand.

**Macros:** Automate repetitive tasks with programmable scripts, saving time and effort. Perform complex tasks with one click, improving consistency and accuracy.

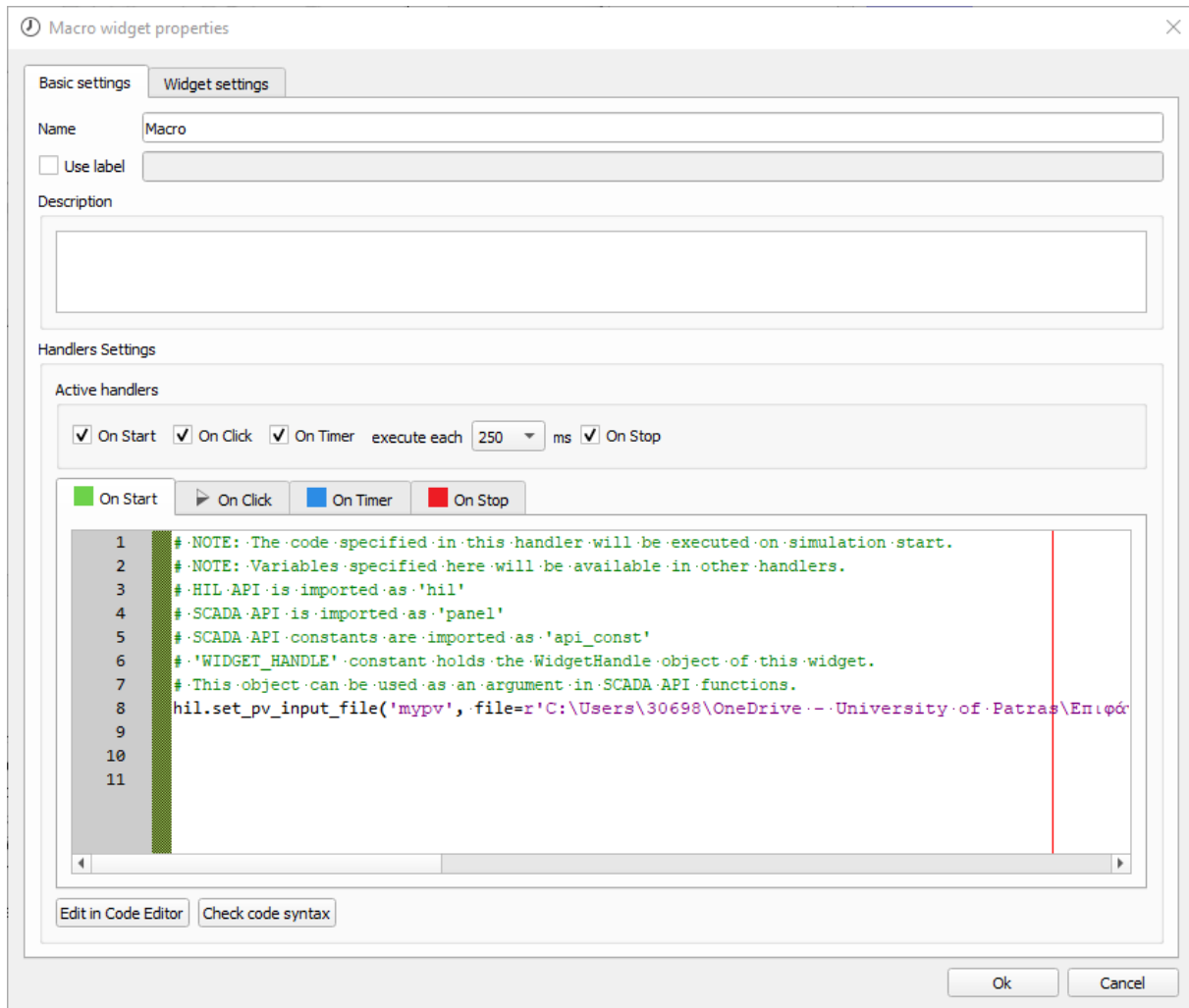


Figure 47. Macro Widget

As we can see in the image, there is the possibility of executing specific commands for our system in real time, either by starting the model, after clicking, or after a certain time, as well as stopping them.

**PV Monitor:** We monitor and analyze measurements in real time, identifying and troubleshooting problems during the simulation. In this way, we optimize the performance of the circuit and evaluate the behavior of the system under various conditions.

**Probes:** We place virtual sensors and meters at any point in the circuit to take measurements, obtaining detailed analysis and access to points that are not measurable in the real system.

**Trace Graphs:** We visualize the temporal evolution of measurements, identifying trends and currents, comparing the behavior of different measurements and evaluating the stability and response of the system.

**Gauge Widgets:** Display measurements in easy-to-use gauge widgets, quickly and easily track important metrics, visualize system behavior in real-time, and customize the appearance and operation of meters.

In our experiment, the model of the Typhoon Hardware In the Loop we used is the HIL402, which is a powerful and versatile Hardware-in-the-Loop (HIL) simulator used to develop and test power control systems. It offers a realistic and interactive platform for testing control systems in real-time, eliminating the need for costly and time-consuming prototypes.

#### **Features:**

- 4 Intel Xeon processor cores
- 16 GB RAM
- 256 GB SSD
- 2 x Gigabit Ethernet ports
- 4 USB 3.0 ports
- 1 HDMI port
- 1 VGA port
- Windows 10 IoT Enterprise Operating System

### *5.3 Circuit System Model in Typhoon Hardware In the Loop:*

The logic with which the model was designed is based on the connection of the photovoltaic array to the voltage boosting inverter, the inverter, and finally the main grid. As already mentioned, the control of this system is a key aspect of the design, since the voltage at which the PV output is raised and the amount of energy transferred to the grid through the Inventor are a key objective.

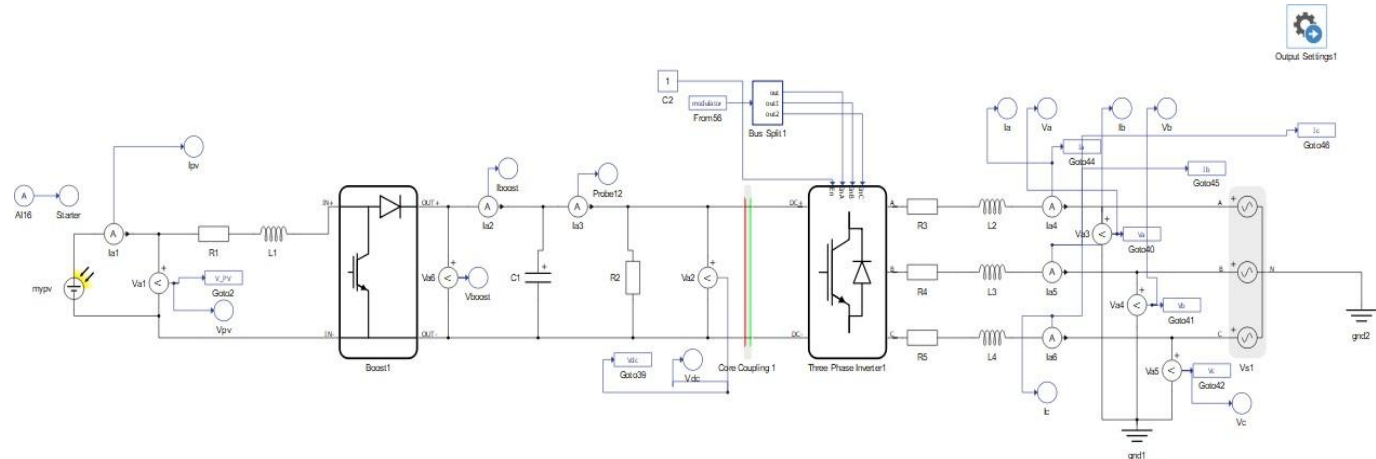


Figure 48.Schematic Editor of HIL

The overall implementation of the dispersed production system, which was designed using the Schematic Editor of the Typhoon HIL software, is presented in the image above. The flow of energy in the system is intended to be from the photovoltaic system to the main grid. So we first observe our photovoltaic array, in which the special scenario of partial shading is simulated, to be in line with the Voltage Lifting Inverter. It is worth commenting that this particular converter does not receive pulsation from any element in the Schematic Editor but is controlled by Digital Inputs. This means that it is controlled by the Texas Instruments C2000 microcontroller that we connect to the HIL, and which is responsible for properly raising the voltage at the Inventor input.

Then there is the DC Bus and as we observe, there is a circuit element called Core Coupling. Core Coupling in the Hardware In the Loop (HIL) Schematic Editor is a feature that allows users to connect two or more processing cores into a single system. This can be used to:

### 1. Performance Improvement:

- Multi-cores connection can distribute the computational load, improving the speed and performance of the simulation.
- This is especially useful for complex circuits that require significant computing power.

### 2. Capacity Increase:

- Multi-cores connection can increase the number of variables and signals that the simulations can handle.

- This allows users to simulate larger and more complex circuits.

### 3. Implementation of complex functions:

- Multi-cores connection can implement complex operations that require parallel processing.
- This can be It includes artificial intelligence algorithms, image processing and other high-performance processing.

On the right side of the system, we see the placement of the Inverter, which is pulsed by an Internal Modulator and not a microcontroller such as the Boost, the control of which we will analyze at a later stage, while of course the presence of the RL Filter and the simulation of the main network could not be missing. The different control mode between the two converters aims to highlight the possibilities offered to the user by this Typhoon Firmware system, and the harmonious connection of these two models. At the same time, the existence of 2 different ways of control functioned as an educational tool, contributing to a deeper understanding of its capabilities and differences in control methods as it offered a valuable opportunity for comparative evaluation of their performance and behavior, bringing to light the advantages and the Disadvantages every Method. We also notice that in all parts of the system there is a plethora of probes, which enable us to monitor and analyze the desired signals, which in our case are mainly currents and trends.

Finally, by using the Block Output Settings, the system model is connected to the real-time Hardware In the Loop.



Output Settings

More specifically, using this function, we are given the opportunity to connect the HIL device to the microcontroller and then our Laptop and through the Code Composer Studio, to monitor the changes and values that various parameters receive. We chose to analyze in this way the voltage values in the DC Bus as well as the voltage and current in the Photovoltaic Array. Therefore, when connecting the Typhoon HIL to the microcontroller, we use 1 pin for connection to Digital Input which aims to pulse the voltage booster inverter and 3 pins as Analog Ouput which serve to measure the above signals.

## *5.4 Shapes Control Converter System Power:*

Analyzing above the circuit model of the system we created, we referred to the different way in which we chose to implement the control and pulsation of the two inverters. The control of the voltage reversal converter is done with the circuit implementation in the Schematic Editor and follows the course we followed in chapter 3.

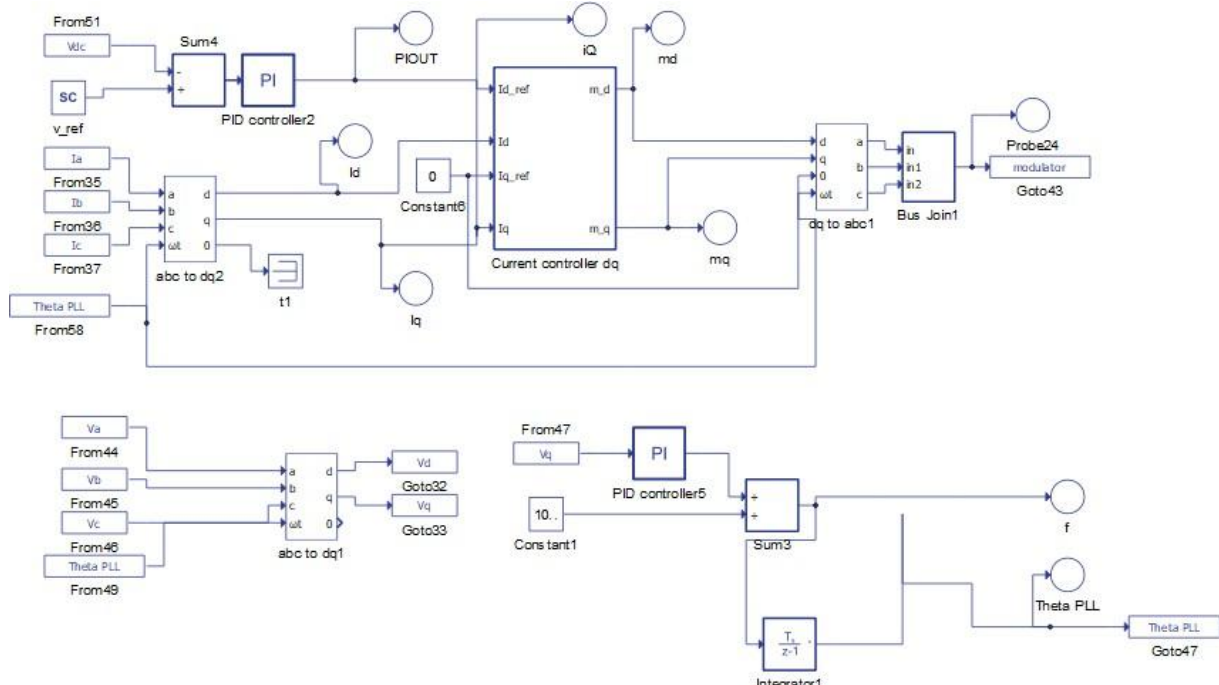


Figure 49.Inverter Control Design in Schematic Editor

More specifically, in the image above we can see how the controls on the load side are implemented. At the bottom of the image is the control for the operation of the phase lock loop (PLL) from which the desired Theta PLL angle is produced, which is required to complete at the controller output and enter the Park transform. Also On the upper left side of the image, the external voltage control loop is implemented. We use a SCADA INPUT component to define the reference voltage, so that we are able to make changes in real time through the HIL SCADA environment and observe the stability of our system and the response time of the control system we have built. The internal current control loop is implemented inside the Block called the Current Controller and is shown below.

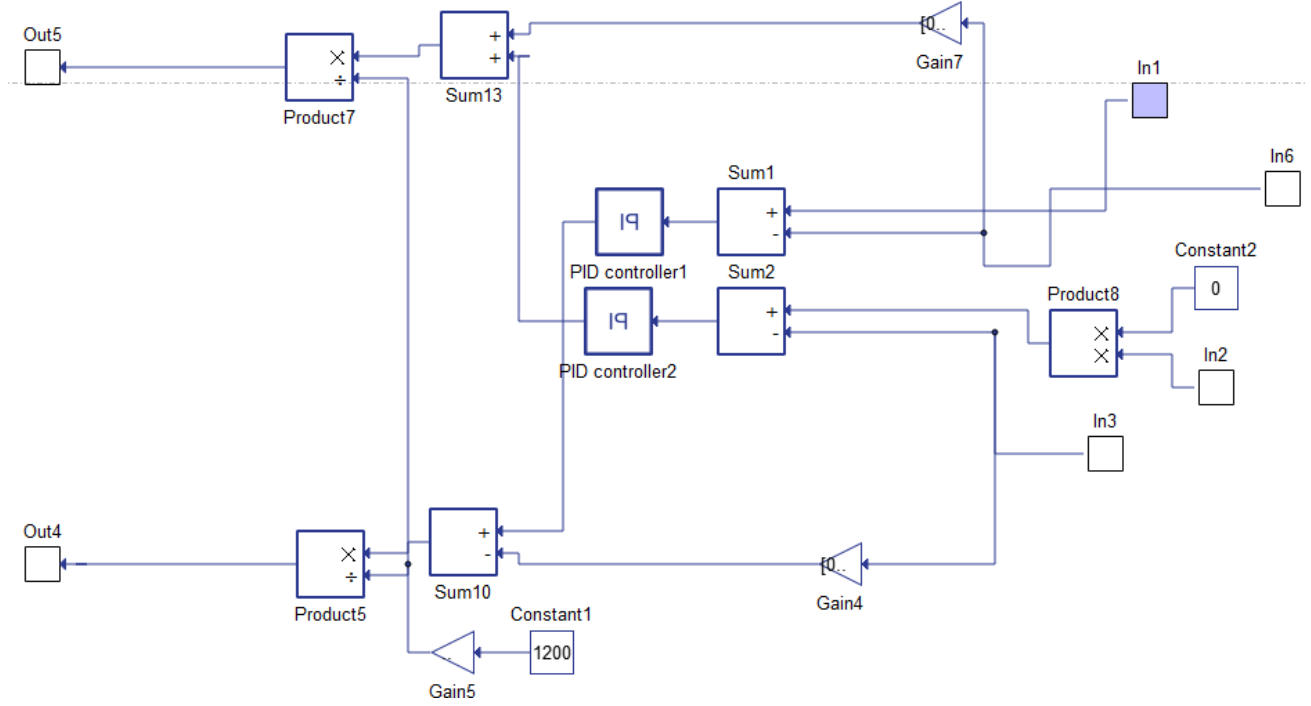


Figure 50. Internal Control of Current Components  $d, q$

The mathematical tools and the logic behind the design of these controllers have been described in detail in Chapter 4, which is why their explanation will be omitted at this point.

On the contrary, the control of the voltage lifting converter is done by creating a Simulink file in which we implement the appropriate connections, "load" it to the microcontroller and the pulsation is done through it by connecting a Digital Input to the HIL. Then, by receiving through Analog Outputs from HIL the values for the photovoltaic current, its voltage, and the voltage of the DC Bus, We use this FeedBack to recharge the control parameters and drive the system to the desired state. We list images of the control system created in MATLAB Simulink.

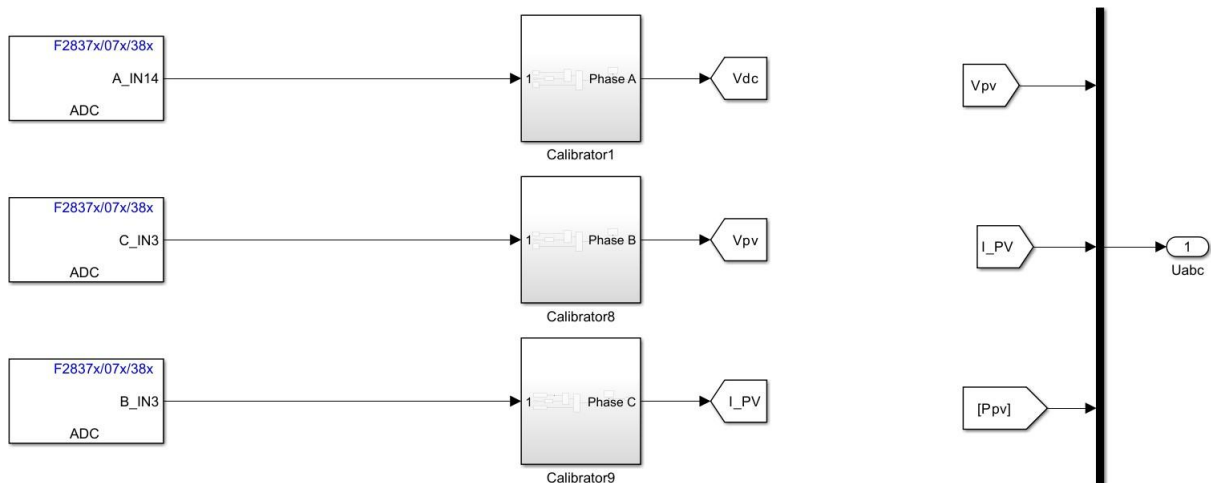


Figure 51. Microcontroller inputs in Simulink

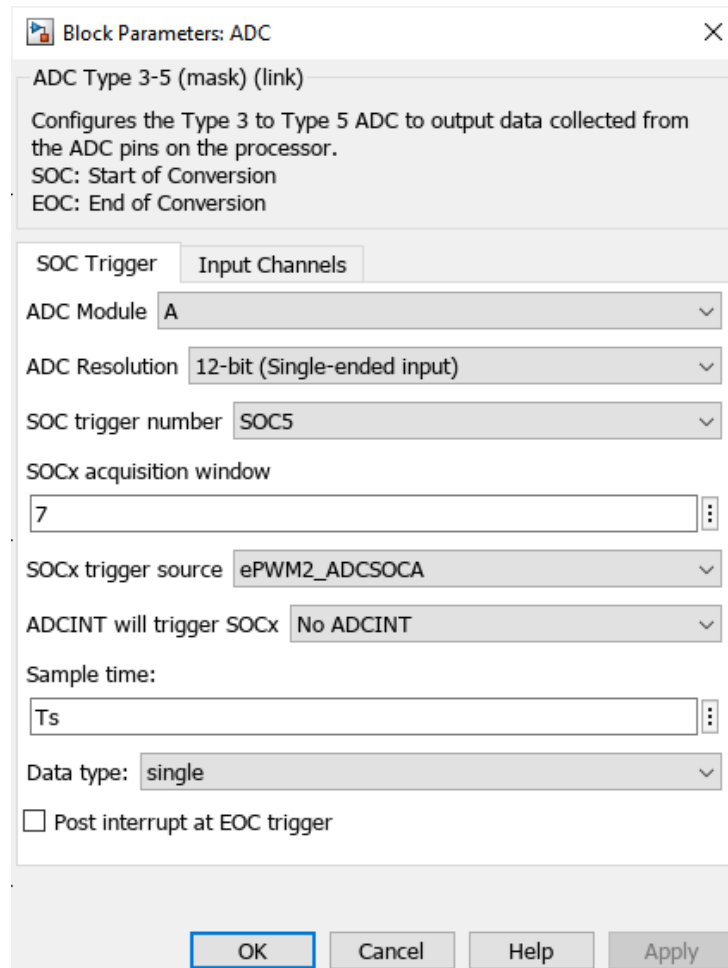


Figure 52. Block Parameters of ADC Block

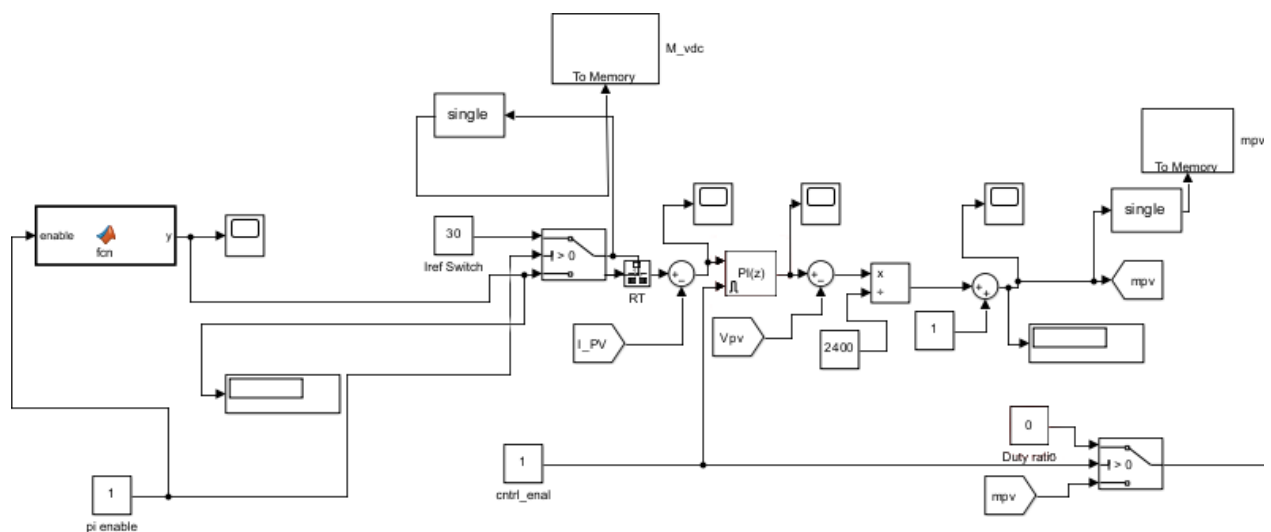


Figure 53. Controlling the Inventor in the Simulink Loaded on the Microcontroller

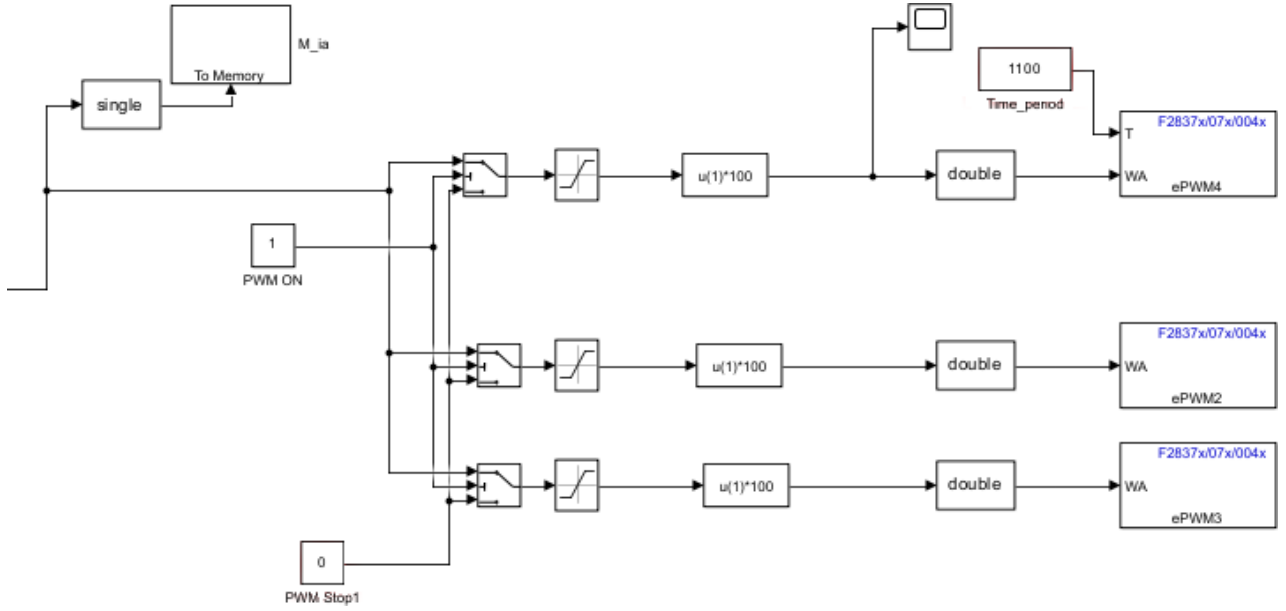


Figure 54. Checking the Inventor in the Simulink Loaded on the Microcontroller

In the first image we see the blocks that enter the measurements of the current and voltage of the PV, as well as the voltage of the DC Bus. As we see in the second, there we define the connection with the microcontroller, i.e. from which pin of the board we will get the corresponding size as well as other characteristics, such as the sampling time. In the third and fourth we present the control, more specifically, we start with the MATLAB FUNCTION BLOCK in which each time we place the algorithm with which we want to control the voltage lifting inverter, whether it is Perturb and Observe, or Particle Swarm Optimization. If we observe carefully, we will distinguish the presence of certain control blocks that aim to enable and disable functions such as PI controllers, Duty Cycle selectors (whether it receives a value that we set arbitrarily or the exit from control) and other elements such as the Rate Transmition Block. The Rate Transition Blocks (RTB) in Simulink are used to manage rates sampling in different parts of a model. Essentially, they act as bridges between subsystems running at different frequencies, ensure that data is exchanged in a synchronized manner, avoiding rate incompatibilities, handle any data loss that may occur, and allow easy modification of the sampling rate in any subsystem, without affecting the rest of the model. They therefore offer simplicity, flexibility, accuracy and stability. In our case, we used RTB to ensure compatibility between the sampling rate of the MPPT control algorithm and the sampling rate of the system. Thus, by applying all of the above, we manage during the experiment through Code Composer Studio to change the way the system works, and to observe the various changes as well as to confirm the correct functioning of our control. last image, we see the blocks with which the pulses are loaded as digital outputs and enter through the C2000 into the HIL 402 that we used for pulsation

of Boost. The above is achieved by Build this model on the microcontroller using TI Delfino F28379D LaunchPad.

## 5.5 The C2000 Launchpad XL tms320f28379d microcontroller:

### 5.5.1 Import:

The C2000 Launchpad XL TMS320F28379D is a powerful development tool for digital control systems. It is based on Texas Instruments' TMS320F28379D microcontroller, which offers high performance, flexible configuration, and a multitude of peripherals.

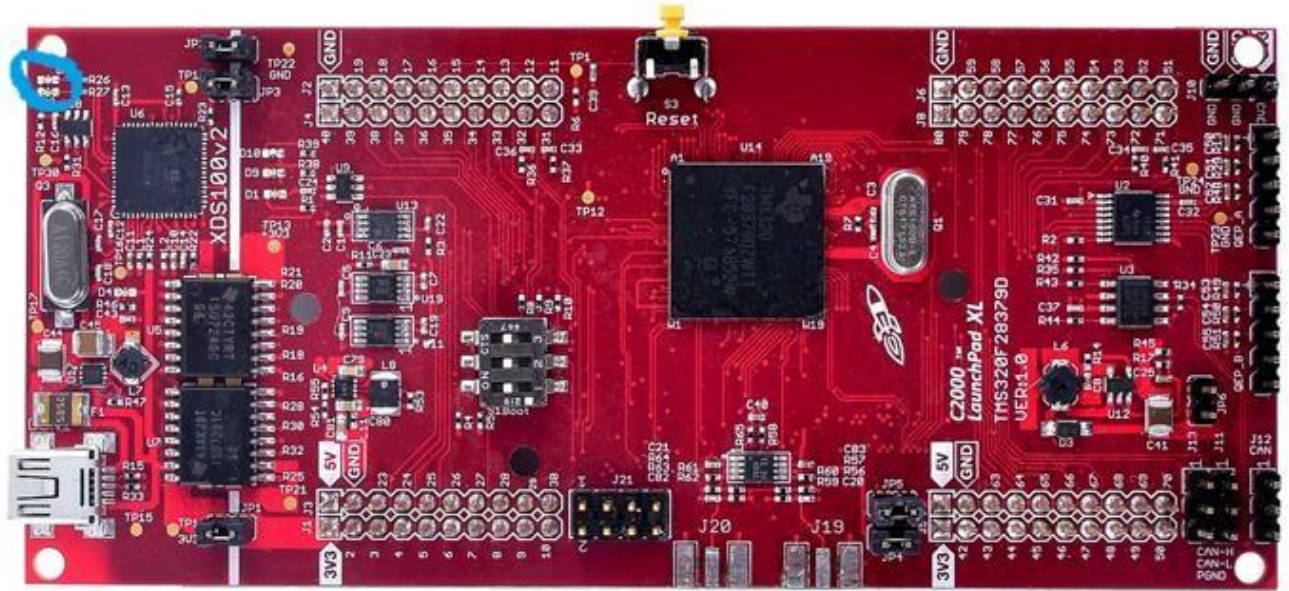


Figure 55. The C2000 LaunchPad microcontroller

### 5.5.2 Features:

Processor:

- Type: TMS320F28379D
- Architecture: C28x
- Speed: 32-bit, 100 MHz
- Resolution: The processor offers high speed and power, necessary for the implementation of MPPT algorithms and the control of the photovoltaic system. The 32-bit architecture and high operating frequency ensure fast data processing and flawless operation.

Memory:

- Flash: 256 KB
- RAM: 128 KB

- Resolution: The available memory is sufficient to store the system's code, data, and measurements. Flash memory retains the code even after the power supply is disconnected, while RAM provides quick access to essentials

Regional:

- ADC: 12-bit, 16-channel
- DAC: 12-bit, 2-channel
- PWM: 6 outputs
- SPI: 2 modules
- I2C: 2 modules
- UART: 2 modules
- USB: 2.0
- Ethernet: 10/100 Mbps
- RTC: Real-time clock
- Analysis: A variety of peripherals allows:
  - Connection to a number of sensors and actuators.
  - Communication with computers and other systems.
  - Digital control of the boost converter.
  - Storage of data in memory.
  - Networking and remote access.

### ***5.5.3 Applications:***

- Industrial Control:
  - Drive systems: Motor control, servo drives, speed controllers.
  - Automation: Industrial processes, robotic production lines, assembly systems.
  - Robotics: Controlling robots, arms, manipulators.
- Energy Systems:
  - Photovoltaics: MPPT control, voltage regulation, monitoring.
  - Wind: Turbine control, power adjustment, yaw control.
  - Smart grids: Energy management, power control, monitoring.
- Signal Processing:
  - Digital filters: Noise filtering, signal analysis, signal quality improvement.
  - FFT: Frequency analysis, harmonic finding, frequency identification.
  - Spectrum analysis: Study of signal spectrum, find characteristics, identify components.
- Integrated systems:
  - Medical devices: Imaging devices, patient monitors, medical instruments.
  - Telecommunications: Networking systems, routers, switches, base stations.
  - Electronic vehicles: Engine control, battery, safety systems.

### **5.5.4 Advantages:**

- High performance: The TMS320F28379D offers high processing speed and support for floating-point operations.
- Flexible configuration: The Launchpad XL includes a variety of jumpers and headers for easy connection to sensors, actuators and other peripherals.
- Number of peripherals: The Launchpad XL has a number of built-in peripherals for digital control systems.
- Connectivity: The Launchpad XL supports Ethernet and USB 2.0 to communicate with other systems.
- Educational environment: Launchpad XL comes with a host of educational resources, tutorials, and software libraries.

### ***5.5.5 Detailed use his C2000 Launchpad XL In the photovoltaic experiment:***

As part of the experiment, the C2000 Launchpad XL TMS320F28379D was used to control and monitor a grid-connected photovoltaic (PV) system.

#### **Pulse Boost:**

- The microcontroller implemented MPPT (Perturb & Observe or Particle Swarm Optimization) algorithms for maximum power extraction from the photovoltaic arrays.
- The PWM signal, based on the algorithm, adjusted the power switch on the boost converter, ensuring a constant DC voltage at the DC link.
- The PWM frequency and pitch adjustment (for P&O) were appropriately adjusted for optimal operation.

#### **Communication:**

- The Launchpad acted as a communication hub, taking measurements from sensors (e.g., current, voltage) and sending commands to the HIL
- The USB port was used to connect to a computer, download data, display graphics, and store for later analysis.
- We used the pins to connect between the microcontroller and the HIL, depending on whether the theme signal was Digital or Analog and Input or Output.

**Data processing:** The microcontroller performed real-time calculations to monitor and optimize the performance of the PV system.

- Measurement of power, voltage, current, and other quantities.
- Application of MPPT algorithms for maximum power extraction from the PV panels.
- Save data in memory for later analysis.

# CHAPTER 6: Simulations

## 6.1 Import:

In this chapter we will analyze the system we created in the simulations using the MATLAB SimPower library. The systems are divided into two main categories, that of normal shading and that of partial shading. For each of them we created the model in Simulink and ran simulations, while also to find the maximum operating point of the photovoltaic array we created the models from which we extracted the P-V and I-V characteristics. This is achieved by seriously connecting a power source to the photovoltaic array and taking appropriate measurements.

## 6.2 Photovoltaic Array without Shading:

The system we created in Simulink for the scenario where a photovoltaic array is under normal shading conditions is the following:

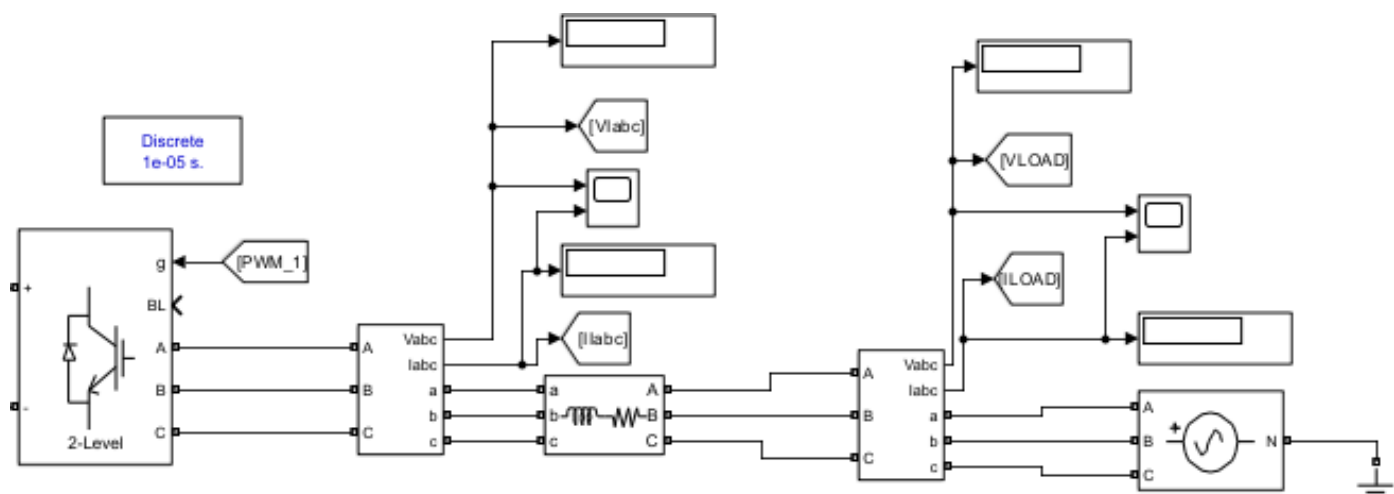
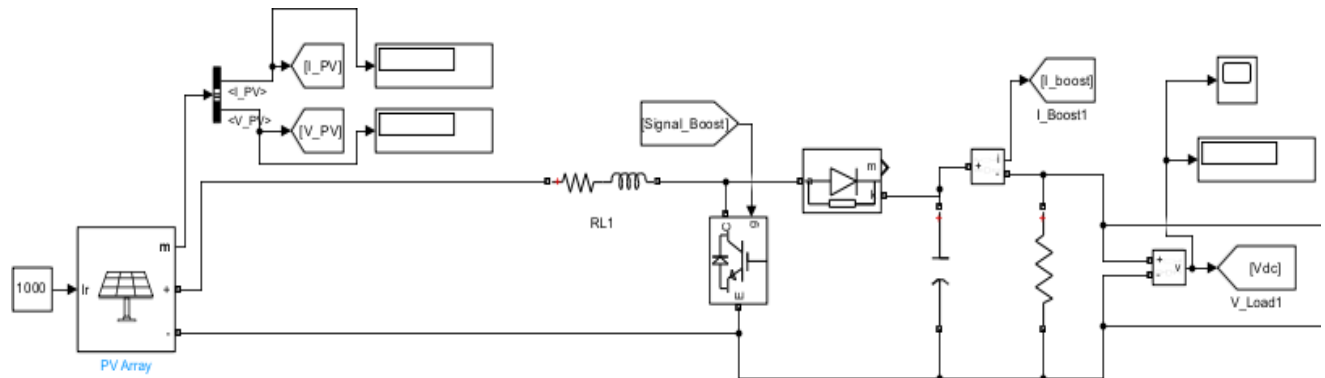


Figure 56. Simulink Model System

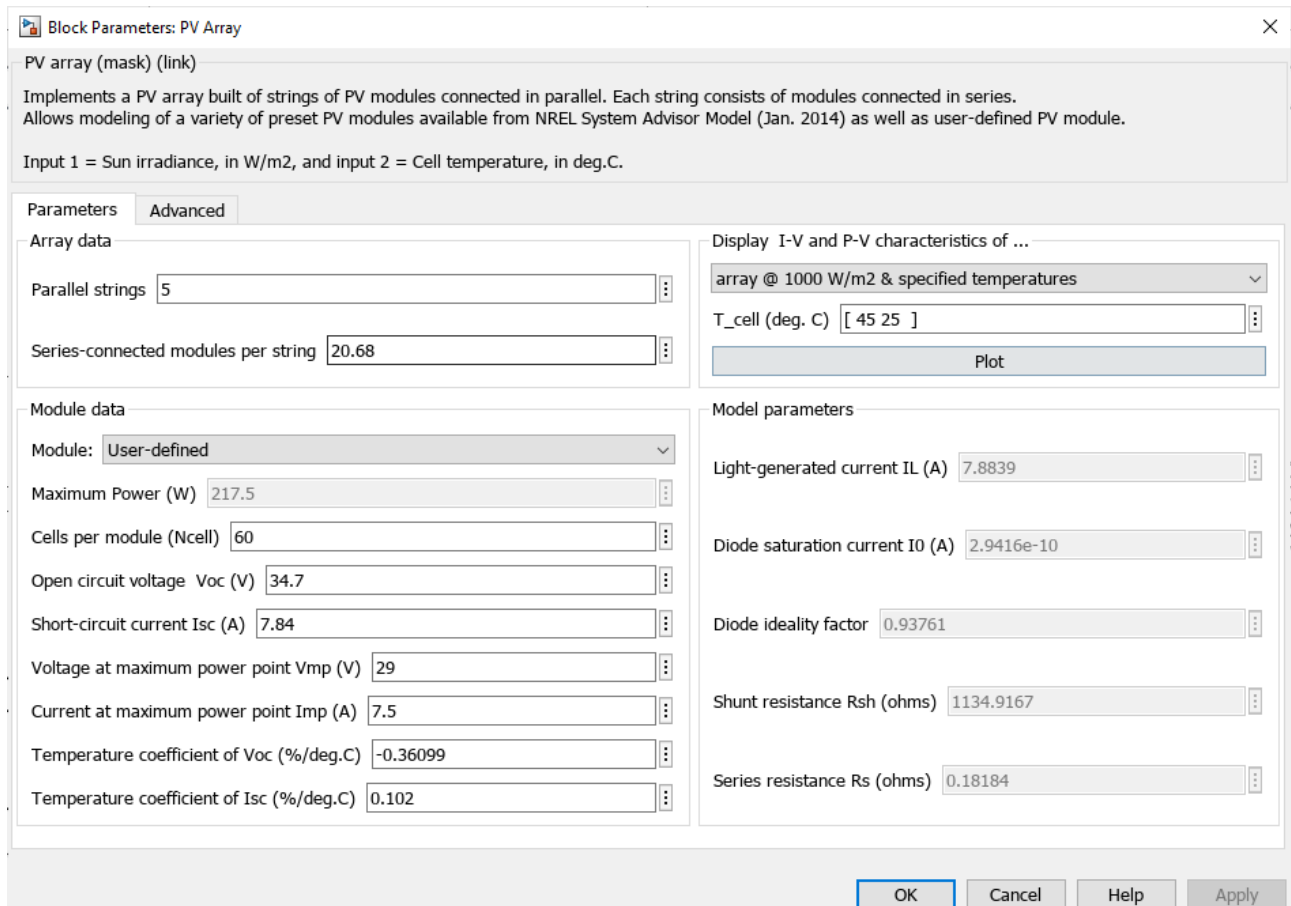


Figure 57.Photovoltaic Array Parameters

In the images above, we can see how we connect a photovoltaic array to the grid. Immediately after the PV there is an RL filter that precedes the connection to the Boost Voltage Booster converter. Then there is the Two Level Converter, Voltage Inverter and an RL filter to reduce the harmonics before connecting to the grid. Along the model we observe a series of meters from which we get values for Current and Voltage of the photovoltaic, the voltage of the DC Bus and other variables which will serve us in the control but also in our general image for proper operation. It is also worth noting that our system is characterized by a discrete time simulation with a step of 1e-5s, and the characteristics of the photovoltaic array were chosen so that at the output we have a voltage close to 1200Volt which is the desired voltage for the DC Bus. operate with a duty cycle close to 0.5 for optimal operation, therefore

from the formula  $\frac{V_{out}}{V_{in}} = \frac{1}{1-d}$ , it follows that  $V_{in} = 600\text{ Volt}$ , therefore

$\frac{V_{in}}{V_{MPP}} = 20.68$  photovoltaics in series to achieve 1200 Volt with 0.5 Duty Cycle.

We have analysed the audit for this system in Chapter 4 and it is presented as follows:

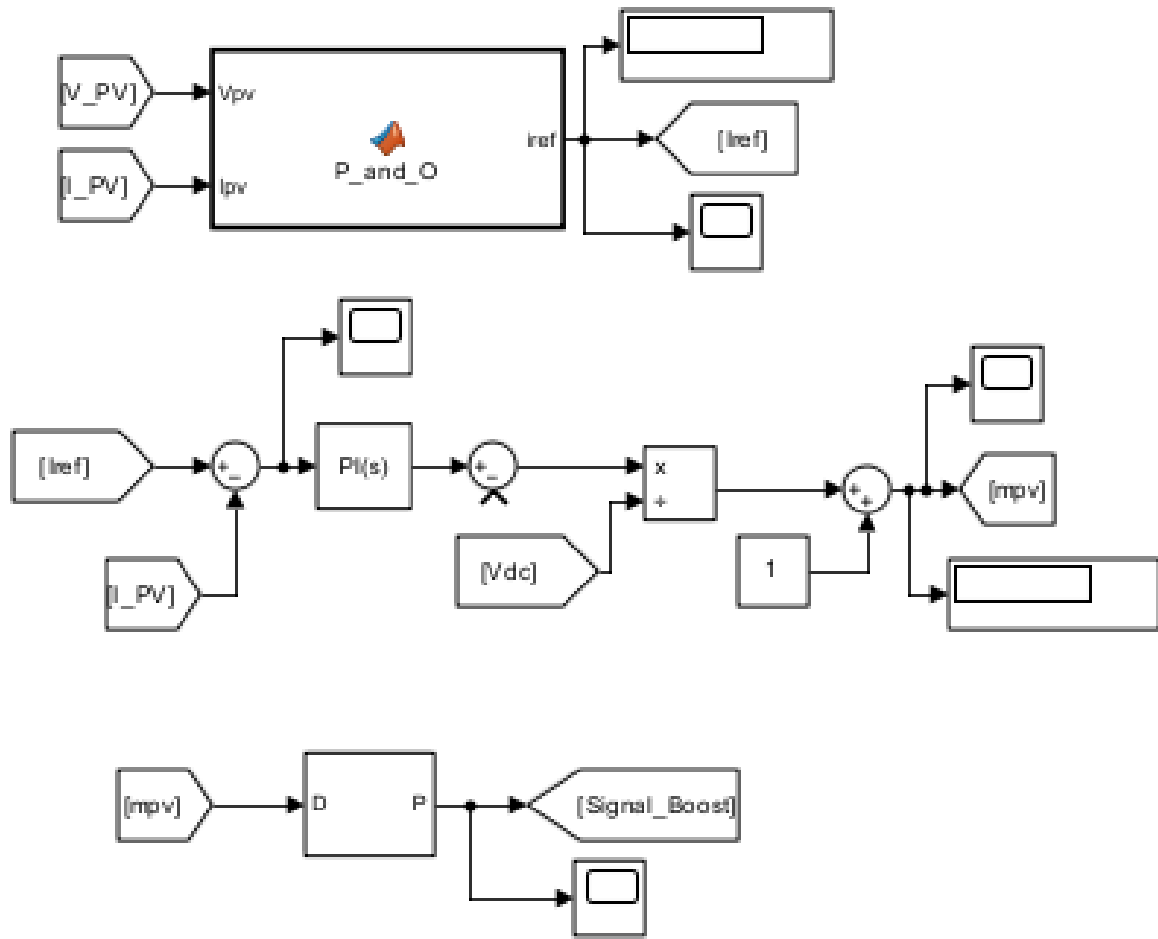
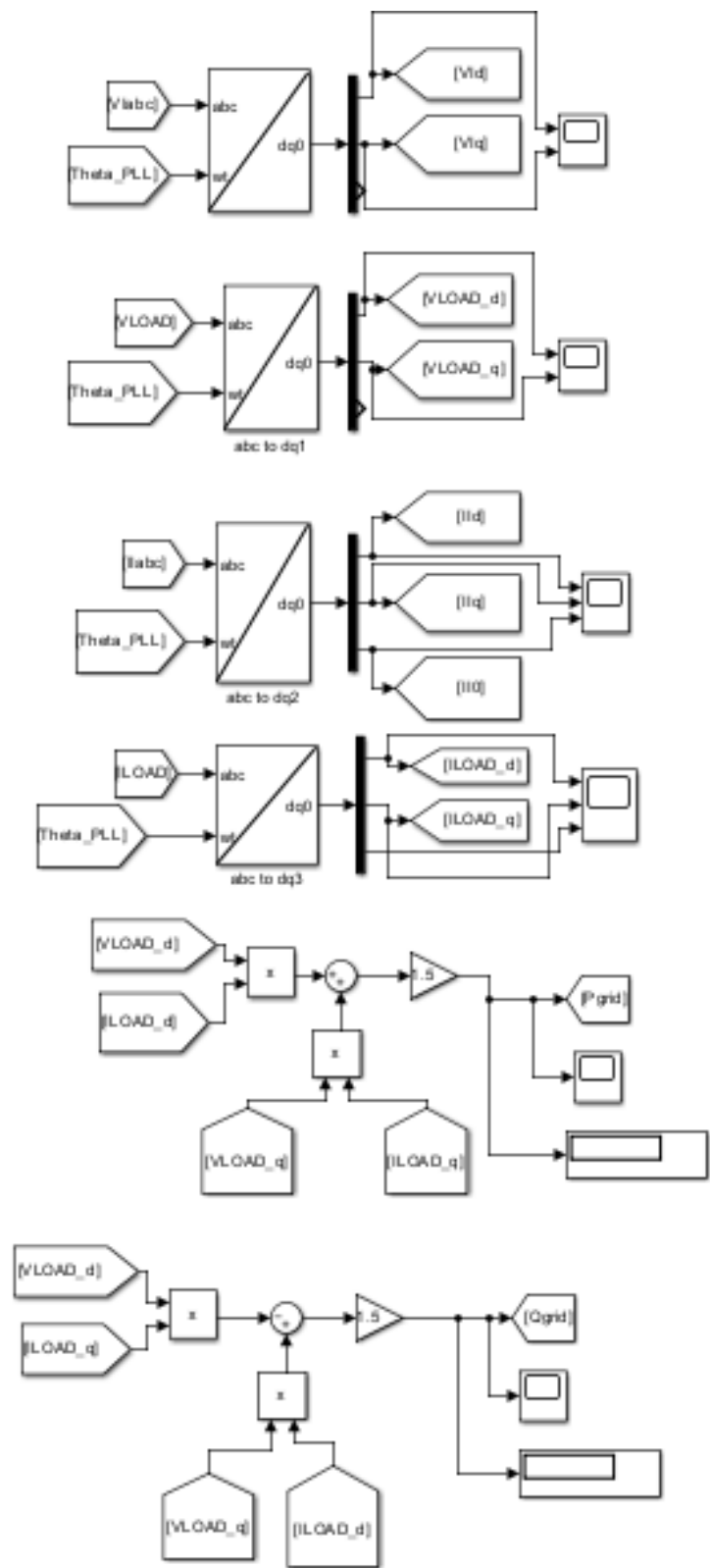


Figure 58. Checking Boost Converter in Simulink

Here we see the MATLAB Function Block which contains the desired algorithm, in this particular snapshot Perturb and Observe, and the internal current control loop from which we finally receive the pulse of the Boost.



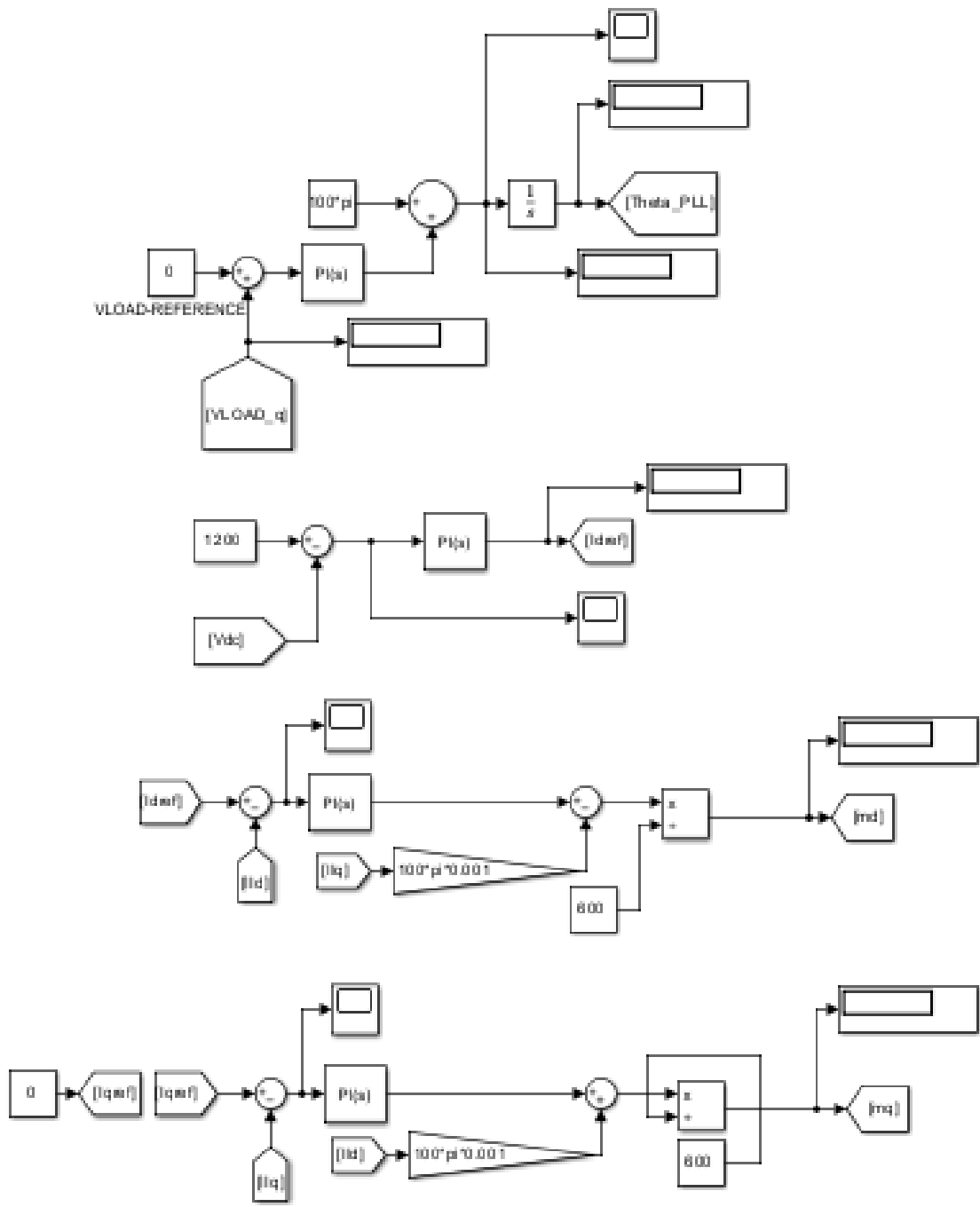


Figure 59. Inverter Control and Network Synchronization in Simulink

The 2 images above show the load side control, the internal current control loop and the external voltage control loop as well as the PLL, the Park transforms and the calculations required to extract the necessary quantities for the control, which ultimately lead to the pulse of the inverter and the finding of the Active and Reactive Power value that characterizes the network side.

In order to be sure of the proper functioning of our system and the algorithms for finding the maximum power output point, we will extract the characteristics

equations of the photovoltaic array. To achieve this, we will connect a power source in series as in the image below:

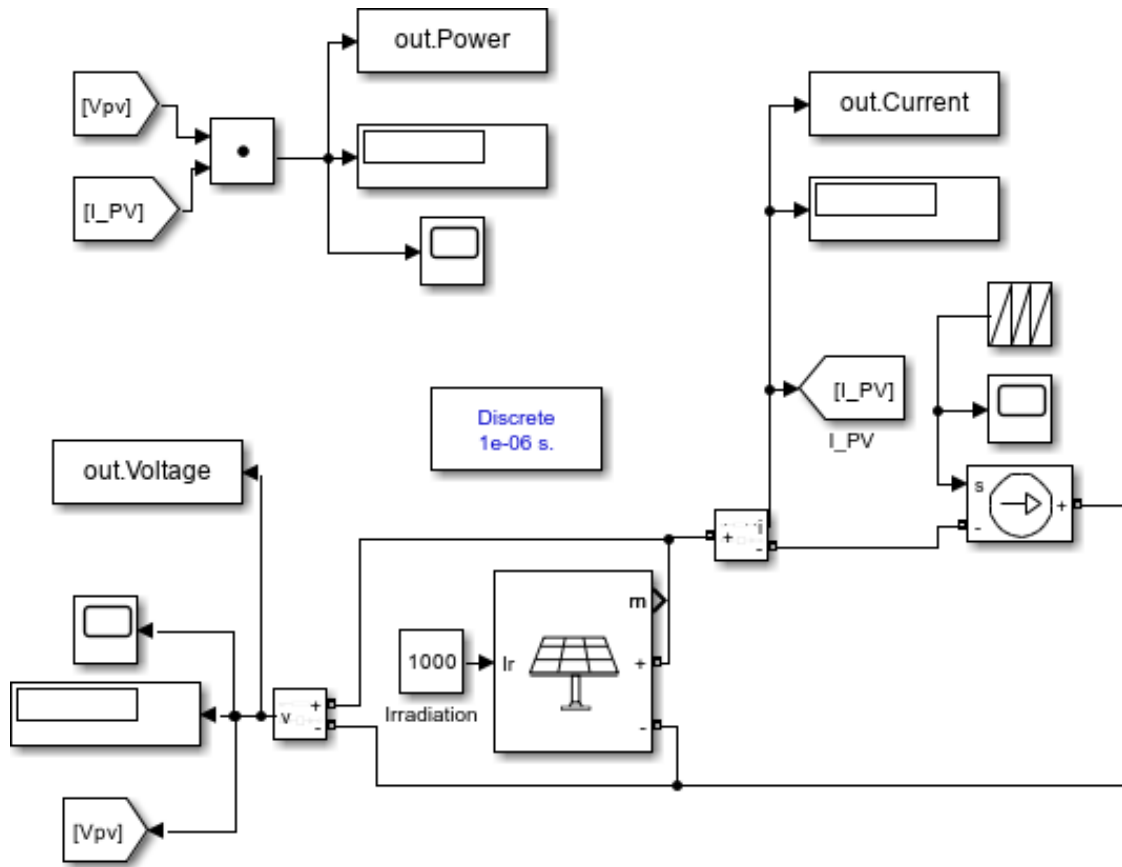
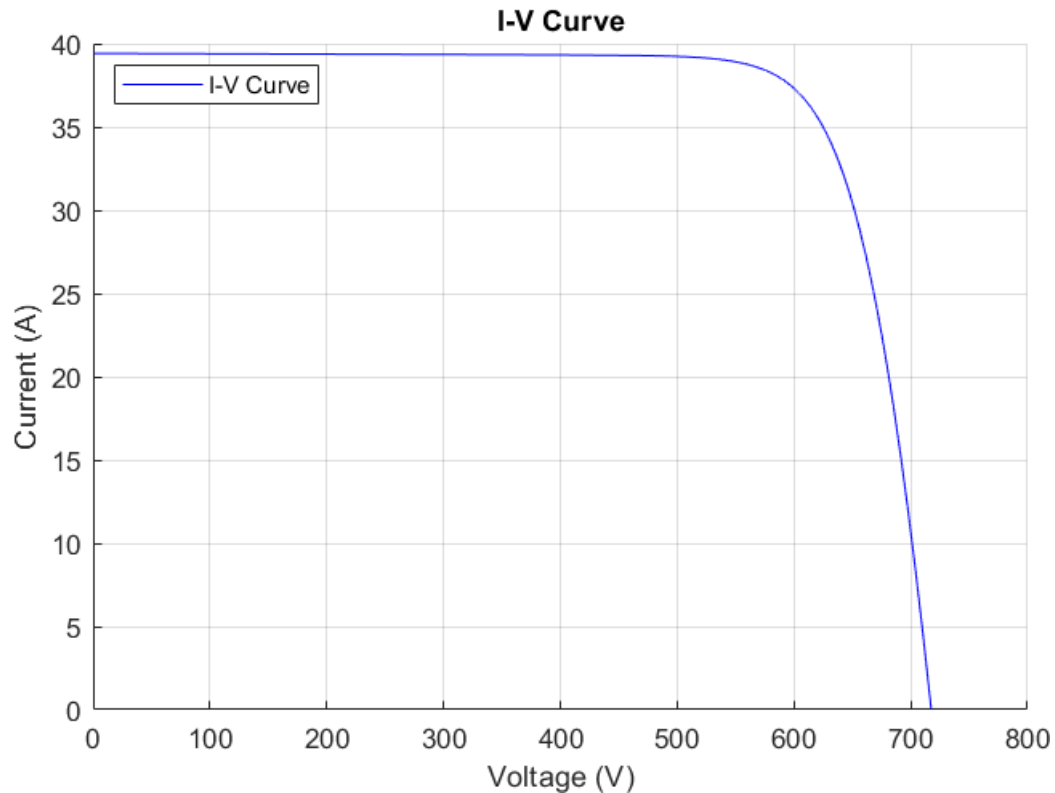


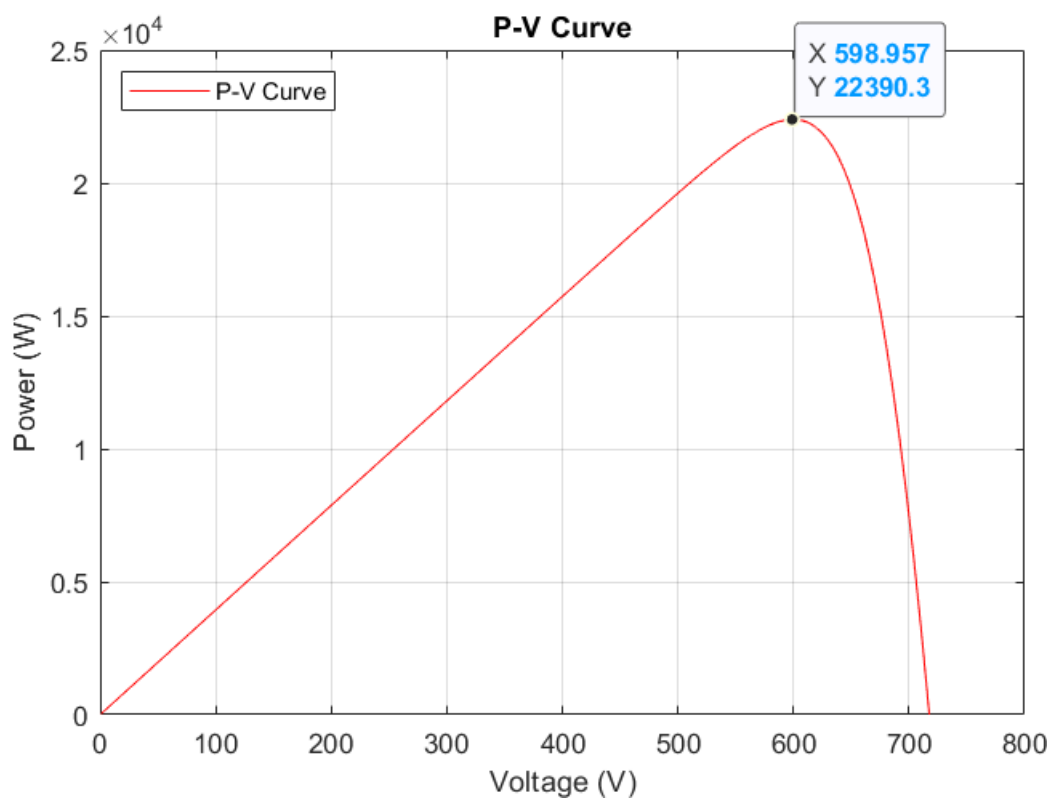
Figure 60. Photovoltaic System Characteristics Extraction Model under Normal Shading Conditions in Simulink

From the above simulation we get the following graphics for the characteristics:

### System Characteristics



### System Characteristics

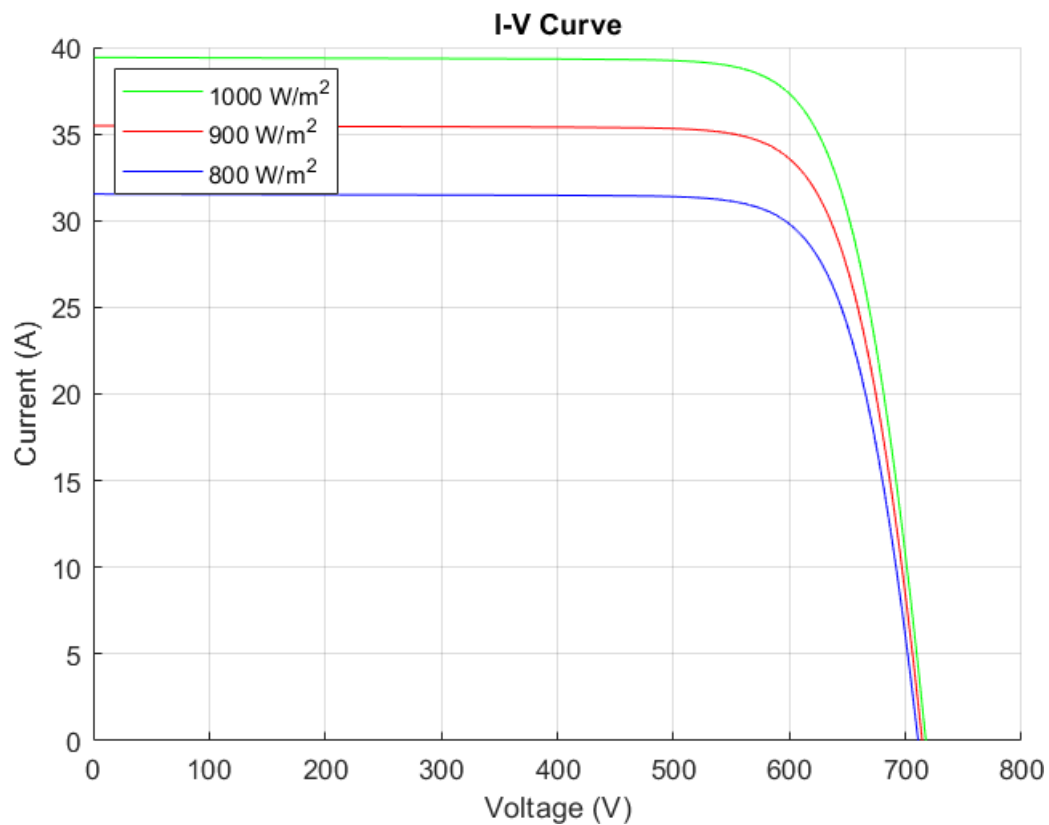


From these we can distinguish the basic characteristics of the system, namely the open circuit voltage, the short-circuit current and most importantly the operating point of maximum power production which, as we can see, is located at 22.39kW with a voltage of 598.95 Volts.

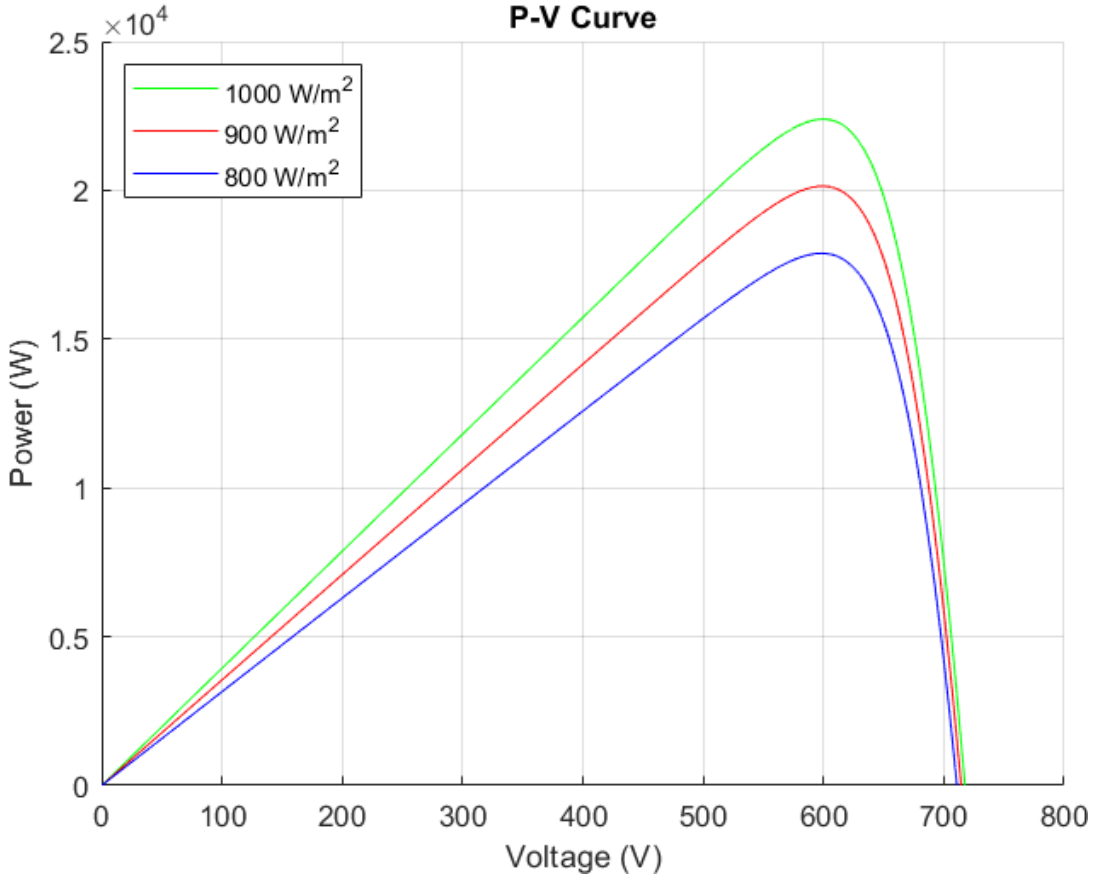
### ***6.2.1 Photovoltaic Array without Shading, radiation change scenario:***

In this scenario we will compare the different responses that result from the system when we apply 800, 900 and 1000 W/m<sup>2</sup> radiations to it.

## System Characteristics



## System Characteristics



We observe in the above characteristics, as expected, that with the increase of incident radiation in the photovoltaic panels, the power production increases at the maximum point of production. However, it is worth noting that this is almost in the same operating voltage as differences in current. We also distinguish the differences in short-circuit current, for 1000 W/m<sup>2</sup> it is at 39.41 Amper, for 900W/m<sup>2</sup> it is at 35.47 Ampere and finally 800W/m<sup>2</sup> is at 31.53 Amper. On the contrary, the open circuit voltage is in all cases almost at the same value, close to 715 Volts.

### 6.3 Photovoltaic Array under Partial Shading Conditions:

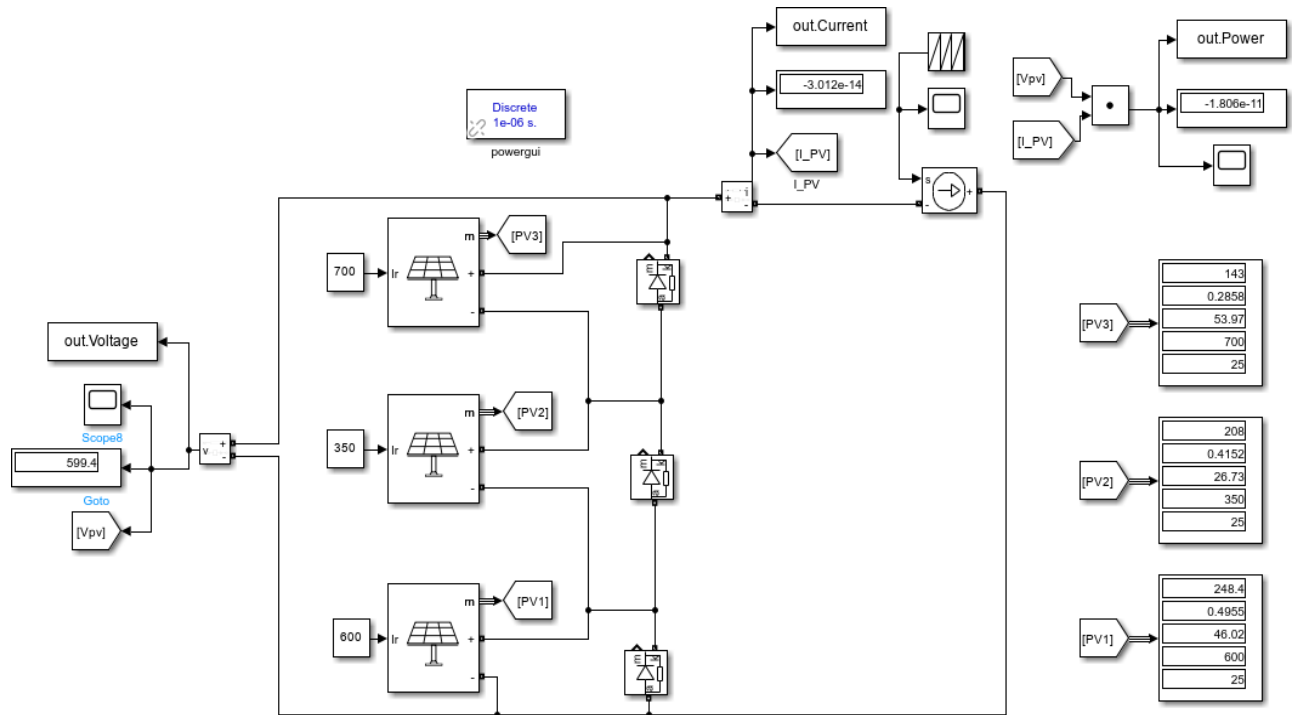


Figure 61. Photovoltaic System Characteristics Extraction Model under Partial Shading Conditions in Simulink

In the system we see above, we observe the connection of three photovoltaic arrays in series, each of which receives different radiation. At the same time, in each of them there is a Bypass diode, and in line with this system a controlled power source and the corresponding meters. Including the losses presented in the system as mentioned in Chapter 2, we compare for these two cases the characteristic P-V, I-V.

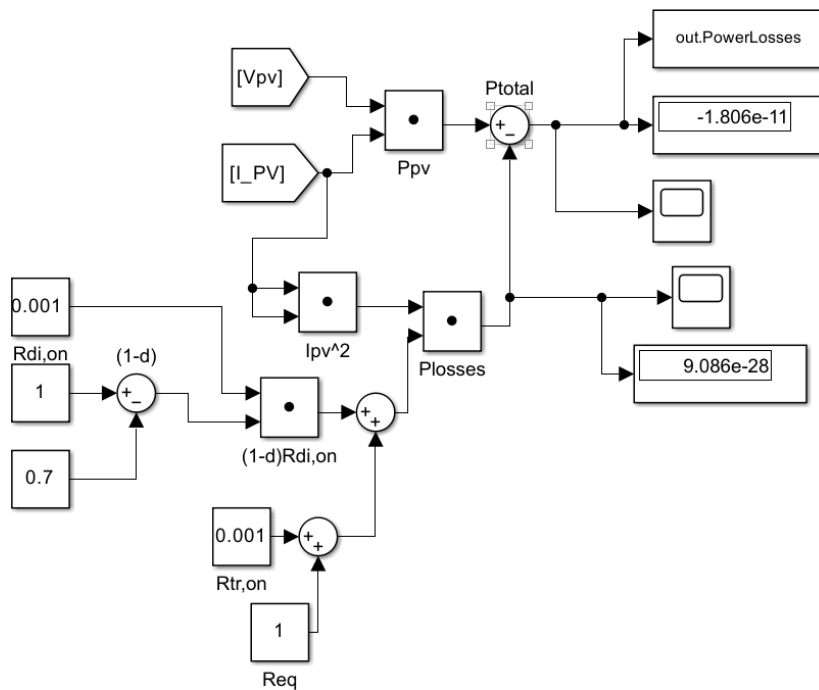
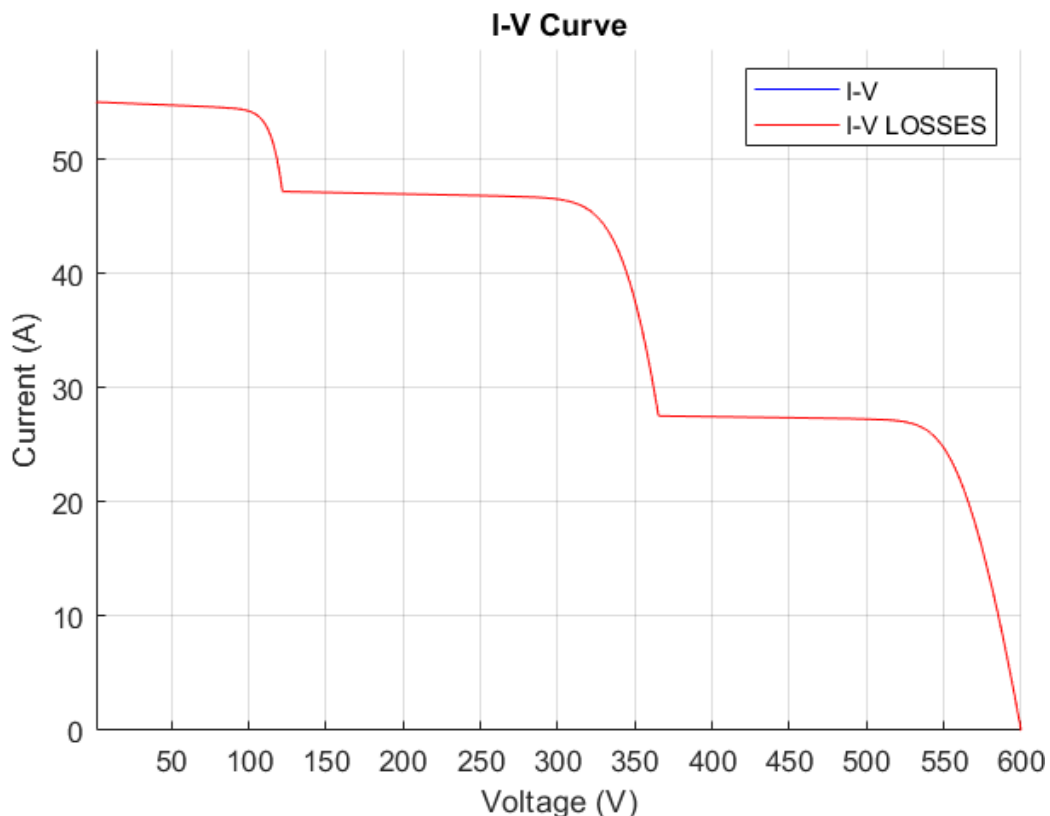
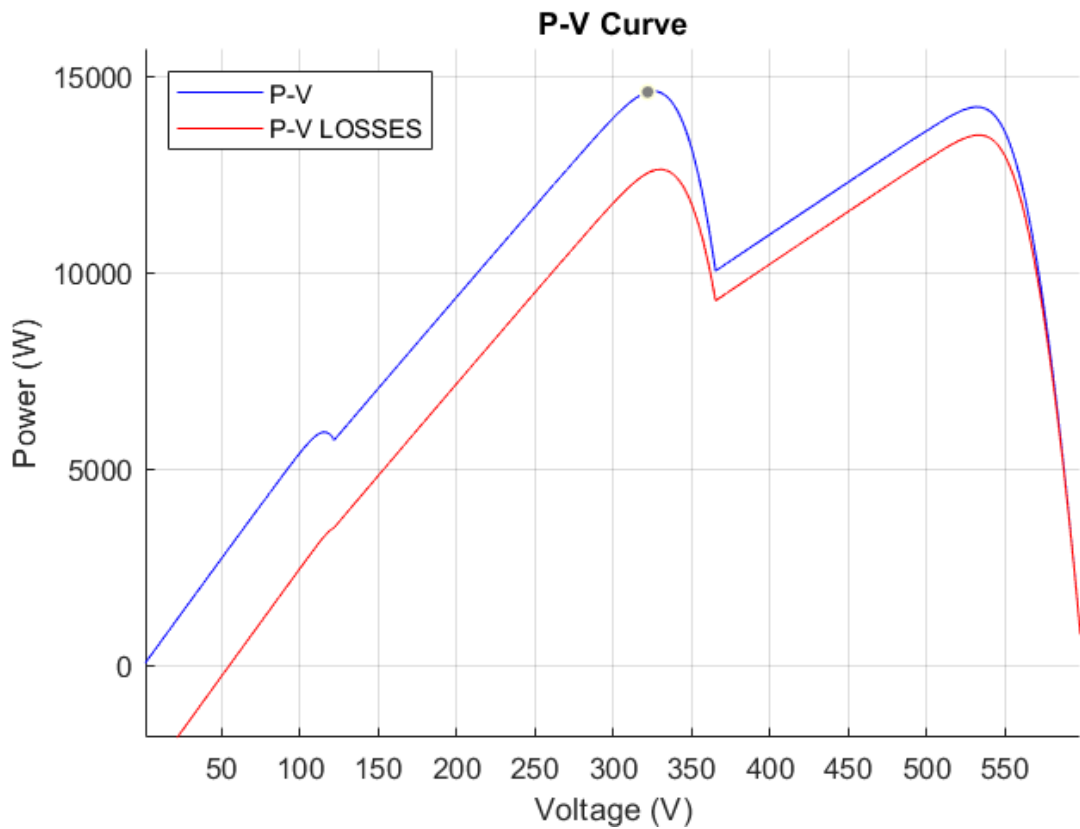


Figure 62. Calculation of Photovoltaic Losses in Simulink

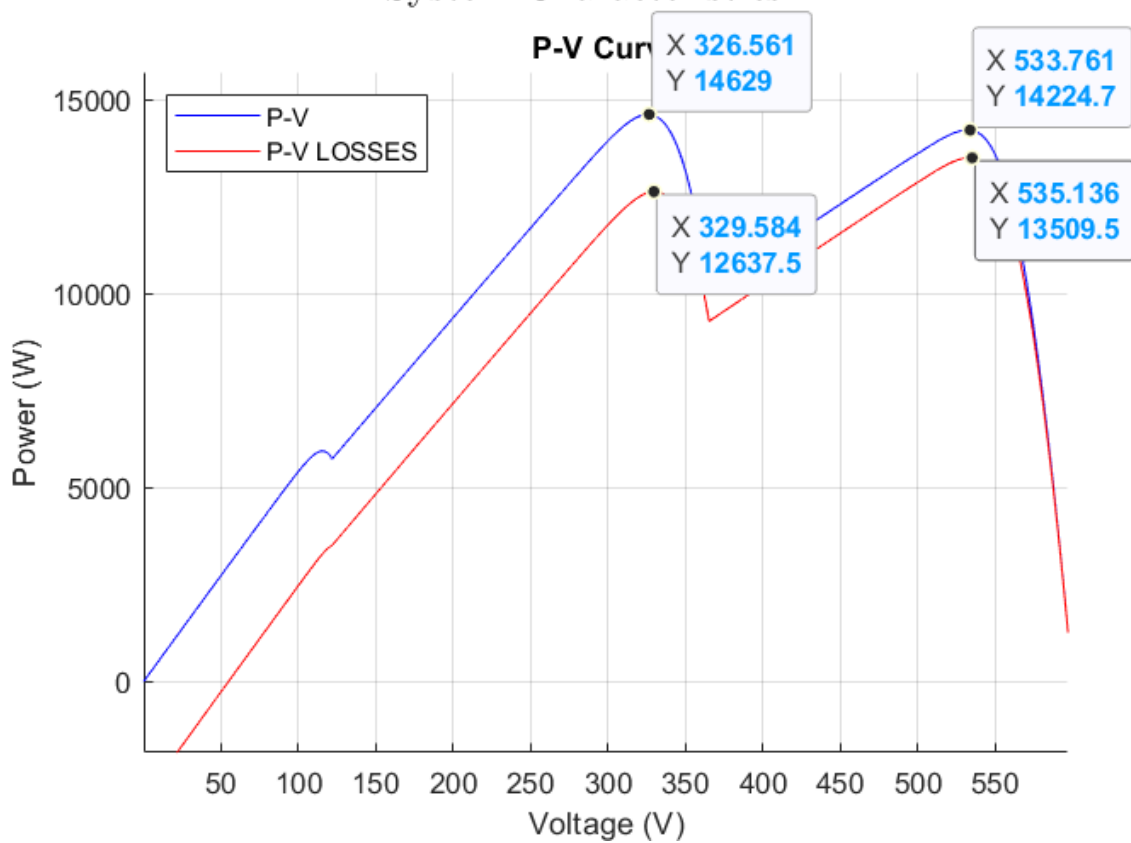
### System Characteristics



## System Characteristics



## System Characteristics



We notice from the above characteristics that the scenario of partial shading is translated into graphics with the presence of local maximums. More specifically, we observe that the Power-Voltage graphics present two maximums very close to each other, both in the case without calculating the losses, and in the case where they are calculated. The main point to comment on is the change in the point of Maximum Power Output when losses are included. More specifically, in the case of no losses, the 2 maximums that concern us receive the values of 14.6kW and 14.2kW for the respective voltages of 327 Volts and 534 Volts, with the first being characterized as the total maximum power output for the system. After calculating the losses, we see that for 330 Volts 12.6kW are produced and for 535 Volts are produced

13.5kW, i.e. now the MPP has changed. This is very important as this optimization in MPPT algorithms can offer us up to a 5% increase in power generation. The reason this phenomenon takes place is that in the formula for calculating total power.

$$PMPP = P_{PV} - [R_{tr, on} + Req + R_{di, on}(1 - d)]_P V^2$$

The losses involve the current raised in the square, so for larger currents and lower operating voltages the losses increase exponentially.

Regarding the Current-Voltage graphics, we notice that as expected, no difference is observed in these 2 cases, since the operation of the system is not affected by the losses in power.

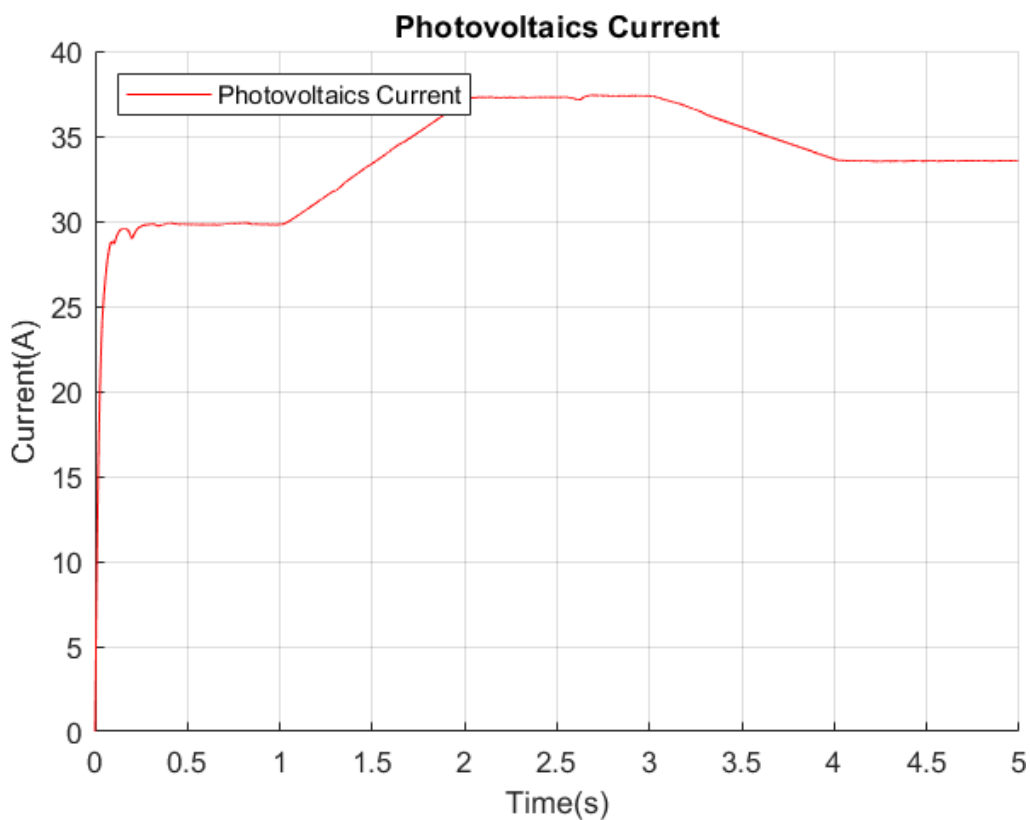
# CHAPTER 7: Results

## 7.1 *Results of Simulations under normal shading conditions:*

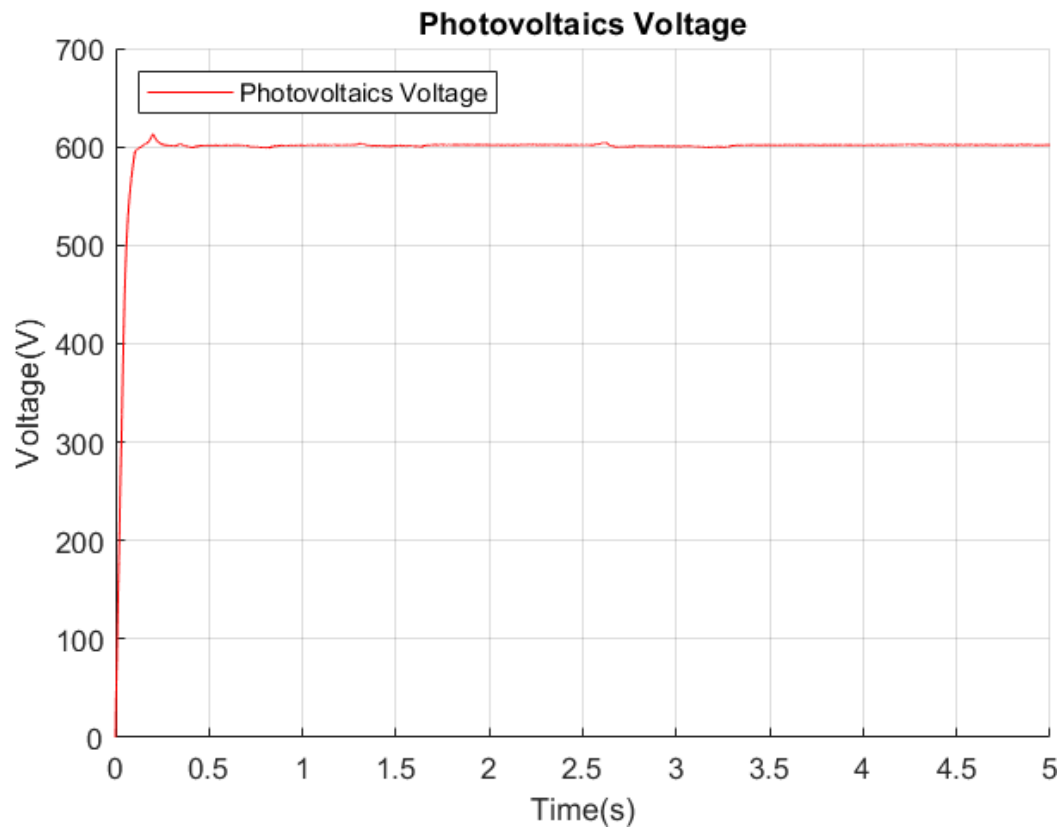
In this scenario, despite the normal incidence of radiation, changes in its intensity take place from  $800\text{W/m}^2$ , to  $1000\text{W/m}^2$  and finally to  $900\text{W/m}^2$ . These changes are made gradually, simulating the fluctuation of sunshine in a landscape as it occurs under real conditions. More specifically, the radiation increases from  $800\text{W/m}^2$  to  $1000\text{W/m}^2$ , between the time moments 1-2second, it is kept constant at  $1000\text{W/m}^2$  from 2-3 seconds, it decreases to  $900 \text{ W/m}^2$  between 3-4 seconds and finally it is maintained at  $900 \text{ W/m}^2$  from 4-5 seconds where the simulation is completed. Then we will present graphs of the most important quantities, which will indicate the response of the system and will lead us to draw some conclusions regarding the system and its operation using different algorithms to find the Maximum Power Output Point.

### 7.1.1 *Perturb and Observe without Losses:*

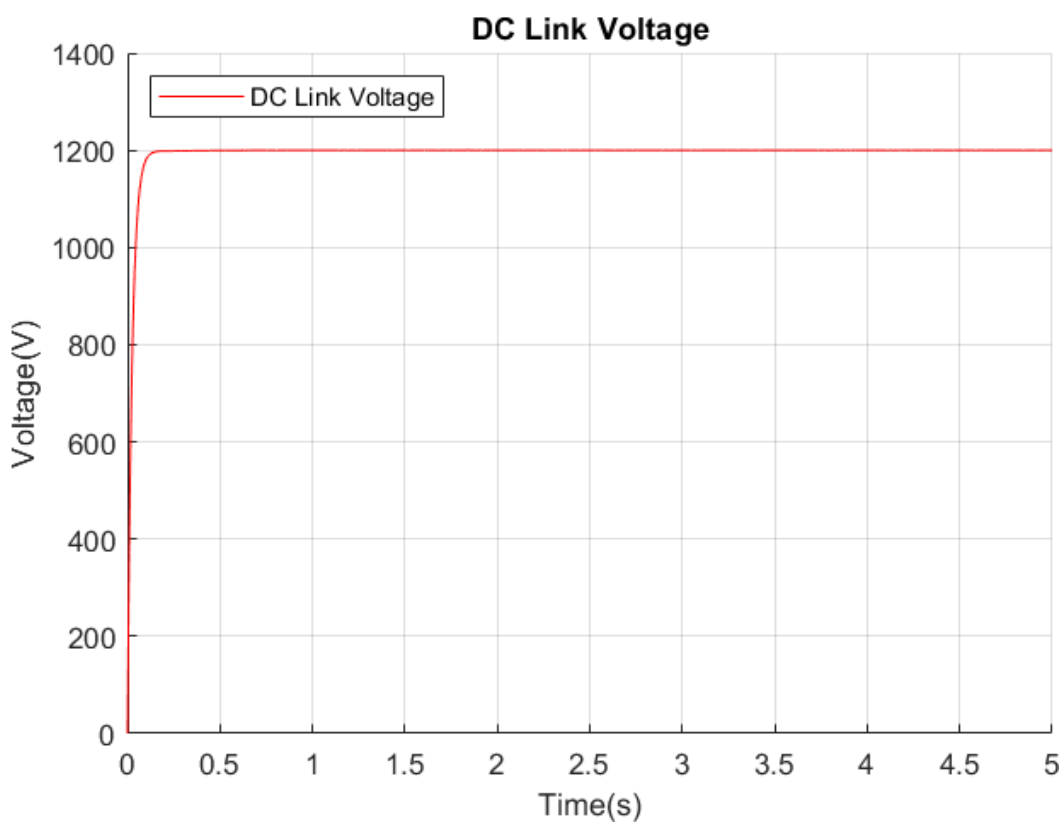
Petrurb and Observe-No Losses



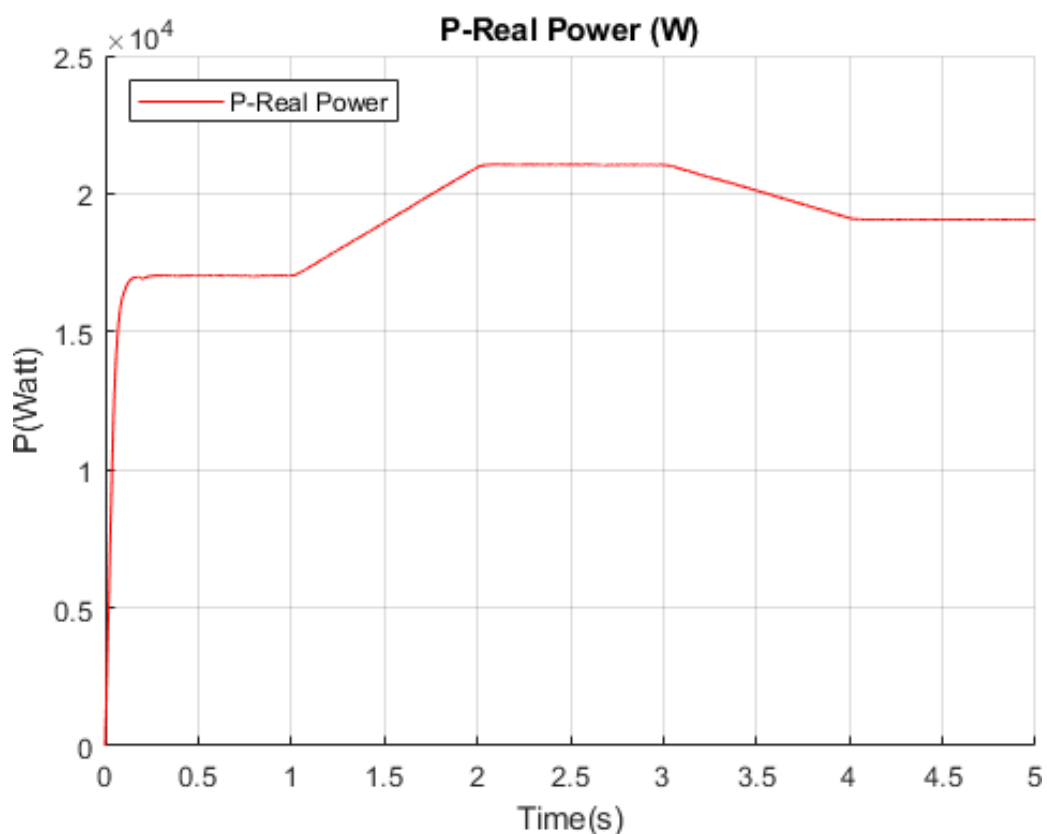
Petrurb and Observe-No Losses



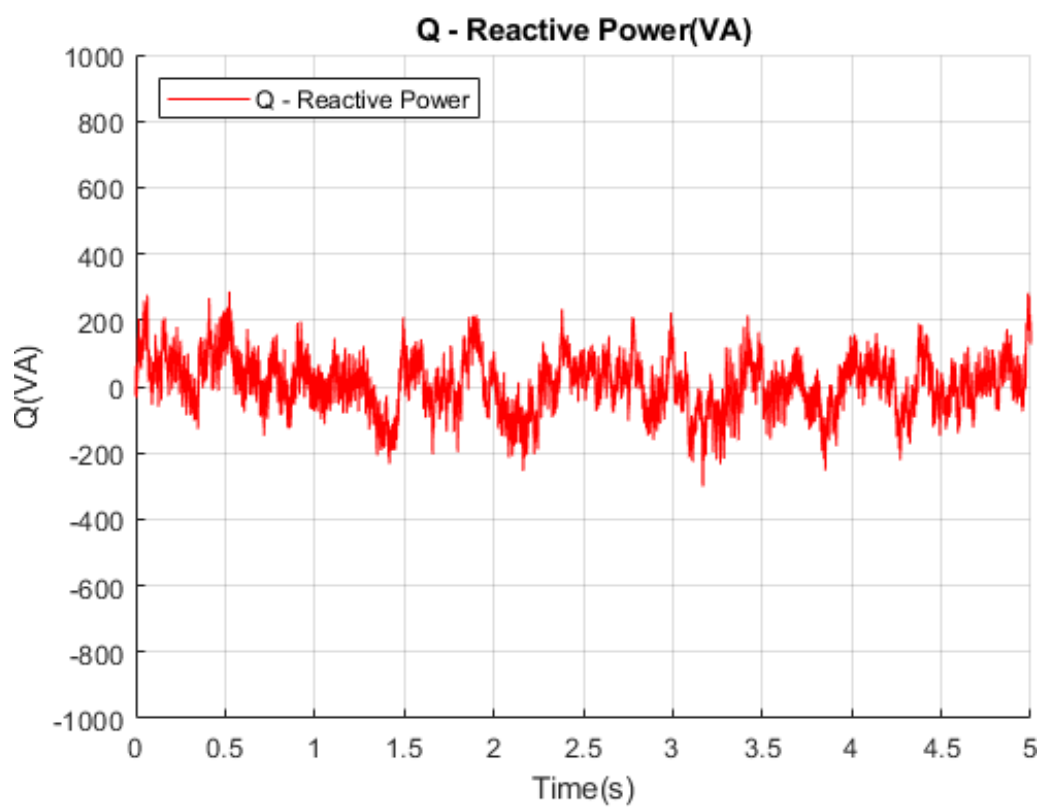
Petrurb and Observe-No Losses



Petrurb and Observe-No Losses



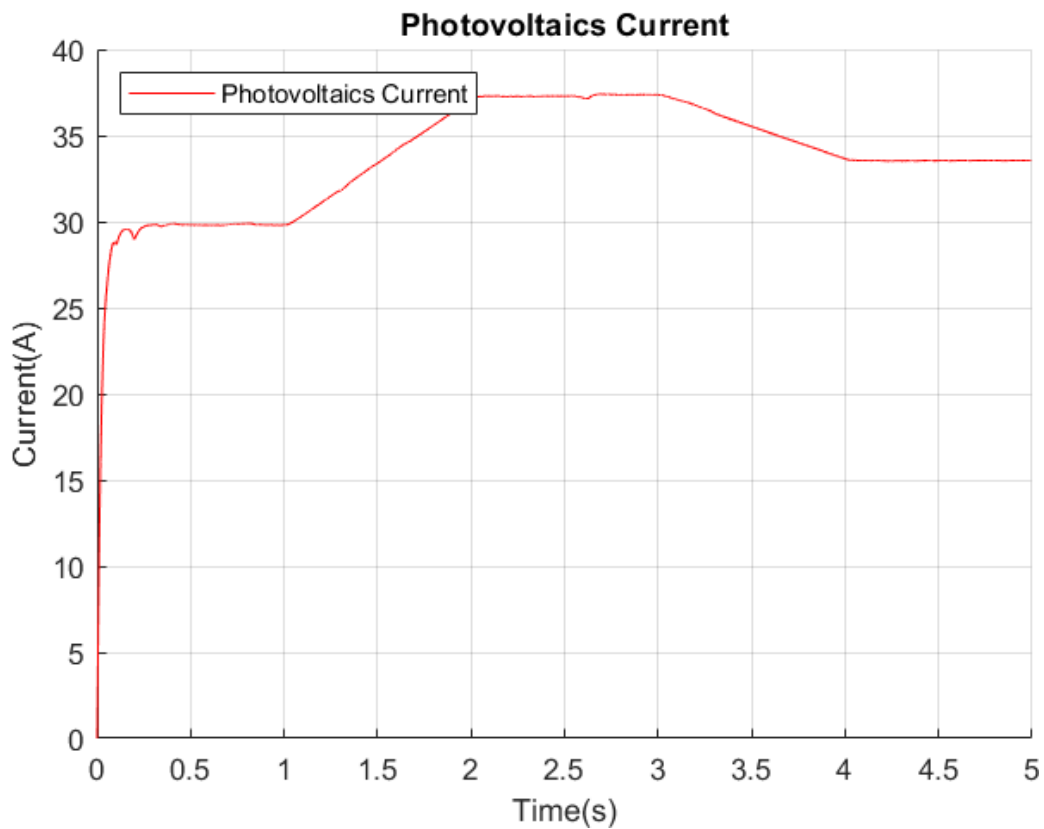
Petrurb and Observe-No Losses



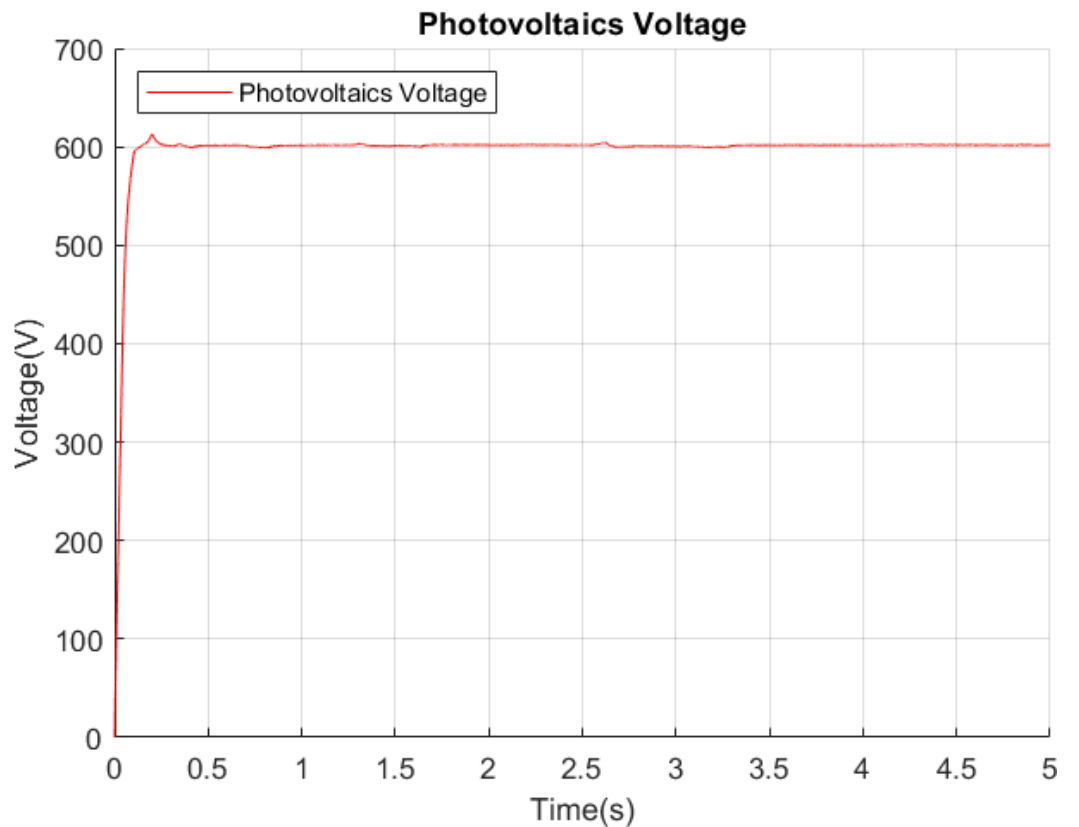
From the above graphs, we first notice that the current values of the photovoltaic system follow the intensity of the radiation. More specifically, when the radiation is at  $800\text{W/m}^2$ , the current that leaks through the photovoltaic array is close to 30 Amper, with its increase to  $1000\text{ W/m}^2$  it changes to 38 Amperes and finally with the decrease to  $900\text{W/m}^2$  it ends up at 34 Amperes. On the contrary, the trend at its extremes remains constant for the entire period of time. These two graphics give us an idea of the graphics of power production, which, as confirmed, follow the intensity of the radiation. Finally, it is worth commenting on the quick operation of the voltage control on the load side, as the Voltage in the Bus is quickly driven to the desired value of 1200 Volts and the values of the Reactive Power are around zero.

### **7.1.2 Perturb and Observe with losses:**

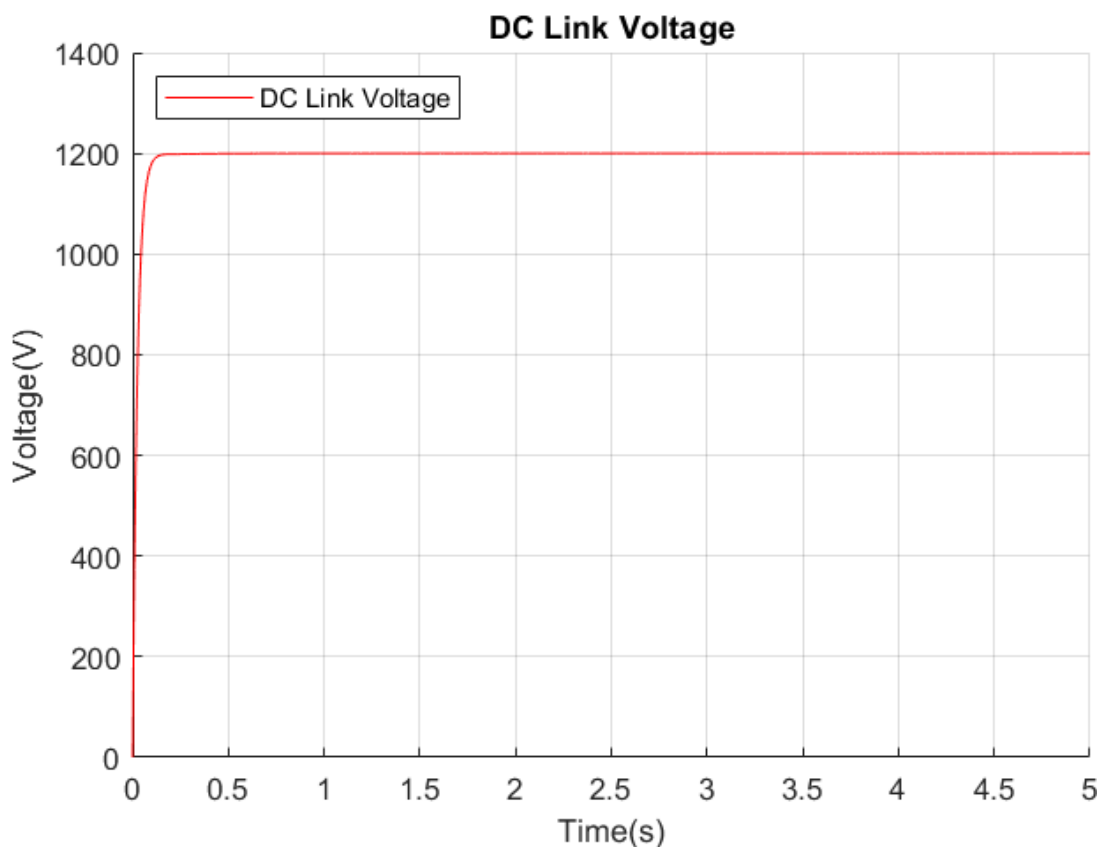
Petrurb and Observe-Losses Included



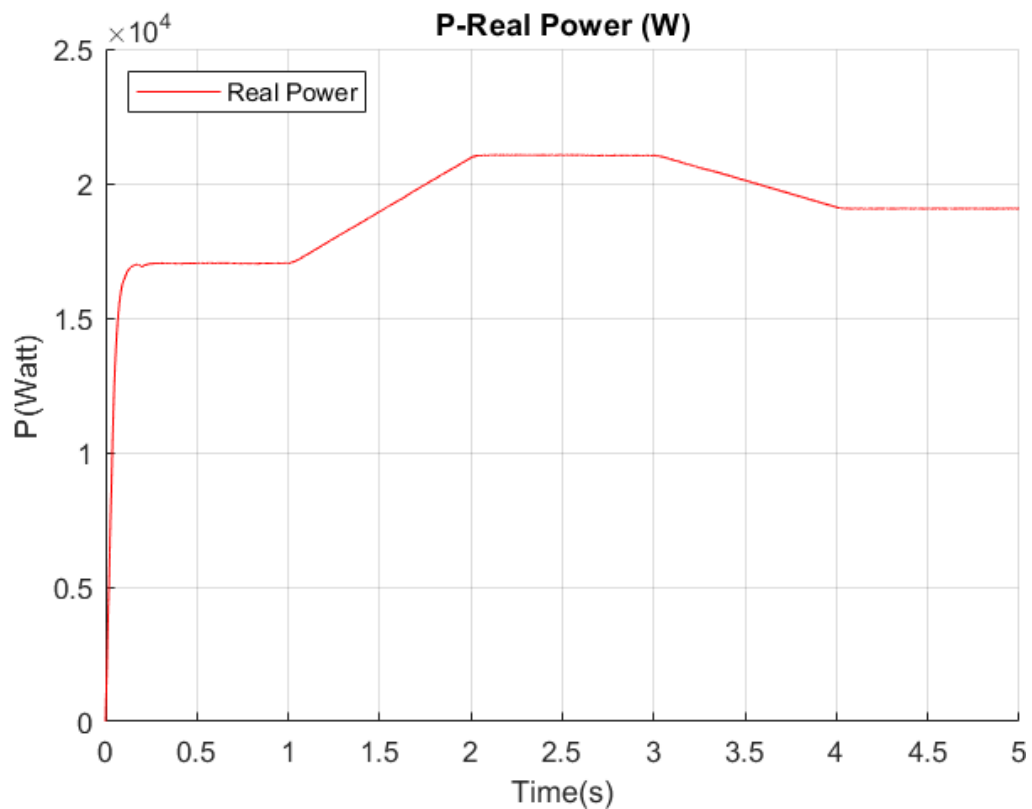
Petrurb and Observe-Losses Included



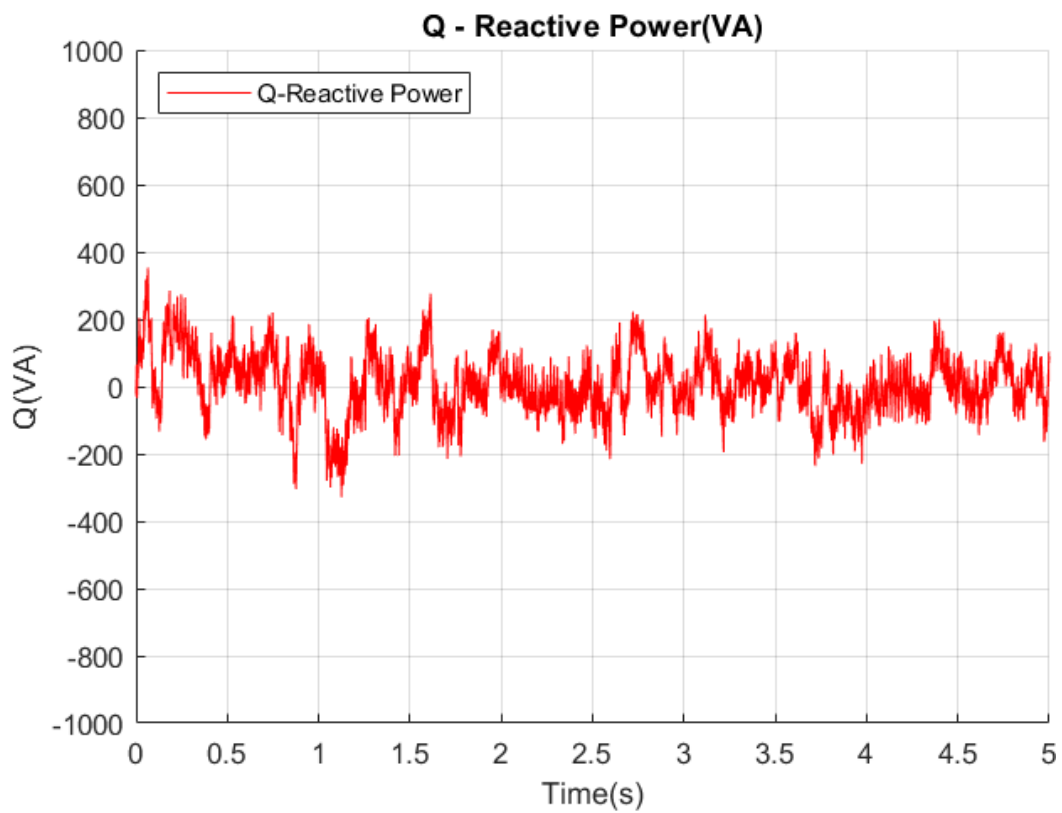
Petrurb and Observe-Losses Included



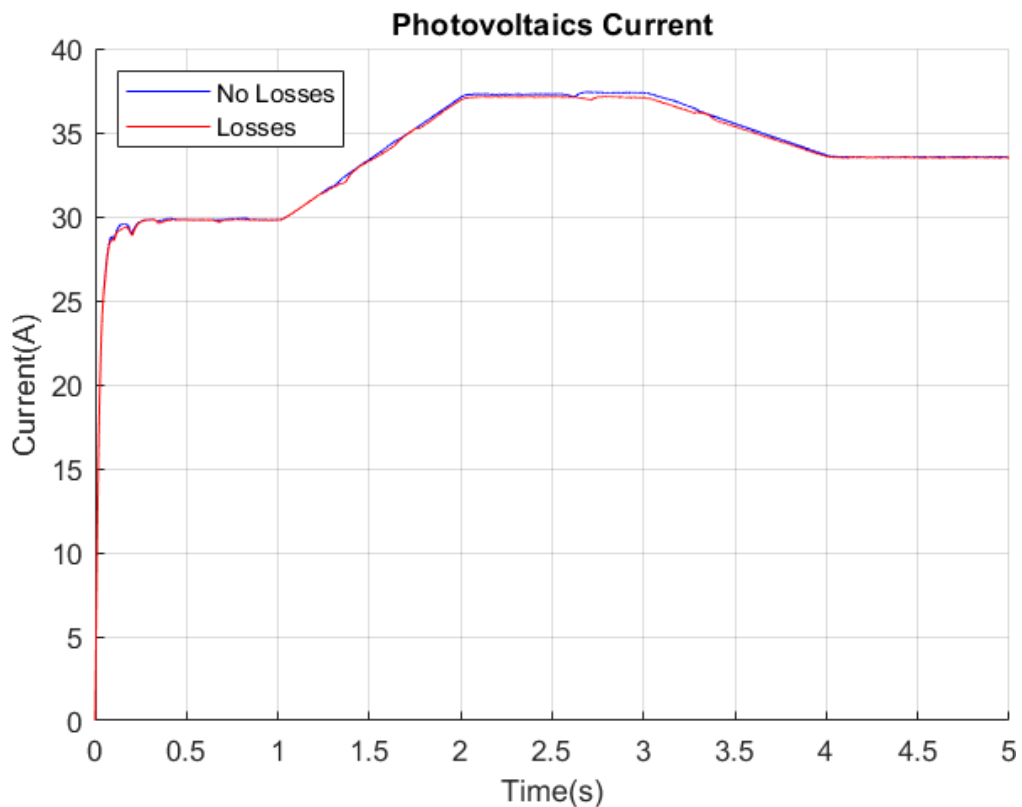
Petrurb and Observe-Losses Included



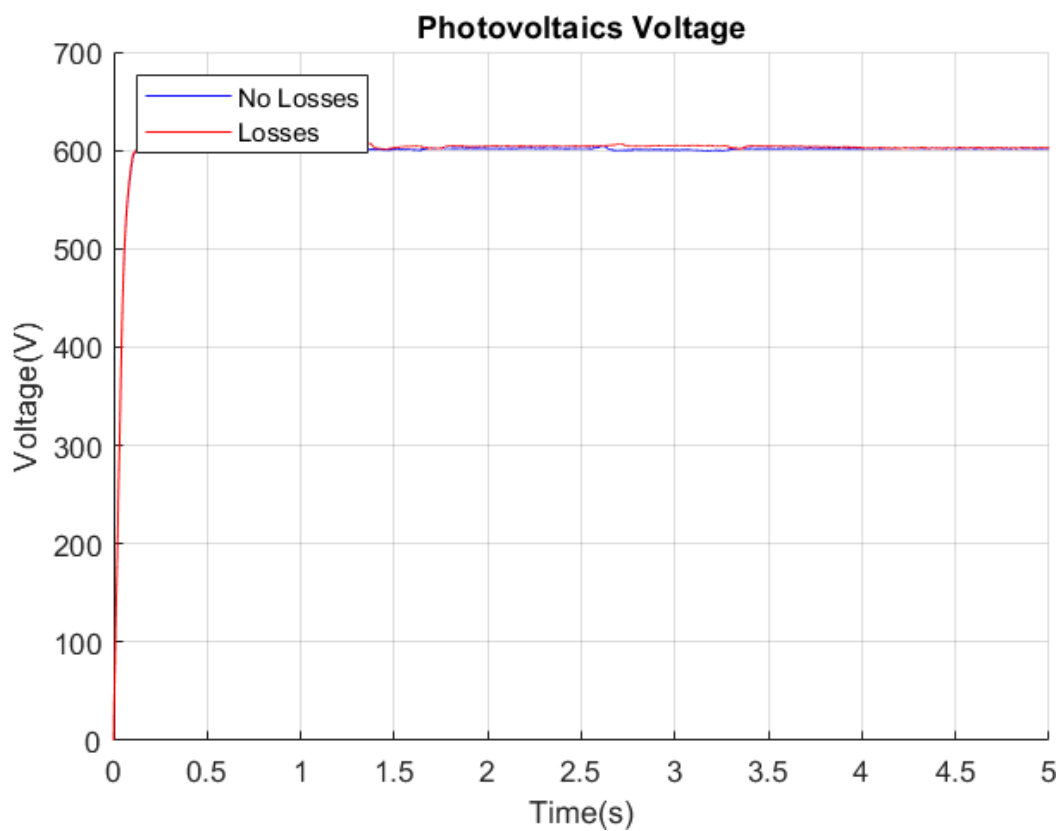
Petrurb and Observe-Losses Included



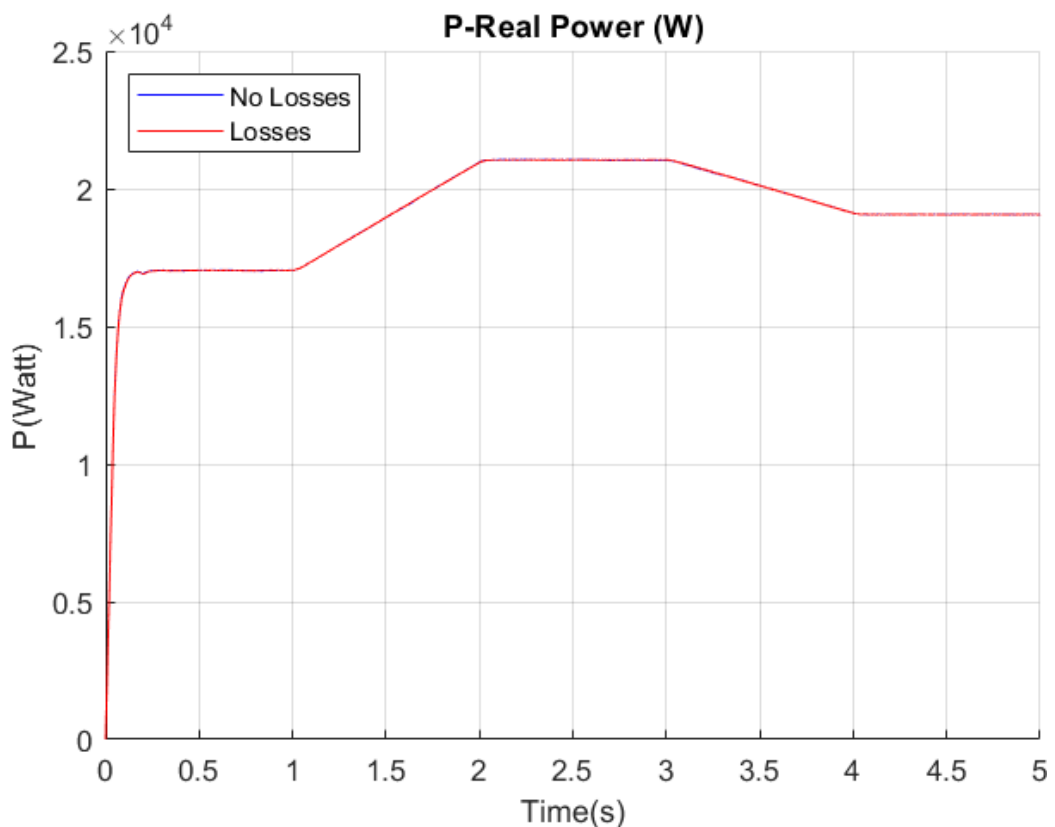
Petrurb and Observe-Losses/No Losses



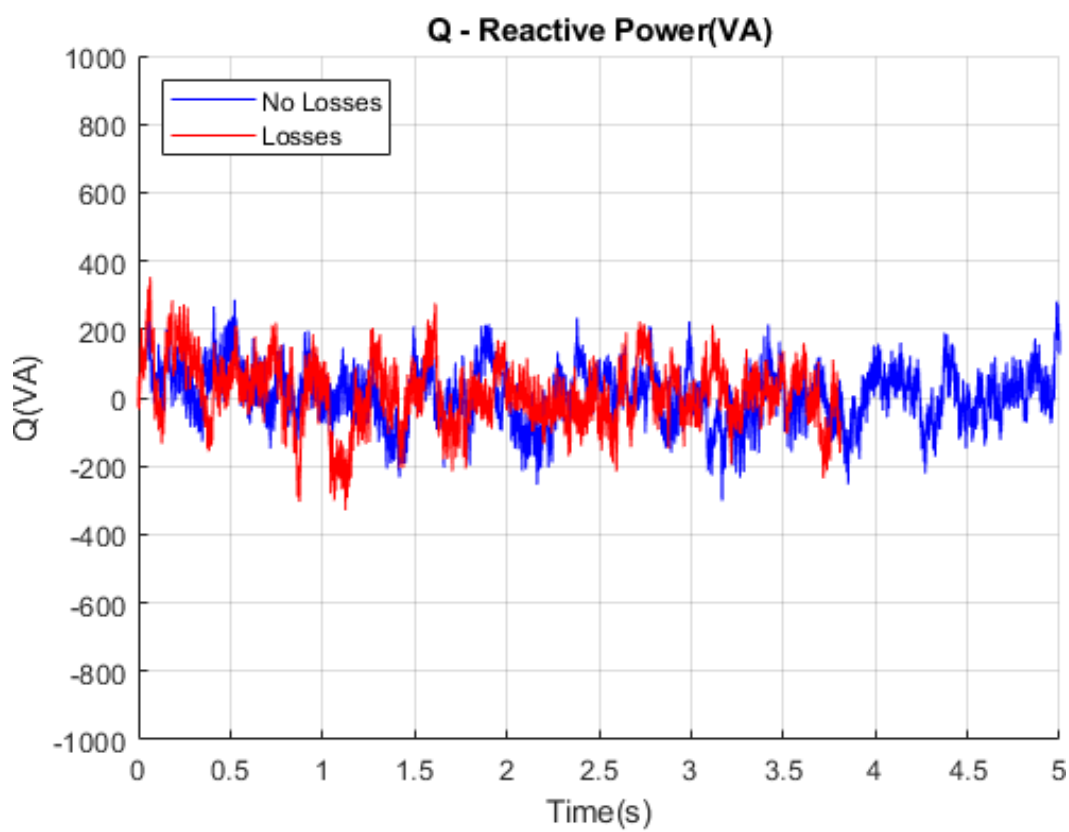
Petrurb and Observe-Losses/No Losses



Petrurb and Observe-Losses/No Losses



Petrurb and Observe-Losses/No Losses



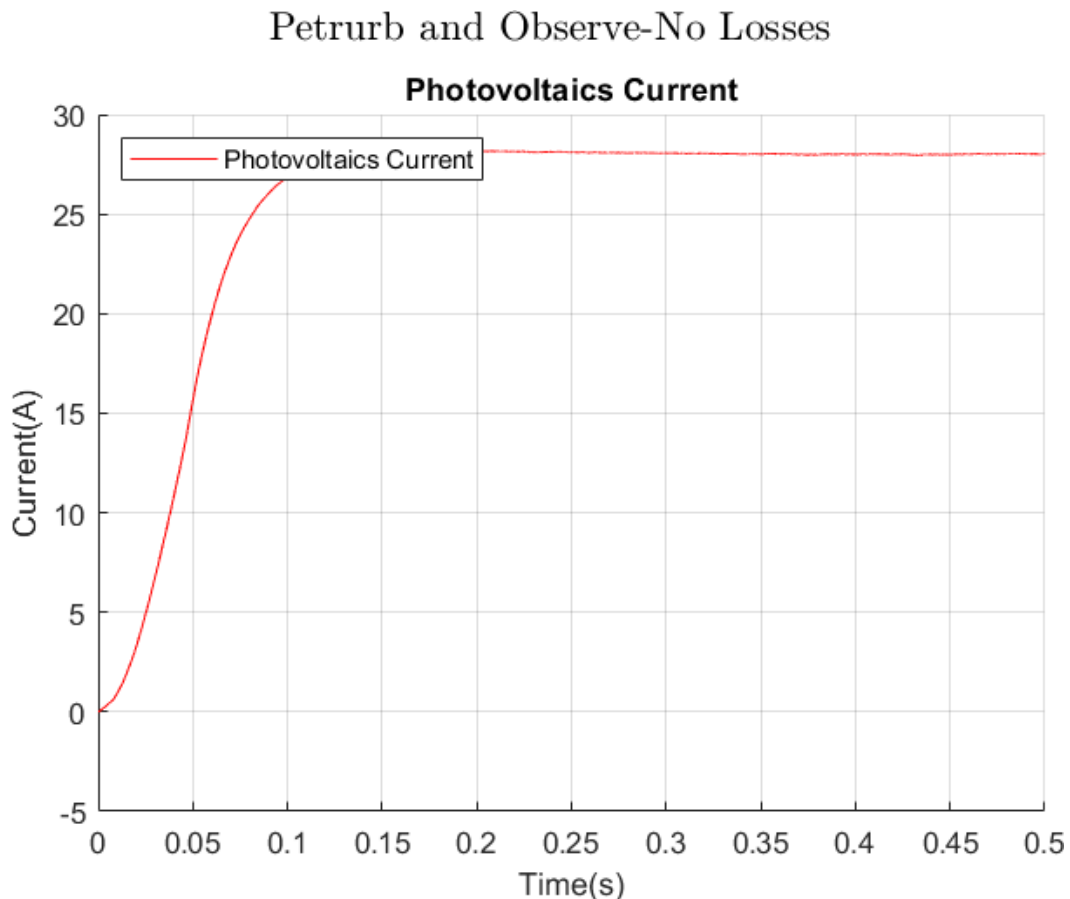
From the above graphs we can easily conclude that for the Perturb and Observe Algorithm, the use of the improved power type, where losses are included, does not show any significant difference at the point of Maximum Power Output. The graphics remain the same, the photovoltaic current and the power produced follow the radiation, its voltage remains constant, the voltage in the Bus reaches 1200 Volts very quickly and the idle power has zero average value.

However, it is worth noting even this small improvement in the performance of our system, as the current is minimally reduced and therefore the losses resulting in a slight increase in efficiency as we expected from the above results.

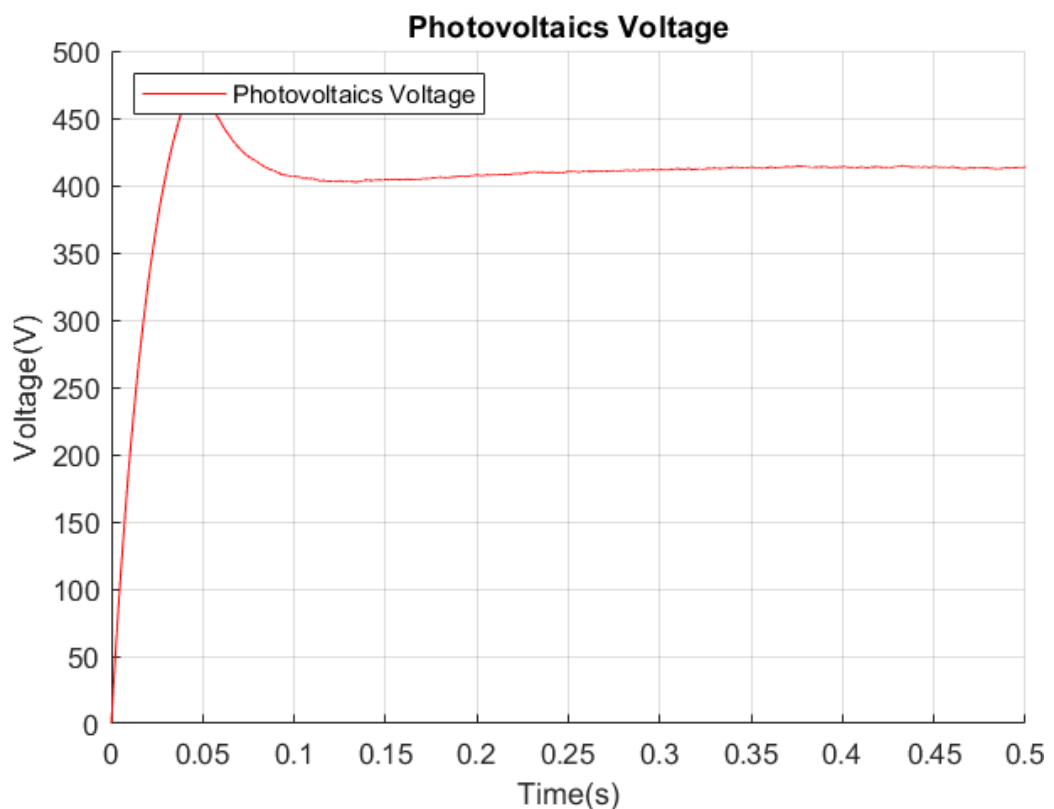
## *7.2 Results Simulations under conditions partial shading:*

In this scenario we apply the different algorithms for finding the Maximum Power Output Point in the partial shading simulation and observe the various responses and graphics that characterize the system. This is how we come to conclusions and can judge their ability to operate under these conditions and lead us to optimal operation, which of course is to minimize losses and produce as much power as possible.

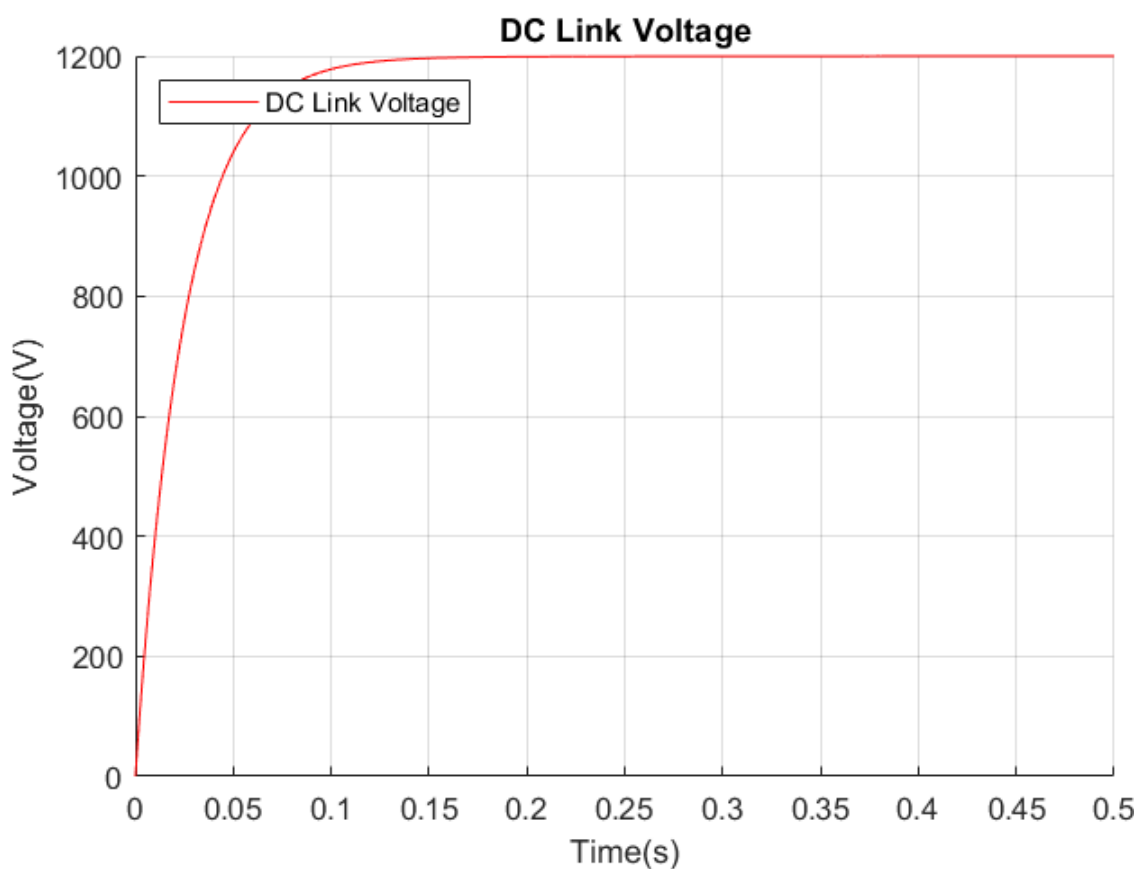
### *7.2.1 Perturb and Observe lossless:*



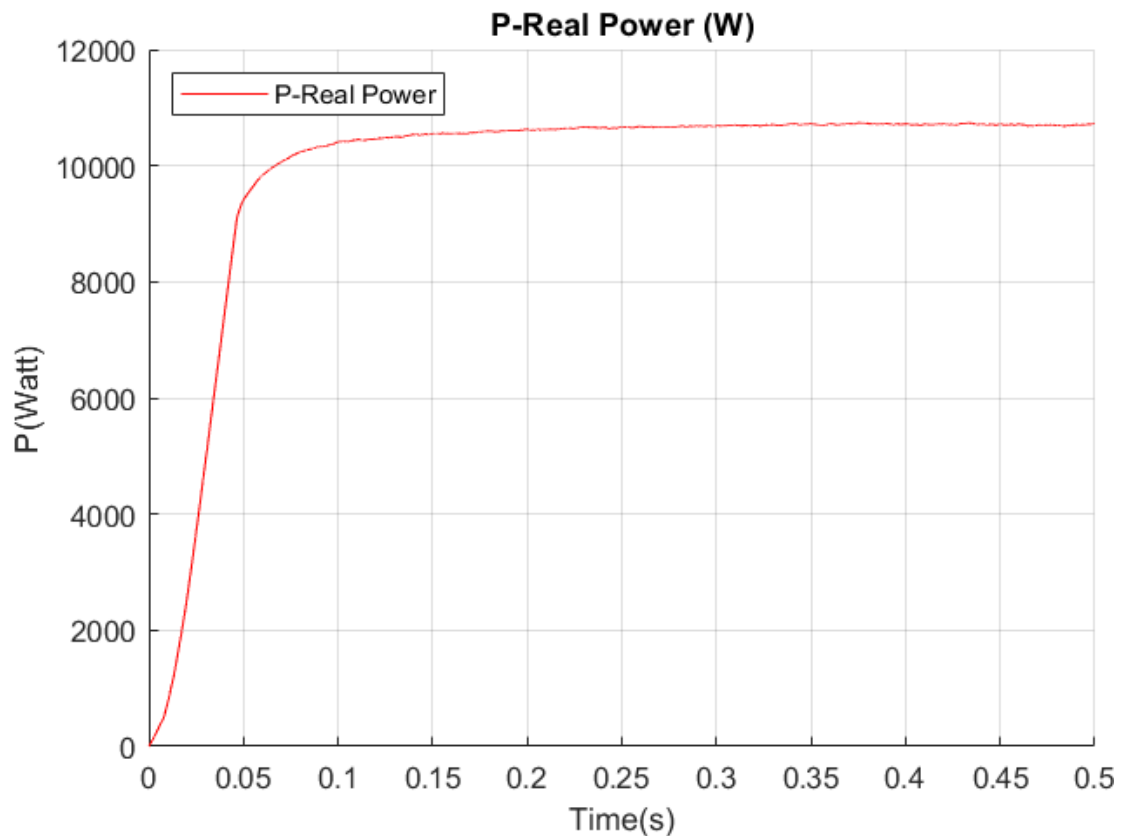
Petrurb and Observe-No Losses



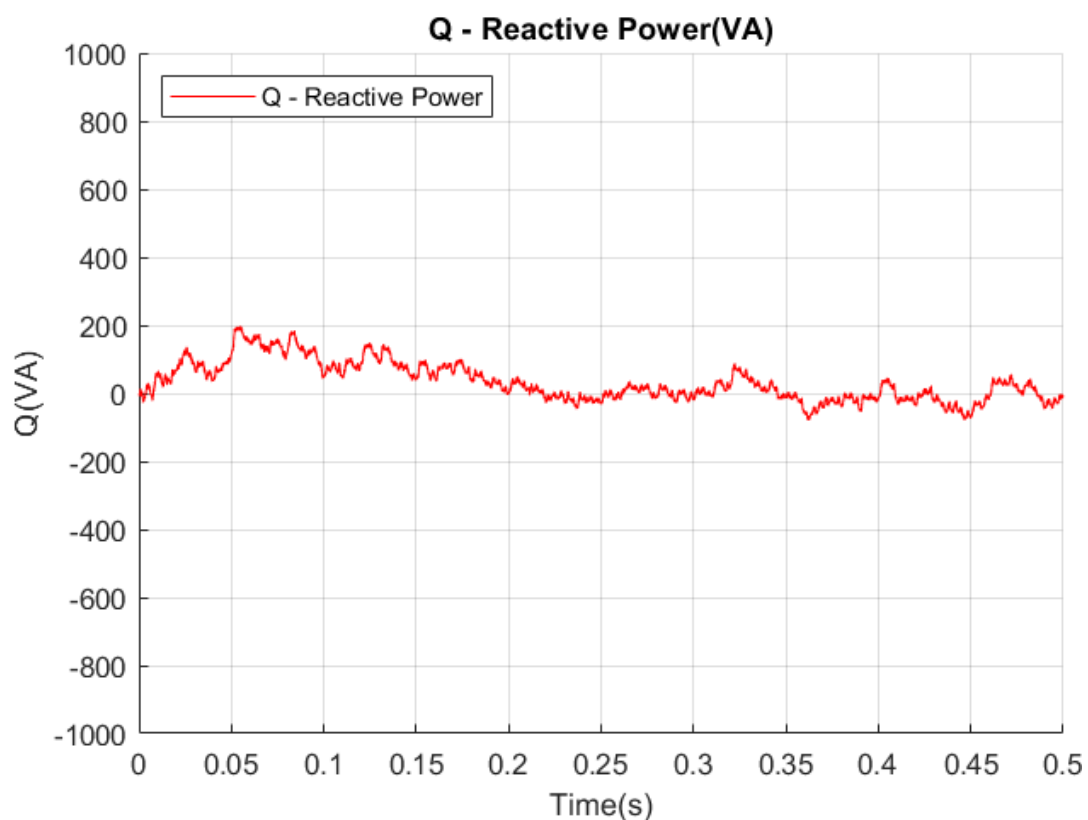
Petrurb and Observe-No Losses



### Petrurb and Observe-No Losses



### Petrurb and Observe-No Losses

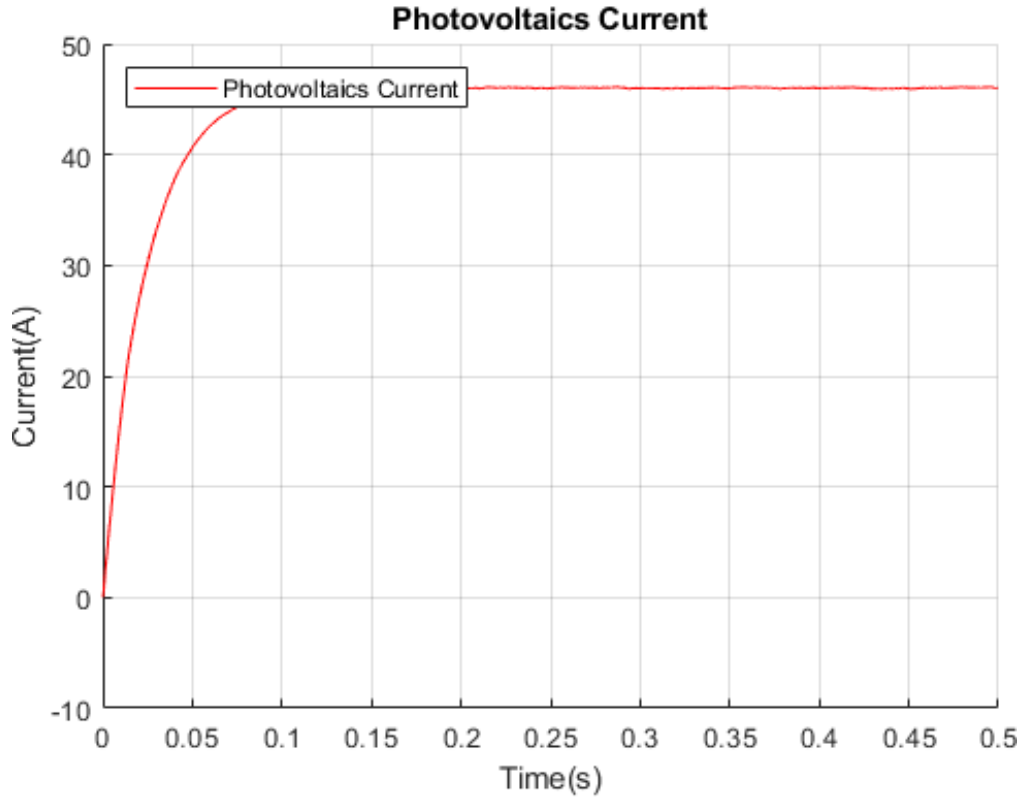


From the above graphs we notice that the Perturb and Observe algorithm drives the simulated system very quickly to 28 Amps, a value that it recognizes as the maximum value of power production from photovoltaics. We also notice that the voltage of the photovoltaic, as well as its current, remain stable, resulting in the same power generated by it at the price of 10.2kW. It is also worth mentioning the rapid stabilization of the voltage in the bus at 1200 Volts, where the desired value is, as well as the zeroing of the average value of reactive power.

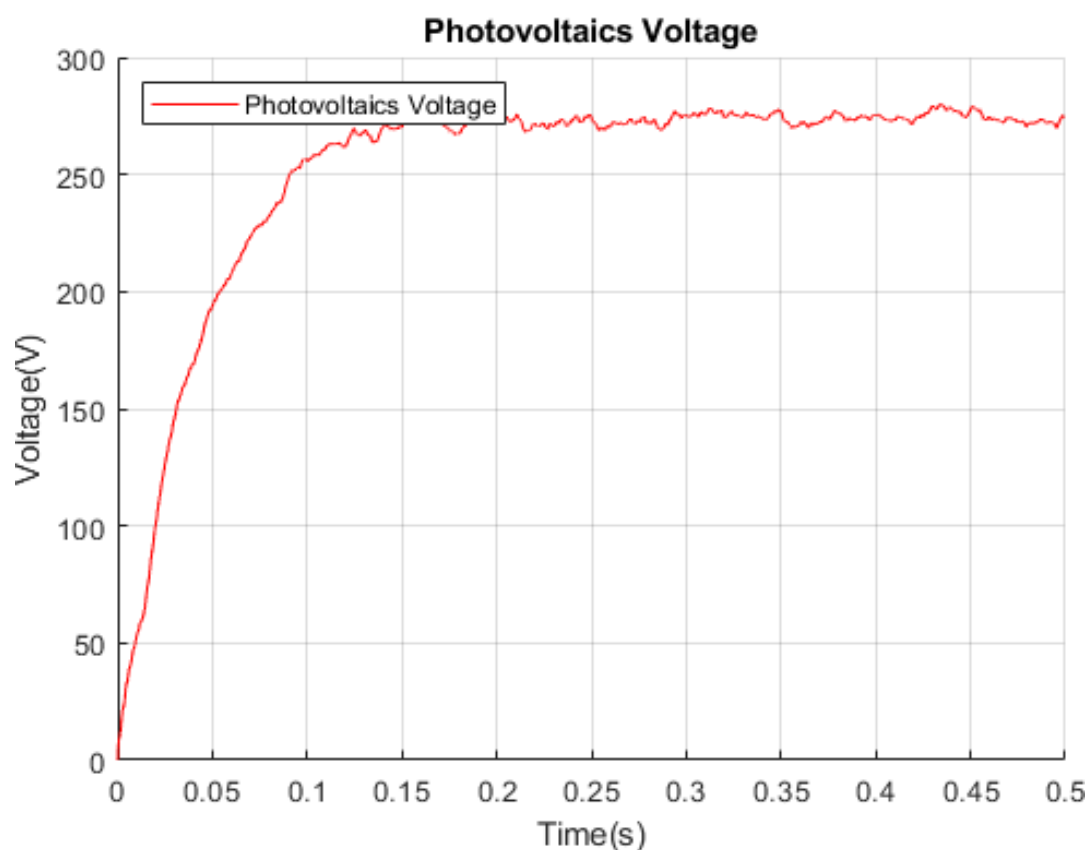
From the graphs that the P&O algorithm converges, we can confidently conclude from the characteristics of the system that we have previously exported that it is driven to GMPP, but this is a random coincidence since the first maximum it encounters during its operation is the total maximum. Otherwise, its function would not be optimal and thus proves its weakness in cases of partial shading.

### **7.2.2 Particle Swarm Optimization without Losses:**

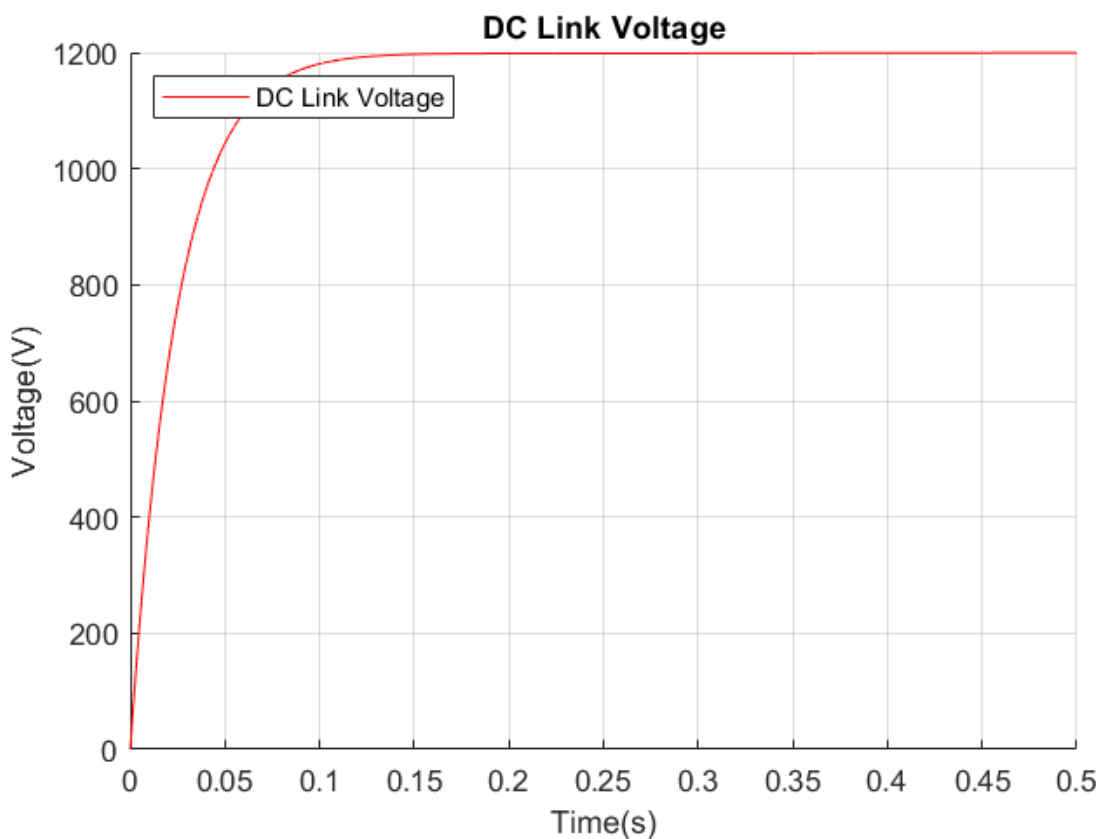
Particle Swarm Optimization-No Losses



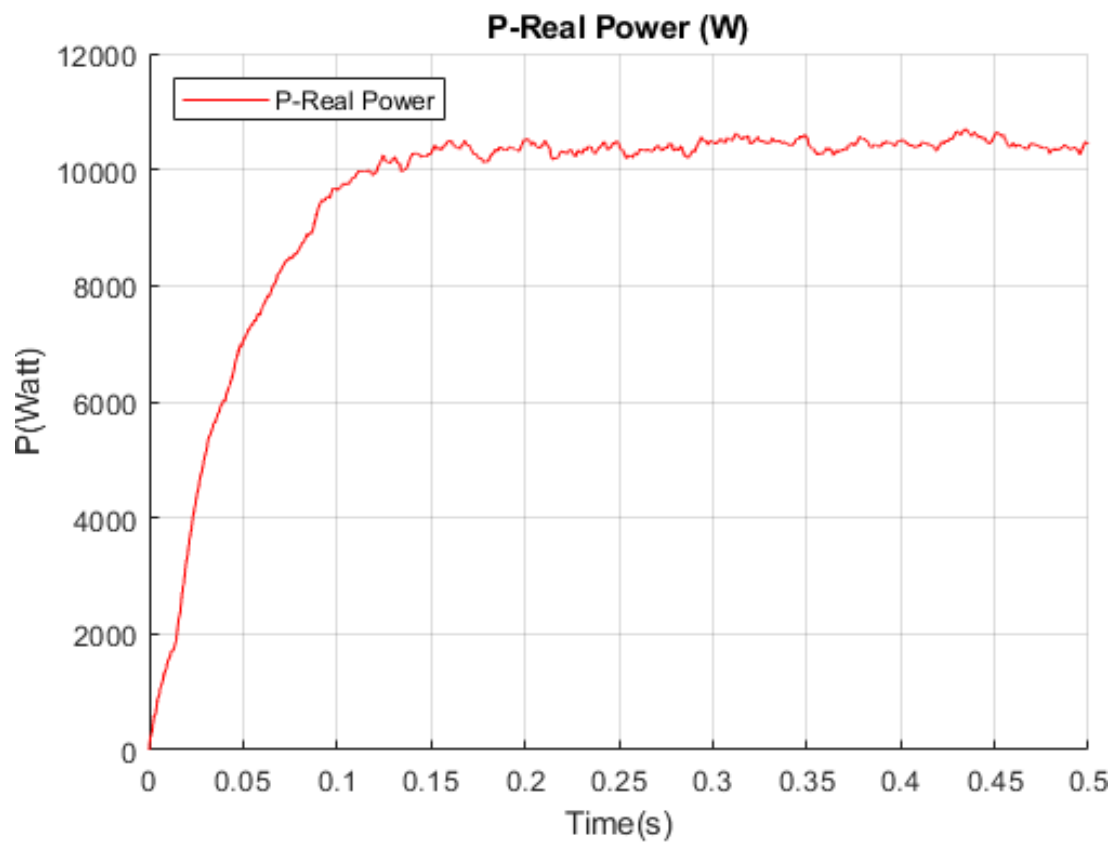
Particle Swarm Optimization-No Losses



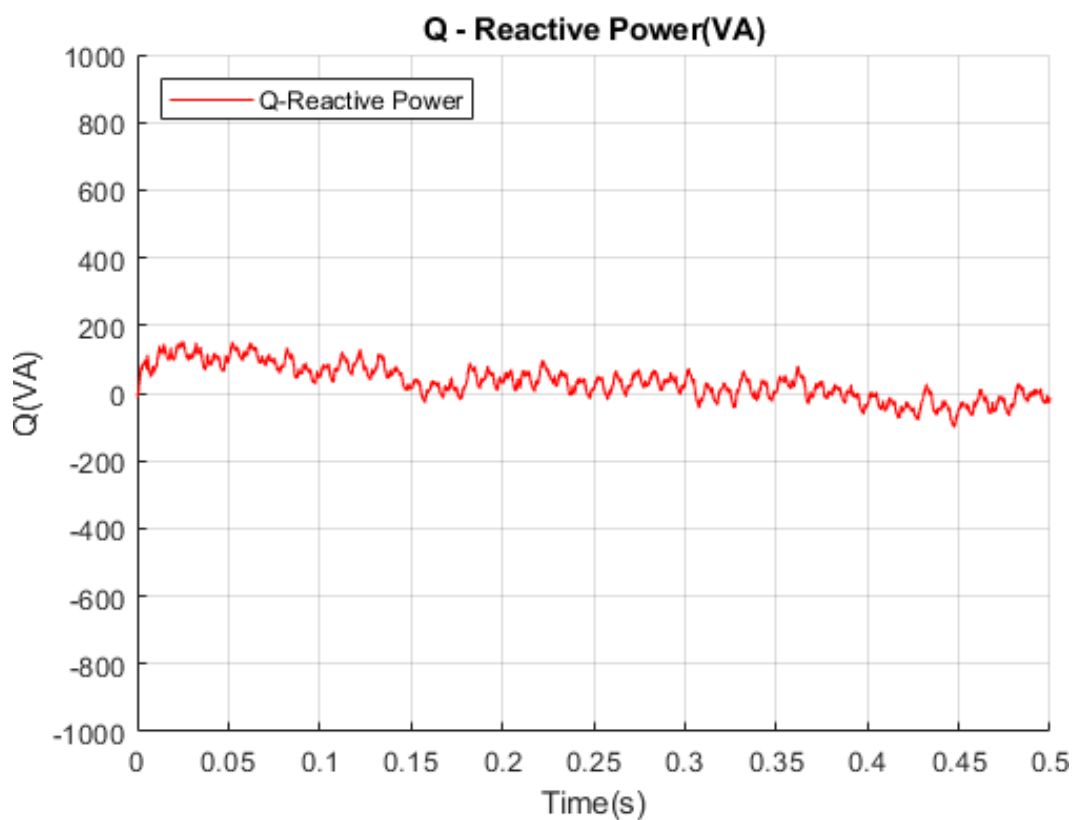
Particle Swarm Optimization-No Losses



Particle Swarm Optimization-No Losses

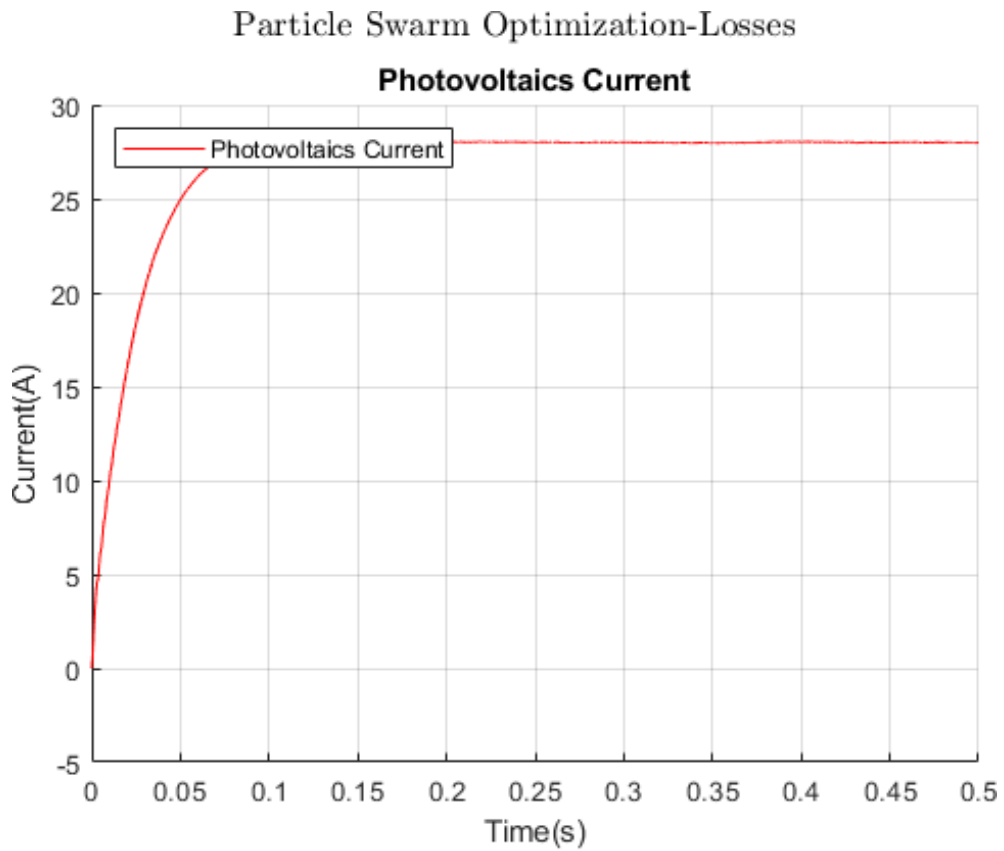


Particle Swarm Optimization-No Losses

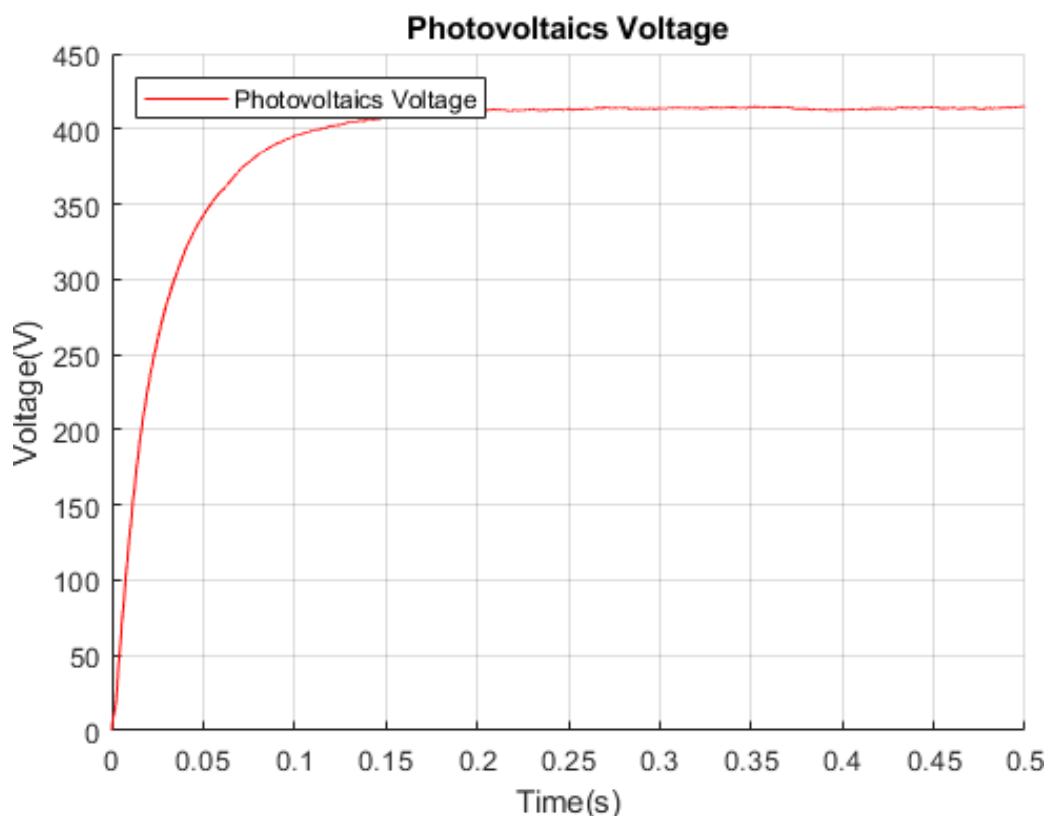


We observe a different response from that of the Perturb and Observe algorithm. More specifically, we see our system being driven to the electricity price of 45Amper for photovoltaics, but a reduced voltage value, which also implies the reduced energy production from our system, and more specifically almost 10kW. As far as idle power is concerned, its average value is zero, while the voltage in the bus is once again rapidly driven to the desired value of 1200 Volts. From the final price driven by the PSO without loss of electricity we can confirm our hypothesis of the importance of including losses in the press. So, based on the characteristics, we see that the algorithm is led to a point that is the seemingly total maximum if we do not take into account the losses, but in reality it is a point of local maximum!

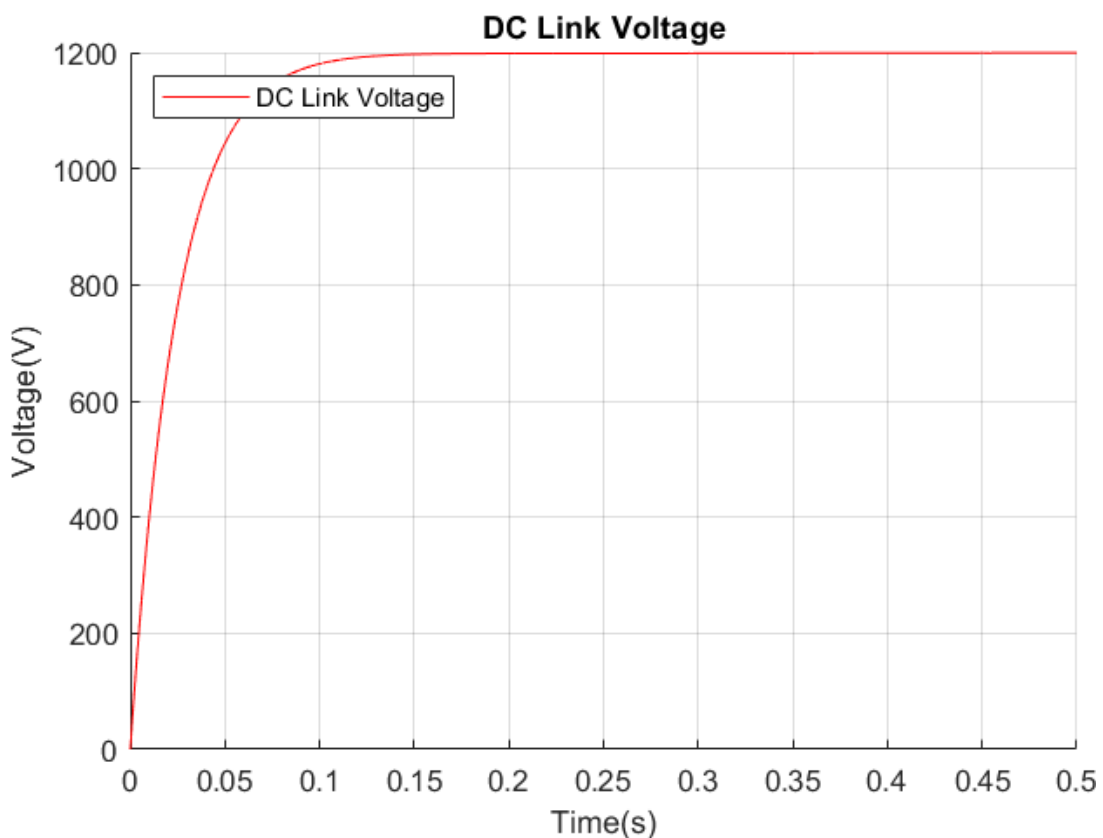
### *7.2.3 Particle Swarm Optimization with losses:*



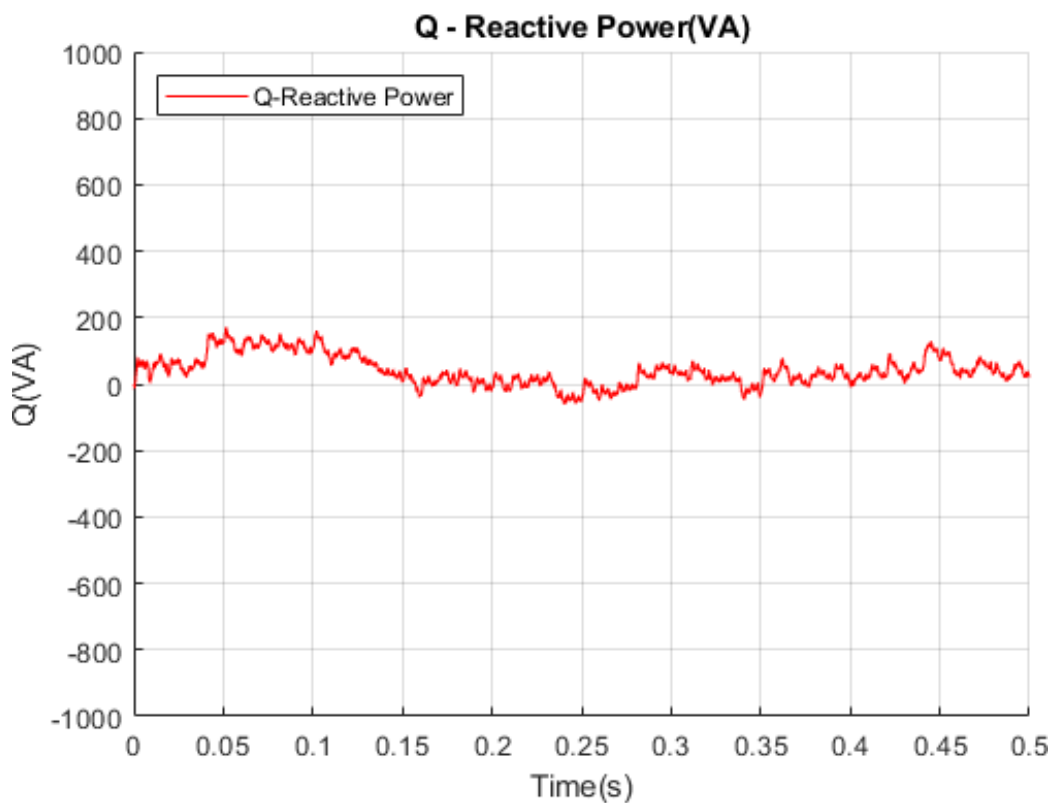
### Particle Swarm Optimization-Losses



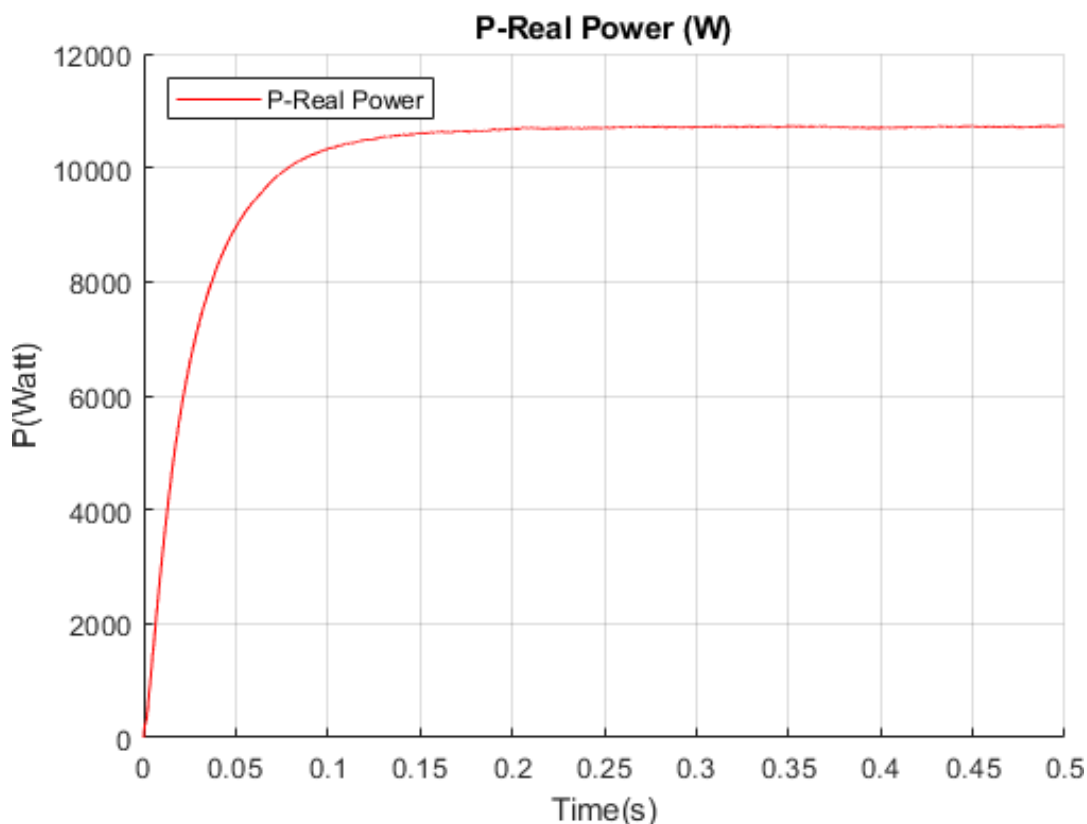
### Particle Swarm Optimization-No Losses



### Particle Swarm Optimization-Losses

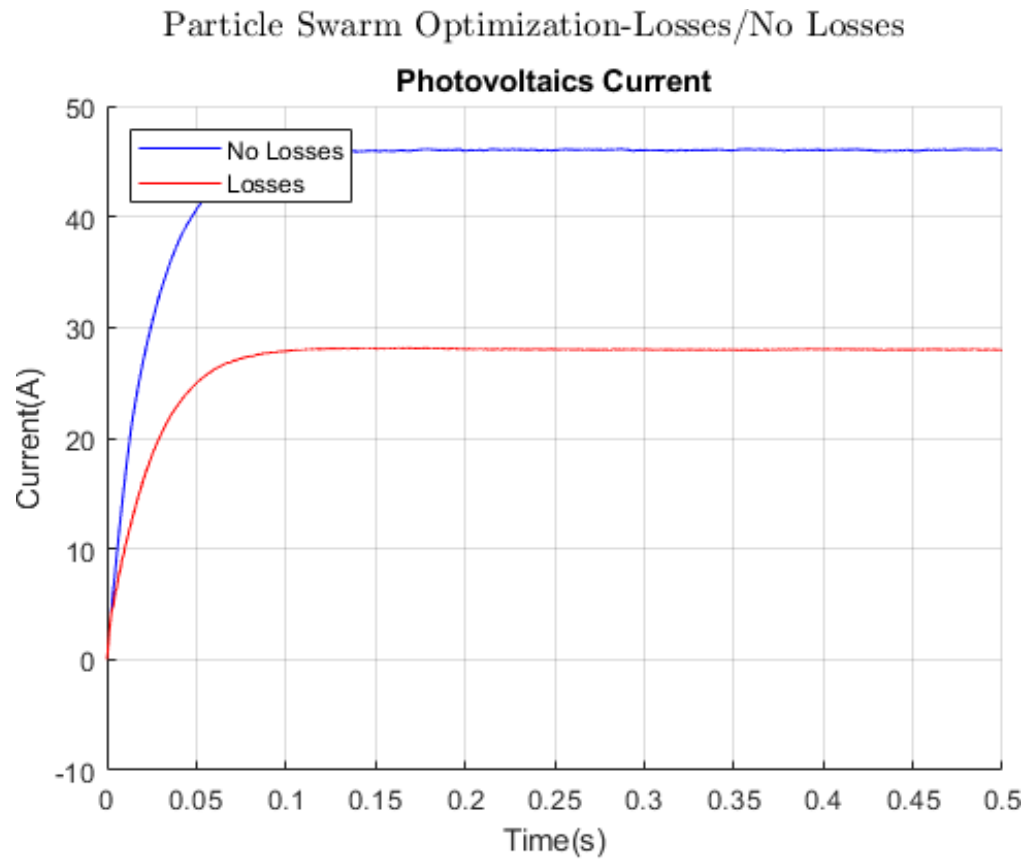


### Particle Swarm Optimization-Losses

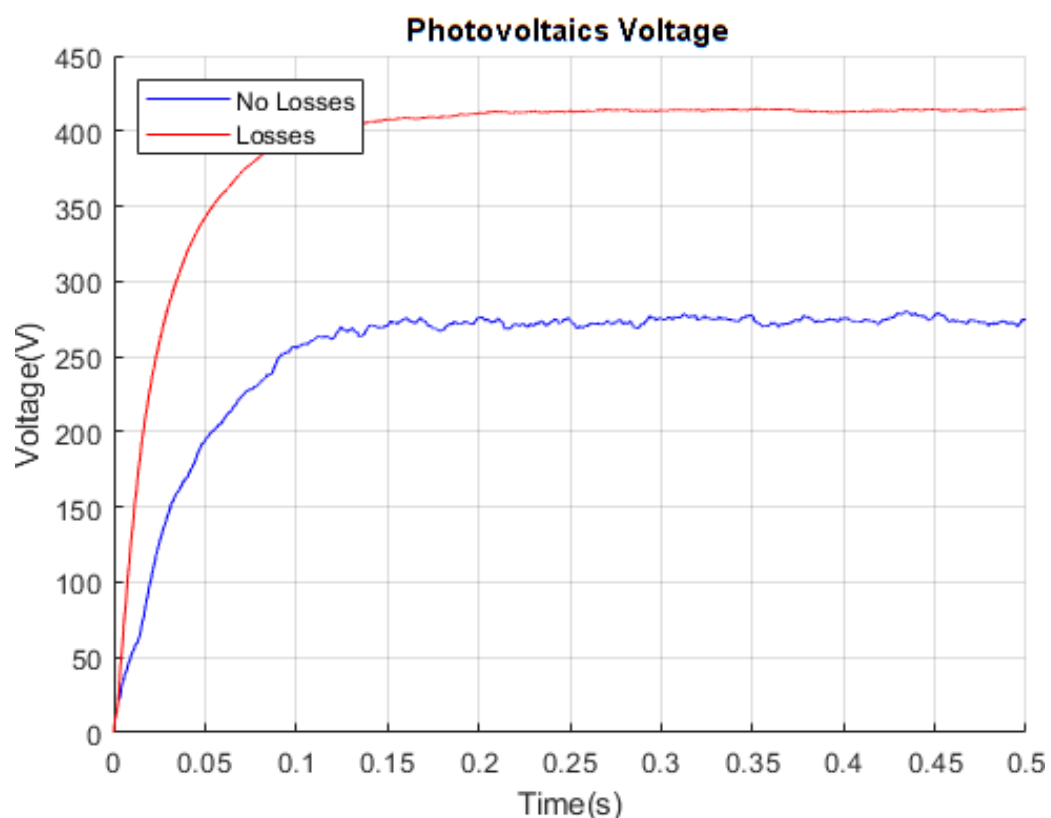


In the above graphics we can see that the current of the photovoltaic system is driven to the value of 28 Ampers and its voltage to 420 Volts. Furthermore, the Power generated is

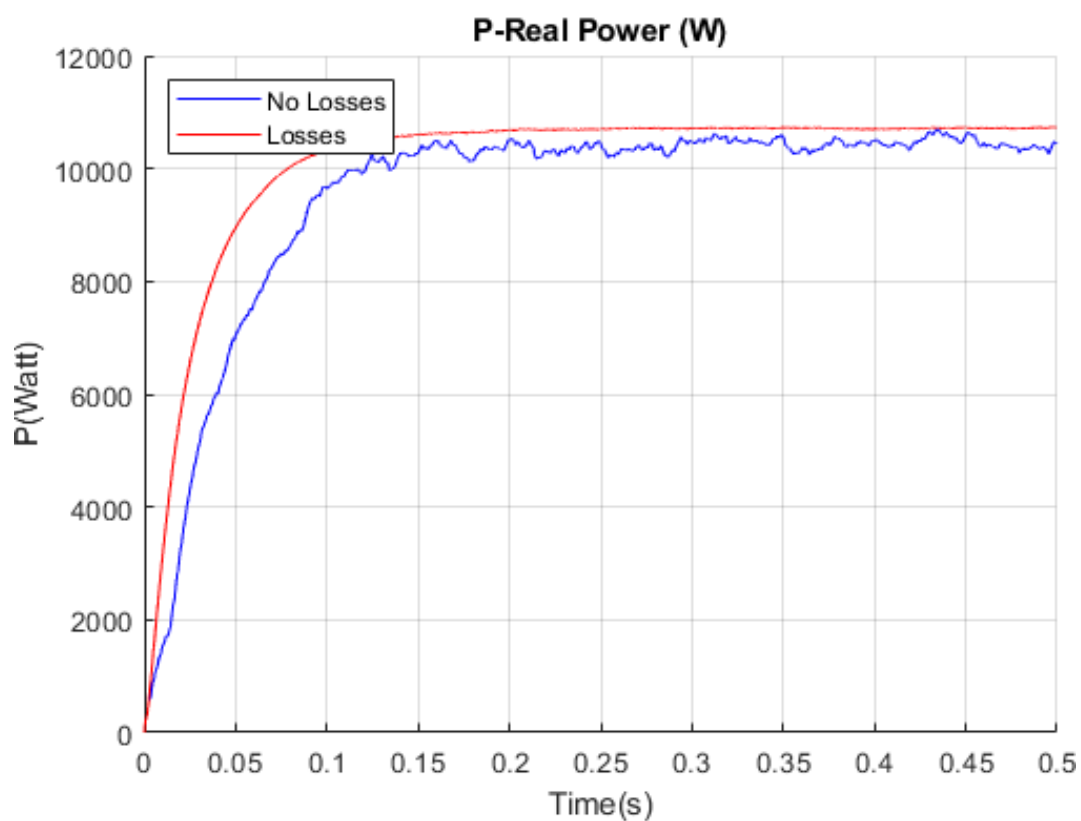
of the order of 10.5kW and the voltage in the DC Bus is quickly driven to 1200 Volts. Finally, once again, the Idle Power has an average value of zero, thus completing the desired function of our control. Next, we will compare the two system functions with the PSO Algorithms with and without losses.



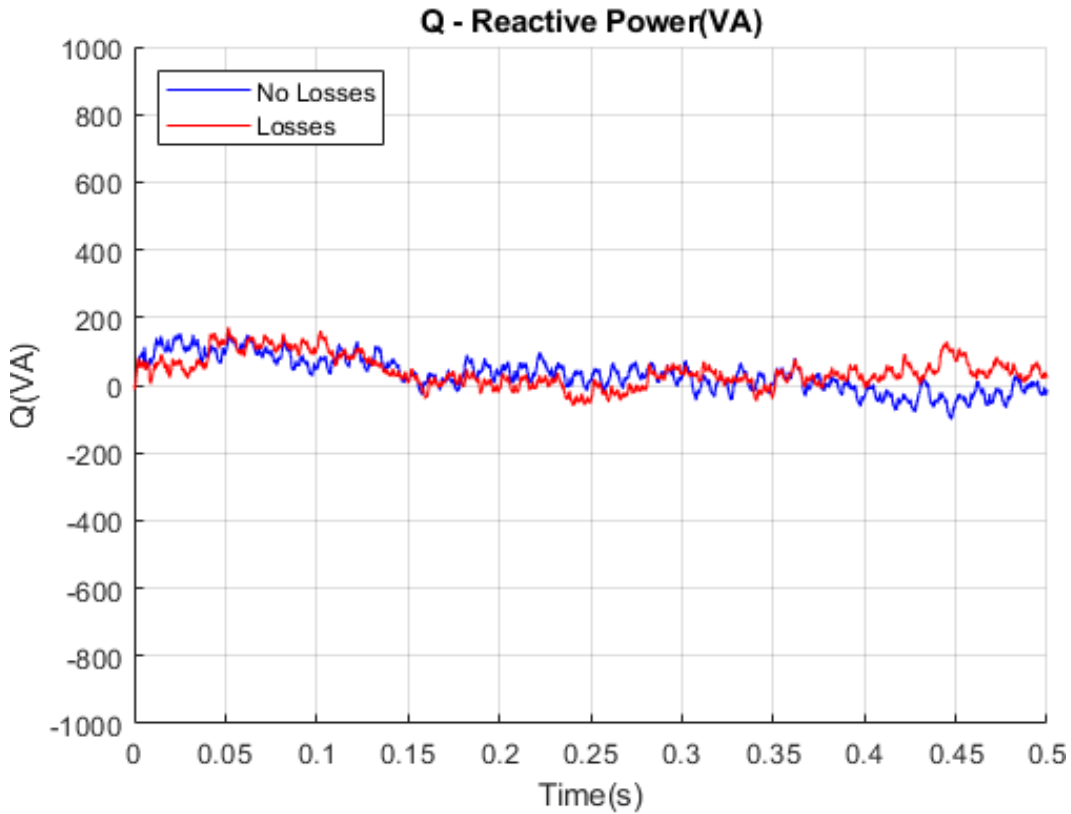
Particle Swarm Optimization-Losses/No Losses



Particle Swarm Optimization-Losses/No Losses



### Particle Swarm Optimization-Losses/No Losses

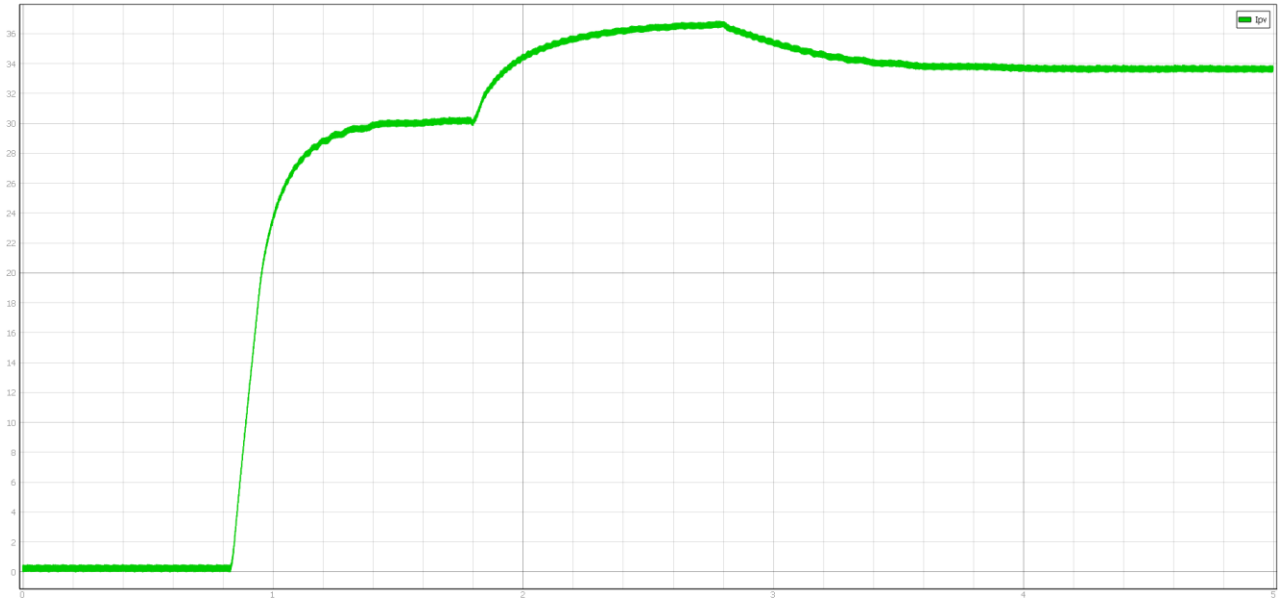


In the graphs above it is easy to distinguish the different functions of the system, even if the only difference between the two algorithms is to include the losses. More specifically, for the photovoltaic current, we observe that in the case without calculating losses, it is led to about 45 Ampers, while taking into account them it is led to 28 Ampers, a significantly lower value. Regarding the voltage applied to the ends of the photovoltaic array, in the case of losses, its value is about 275 Volts, while with losses it is 410 Volts. The idle power has the same behavior in both cases, i.e., as before, it oscillates around zero, while we have left the real power for the end. The actual power generated by our photovoltaic is the most important element in this analysis. Therefore, examining the graph of the actual power production from photovoltaics, we see that in the case of taking into account the losses, the power that is ultimately produced by our photovoltaics is greater than that produced in the case that we do not take them into account. If we recall the characteristics of this system from chapter 6, we will understand why this is the case. That is, the lossless PSO recognizes the first maximum as GMPP while the lossless PSO recognizes the second, hence the big difference in the operating current and voltage of the photovoltaic. We therefore conclude that the inclusion of losses leads our system to an optimal condition, and offers us the ability to produce more power under conditions of partial shading of our photovoltaic system.

### **7.3 Results of Experiments:**

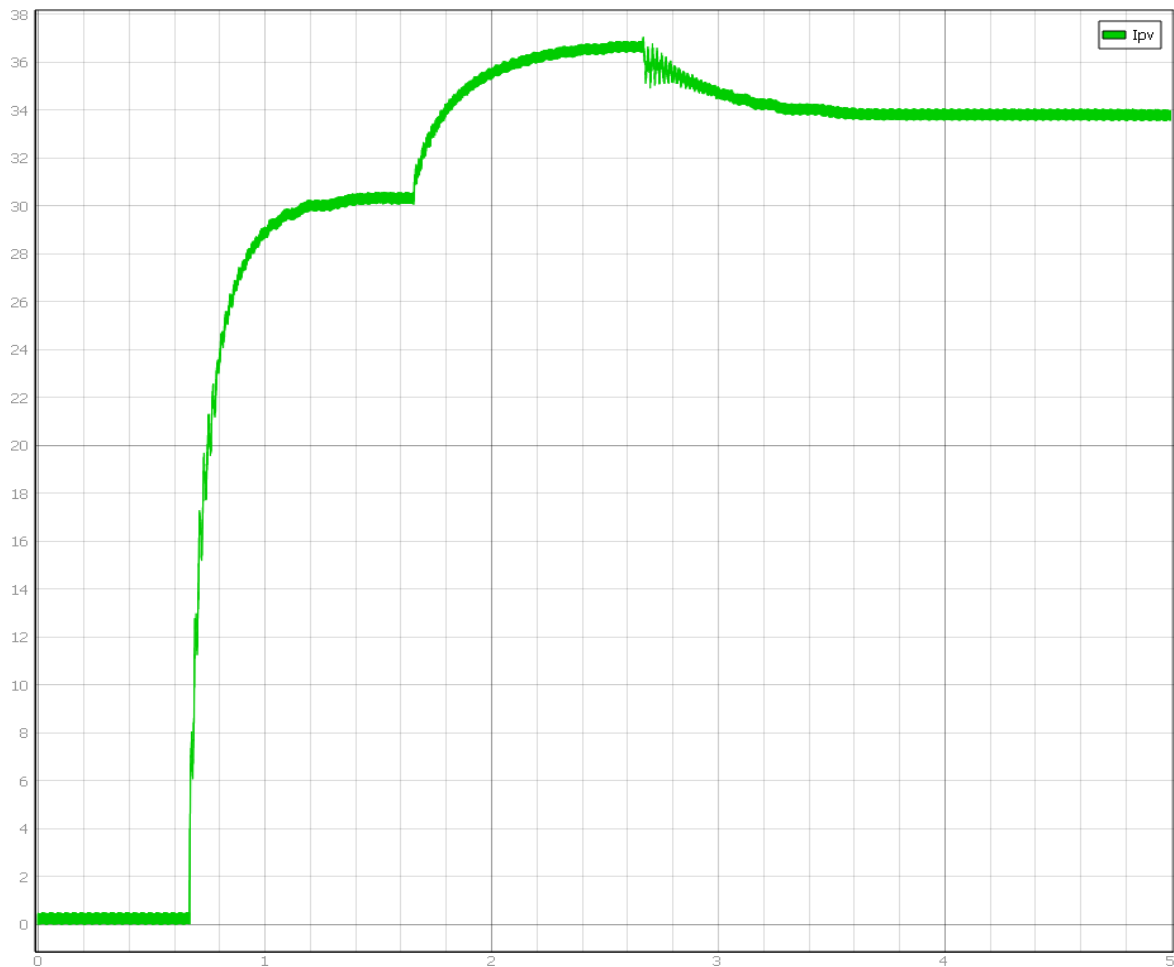
Then, and in order to confirm in practice the results and conclusions we reached through the simulations, we will present the values of the current received by the photovoltaic system using the different algorithms and under the 2 scenarios, without and with partial shading. In this way, we can arrive at the behavior that characterizes the system and the process we must follow for its optimal functioning.

#### **7.3.1 Perturb and Observe without Shading:**



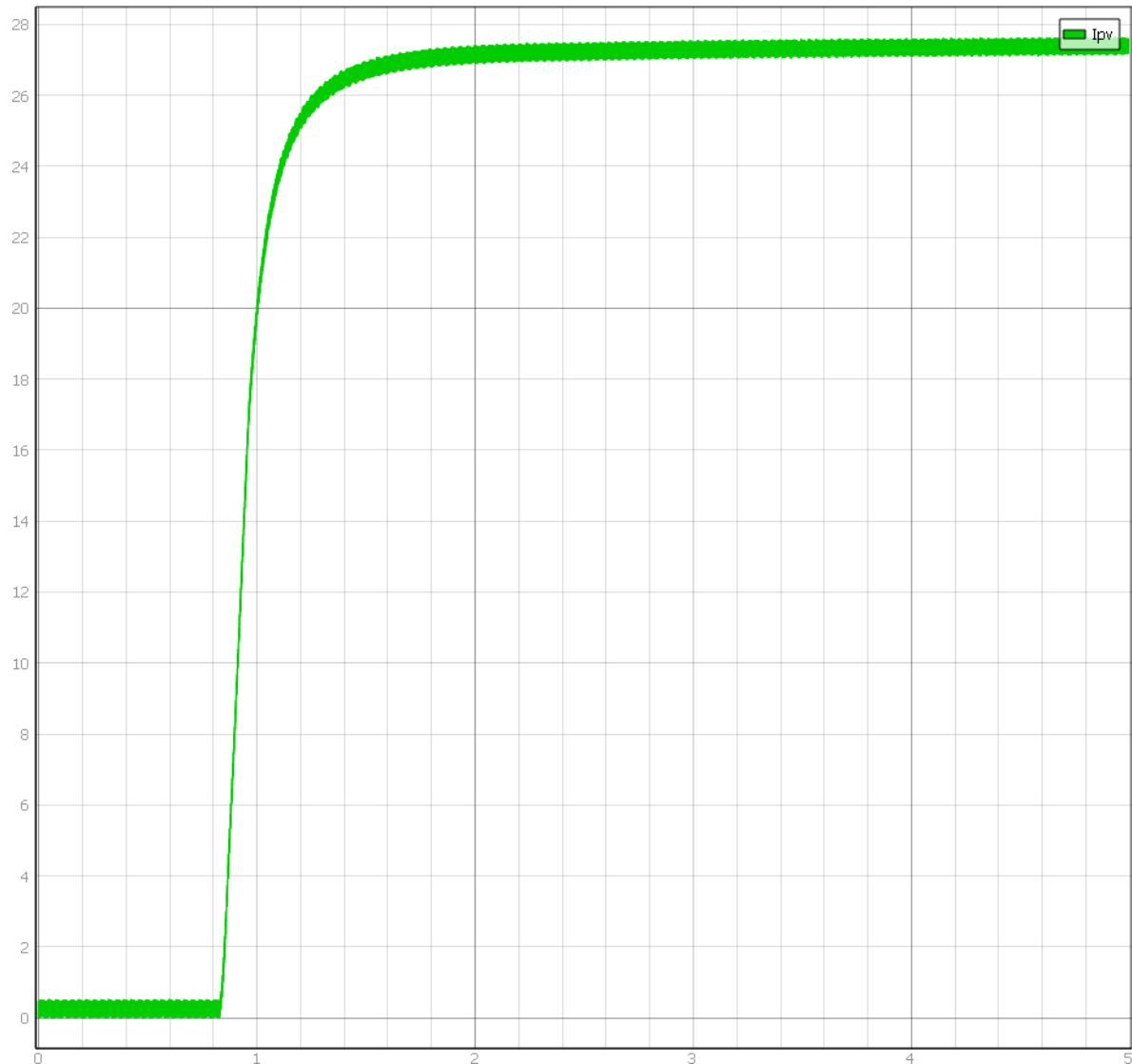
The above graphic shows the current of the photovoltaic system in the case without shading by changing the radiation from  $800\text{W/m}^2$  to  $1000\text{W/m}^2$  and finally to  $900\text{W/m}^2$ , and using the MPPT Perturb and Observe Algorithm. More specifically, we observe that the current follows the course of change of radiation, with its increase we observe an increase in the current and correspondingly with the decrease. The response of the system to changes is good and we can deduce this from the absence of oscillations in the graphics.

### 7.3.2 Particle Swarm Optimization without Shading:



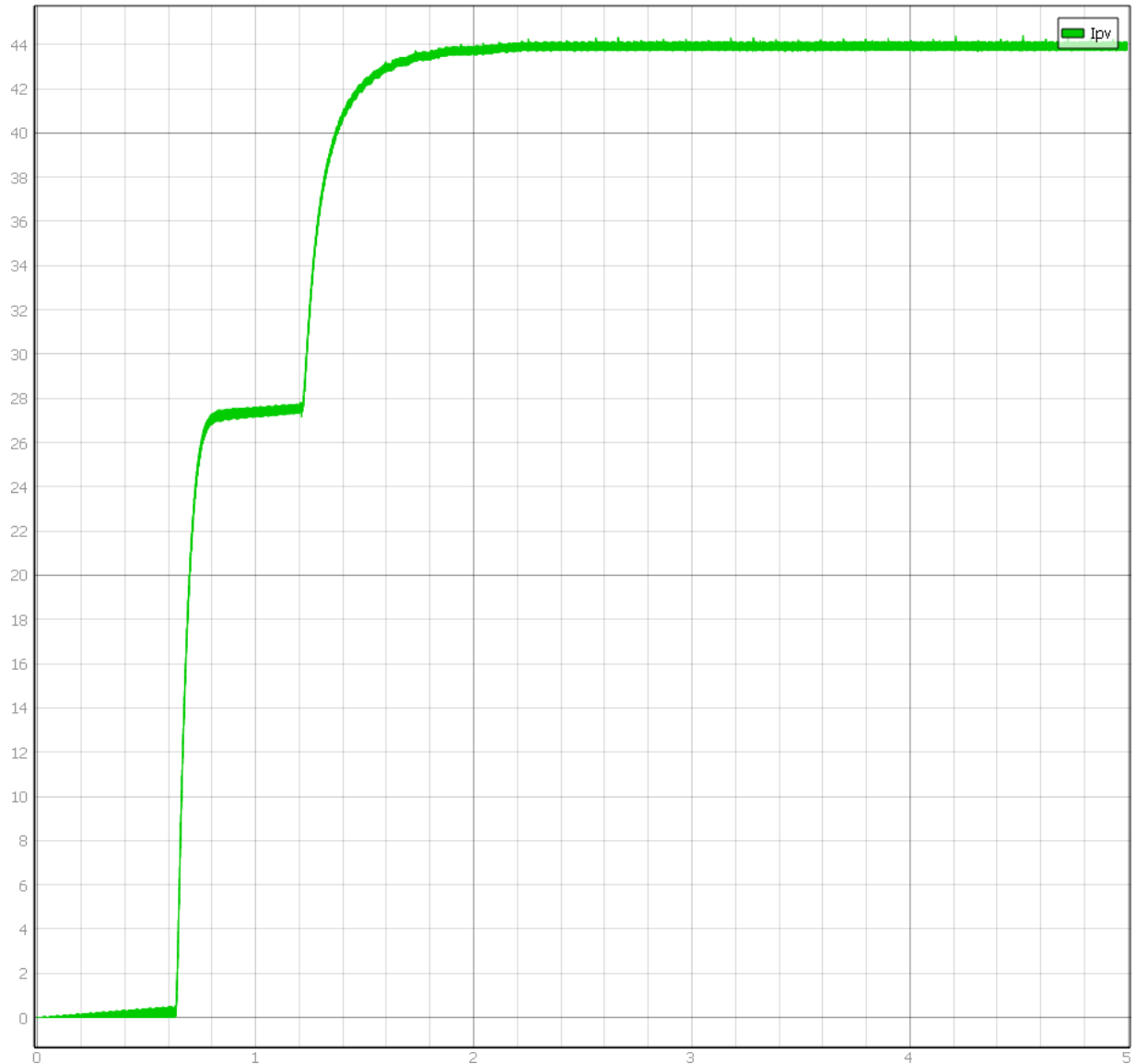
In this case we repeat the scenario using the PSO Algorithm. We notice that this algorithm also follows the path of change in radiation, but it is worth noting that its operation is not optimal. If we look at the graphics carefully, we will notice the oscillation that occurs when the radiation decreases from  $1000\text{W/m}^2$  to  $900 \text{ W/m}^2$ . This shows us that it has a worse transient response.

### *7.3.3 Perturb and Observe partial shading:*



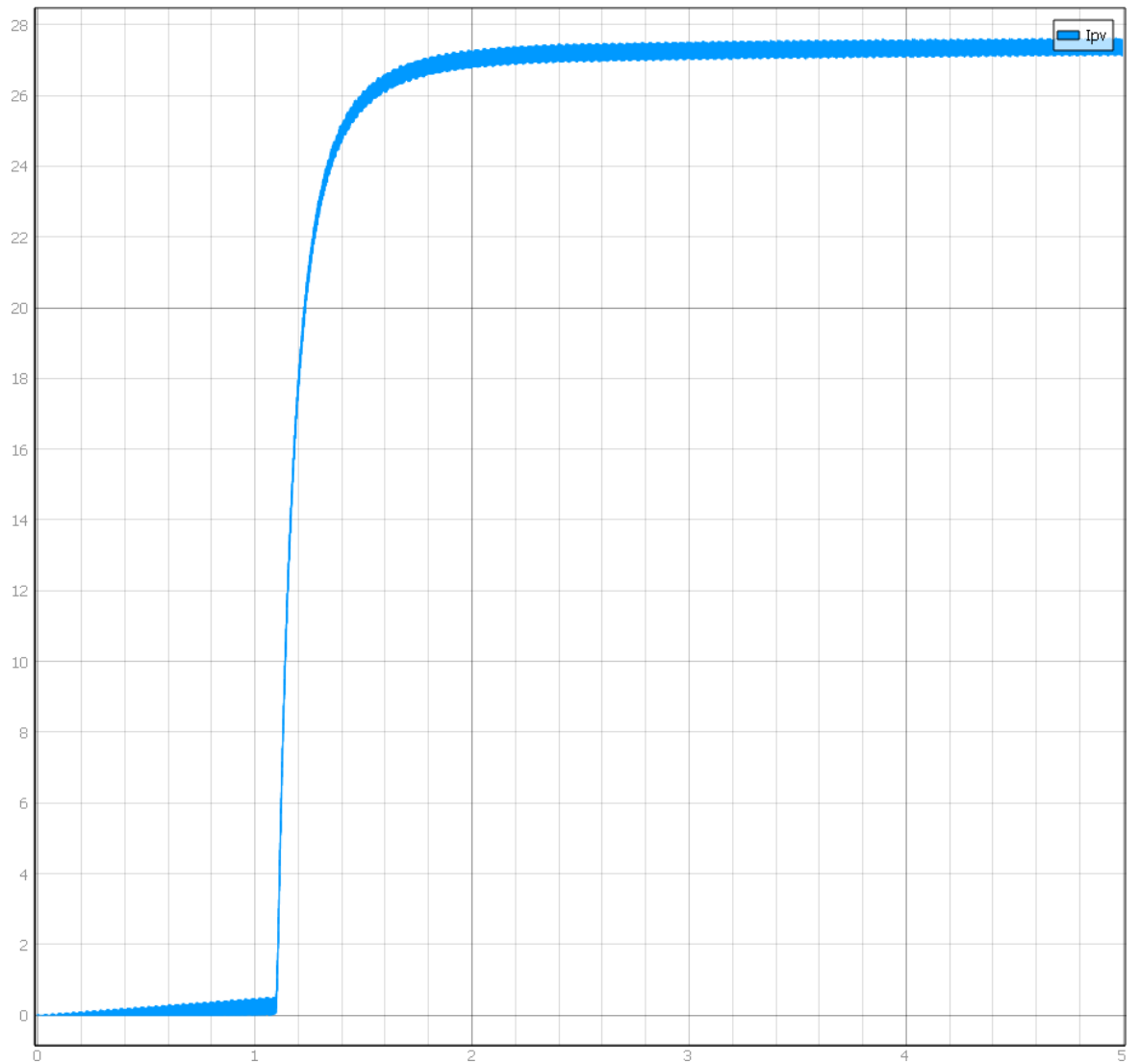
From the above graphic, we confirm what we said in the results of the simulations for the operation of P&O under conditions of partial shading of the photovoltaic systems. That is, the current of the photovoltaic system and therefore the control applied by the algorithm stops at the first maximum it encounters.

#### 7.3.4 Particle Swarm Optimization Partial Shading Lossless:



This is exactly where the difference between P&O and Particle Swarm Optimization can be seen. In more detail, we see that the PSO recognizes both maximums presented by our photovoltaic system, however, since in this particular case we have not taken into account the losses, it ends up at the point of 45 Ampere, where the P&O should also stop in the condition of partial shading since we did not take into account the losses.

### 7.3.5 Particle Swarm Optimization Partial Shading with losses:



By observing the above graphic, we confirm the totality of what we expected to see and we can say with certainty that the experimental results verify the results of the simulations. The current of the photovoltaic converges at 28 Ampere, a current which characterizes the real GMPP. This is accomplished by including losses in the PSO Algorithm.

Therefore, we come to the following final conclusions, regarding the improvement of the efficiency of the photovoltaic array in the grid. The use of the appropriate MPPT Algorithms, depending on the case of shading of the PV is crucial for operation in GMPP, since conventional algorithms seem to underperform under partial shading conditions. Also a key role in our systems are the losses that occur in the power converters, the wiring and other key parts of it, as well as

may lead to a change in GMPP. The combination of these two features, together with the correct control design at the same time, operate our system in optimal condition and lead to an improvement in its performance of up to 5%.

# Bibliography.

- [ 1 ] Bastidas, J., Ramos, C. y Franco, E. (2012). Modeling and parameter calculation of photovoltaic fields in irregular weather conditions. En: Ingeniería, Vol. 17, No. 1, pág. 37 - 48.
- [ 2 ] Kadeval, H. N. and Patel, V. K.. (2021). Mathematical modelling for solar cell, panel and array for photovoltaic system. Journal of Applied and Natural Science, 13(3), 937 – 943.
- [ 3 ] Vibhu Jately, Brian Azzopardi, Jyoti Joshi, Balaji Venkateswaran V, Abhinav Sharma, Sudha Arora. (2021). Experimental Analysis of hill-climbing MPPT algorithms under low irradiance levels. Renewable and Sustainable Energy Reviews.
- [ 4 ] I.William Christopher, Dr.R.Ramesh. (2013). Comparative Study of P&O and InC MPPT Algorithms. American Journal of Engineering Research (AJER).
- [ 5 ] Sumedha Sengar. (2014). Maximum Power Point Tracking Algorithms for Photovoltaic System: A Review. International Review of Applied Engineering Research.
- [ 6 ] Omid Palizban, Kimmo Kauhaniemi. (2015). Hierarchical control structure in microgrids with distributed generation: Island and grid-connected mode. Renewable and Sustainable Energy Reviews, 797-813.
- [ 7 ] Giannakopoulos, G. V., & Vovos, N. A. (2008). Introduction to Electricity Systems. ZITI Publications.
- [ 8 ] Zacharias Thomas. (2003). Mild Energy Forms II. University of Patras Publications.
- [ 9 ] Polyzakis Apostolos. (2019). Energy, Environment and Sustainable Development. P.H.C (Power Heat Cool) Versions.
- [ 10 ] Dervos Th. Konstantinos. (2013). Photovoltaic Systems: from Theory to Practice. University Publications, NTUA.
- [ 11 ] A. Al-Diab, C. Sourkounis. (2010). Variable step size P&O MPPT algorithm for PV systems. 12th Intern.
- [ 12 ] Mohd Rizwan Sirajuddin Shaikh , Santosh B. Waghmare , Suvarna Shankar Labade , Pooja Vittal Fuke , Anil Tekale. (2017). A Review Paper on Electricity Generation from Solar Energy. International Journal for Research in Applied Science & Engineering Technology (IJRASET).
- [ 13 ] Robert Lasseter, Abbas Akhil, Chris Marnay, John Stephens, Jeff Dagle, Ross Guttromson, A. Sakis Meliopoulos, Robert Yinger, and Joe Eto. (2002). Integration of Distributed Energy Resources.

[ 14 ] Kioskeridis, I. N. (2019). Power Electronics 2nd Edition. Tziola Publications.

[15 ]Optimization of MPP tracking algorithms for PVs with the impact of losses minimized Zaint A. Alexakis and Antonio T. Alexandridis, Member, IEEE